The Role of Rho GTPases in Breast Cancer Progression

by

Jeffery R. Smith

A Dissertation

Presented to the Faculty of the Louis V. Gerstner, Jr.

Graduate School of Biomedical Sciences,

Memorial Sloan-Kettering Cancer Center

In Partial Fulfillment of the Requirements for the Degree of

Doctor of Philosophy

New York, NY

November, 2012

Alan Hall, Ph.D.

Dissertation Mentor Date

For Aunt Pearl

Abstract

Cell migration is an essential process involved throughout embryonic development, wound healing, immune cell surveillance, and tumor invasion and metastasis. In order to migrate, cells must interact with and integrate signals from the extracellular matrix (ECM) and adjacent cells. Migration and invasion require cytoskeletal reorganization which is regulated by the Rho family small GTPases.

Rho proteins are best known as regulators of cell migration and morphology through control of the actin cytoskeleton. Rho GTPases exert this control through their function as molecular switches by cycling between the inactive GDP-bound state and active GTP-bound conformation. Once activated, Rho GTPases interact with specific signaling molecules, termed effectors, to promote downstream signaling. Guanine nucleotide exchange factors (GEFs) positively regulate Rho GTPases by promoting the dissociation of GDP, allowing GTP to bind and drive the conformational switch to an activated protein. Conversely, GTPase activating proteins (GAPs) negatively regulate Rho GTPases by enhancing the intrinsic GTPase activity. This causes hydrolysis of GTP to GDP and a conformation change that disrupts the Rho GTPase interaction with effector proteins. The delicate interplay between GEF activation and GAP inactivation of Rho GTPases controls downstream signals with exquisite precision.

When the GTPases and their regulatory proteins are misregulated due to changes in expression level or mutational status, cellular behavior is changed that can result in pathology. Rho GTPases have been reported to contribute to proliferation, survival, and invasiveness of many types of tumor cells. This study sets out to determine which regulators of Rho GTPases are important for breast cancer cell invasion, and gain mechanistic insight into the process. RNAi screens were carried out with siRNA libraries targeting Rho GEFs and GAPs, using the invasiveness of MDA-MB-231 breast cancer cells as a model system. This approach revealed the importance of Cdc42 for invasion, and surprisingly revealed that the Rac GEF Tiam2 expression is correlated to Ras mutational status in cell lines.

Acknowledgements

I would like to thank my mentor, Dr. Alan Hall, for accepting me as his student and allowing me the freedom to pursue my interests while providing thoughtful direction throughout all my pursuits. A huge thank you goes out to the past and present members of the Hall laboratory who made the long days both fun and intellectually stimulating. Particularly, Anastasia Berzat who kept me sane and focused, and Joanne Durgan for suffering my constant barrage of questions. I would like to thank my clinical mentor, Dr. Jacqueline Bromberg, who provided full access to both her clinic and her laboratory, in addition to helping keep me focused on the clinical implications of this project.

I would like to thank my committee members, Dr. Marilyn Resh and Dr. Songhai Shi, for taking the time and care to guide me throughout my studies. Many thanks to Dr. Andrew Koff, who not only agreed to chair my examining committee, but helped recruit me to the GSK Graduate School. I would also like to thank the Gerstner Sloan-Kettering Graduate School and all those involved in its creation, particularly Dr. Kenneth Marians as its first Dean and for setting the highest standards. I would like to thank everyone in the Graduate School Office, particularly Maria Torres for providing expert guidance on institutional procedures and frequent reality checks.

Finally, I would like to thank my parents, Bruce and Gloria Smith, my sister Melanie Grashot, and Robert Fishman, for their unconditional love, support, and encouragement throughout my life and during my Ph.D. None of this would have been possible without friends and family, both near and far, which have supported me along the way.

Table of Contents

List of Tables

List of Figures

List of Abbreviations

a.a.	amino acid
aPKC	atypical protein kinase C
bp	base pair
BRCA1	breast cancer Type 1, early onset
BRCA2	breast cancer Type 2, susceptibility protein
Cdc42	cell division cycle 42
cDNA	complementary DNA
C-terminus	Carboxyl-terminus
CRIB	Cdc42/Rac interactive binding
Dbl	diffuse B-cell lymphoma
DH	Dbl homology
DNA	deoxyribonucleic acid
ECM	extracellular matrix
EGF	epidermal growth factor
EGFP	enhanced green fluorescent protein
EGFR	epidermal growth factor receptor
EMT	epithelial mesenchymal transition
ER	estrogen receptor
FACS	Fluorescent-activated cell sorting
GAP	GTPase activating protein
GCL	Genomics Core Laboratory
GDP	guanine diphosphate
GEF	guanine nucleotide exchange factor
GFP	green fluorescent protein
GH	growth hormone
GST	glutathione-s-transferase
GTP	guanine triphosphate
GTPase	guanine triphosphate hydrolase
HA	hemagglutinin
Her2	human epidermal growth factor receptor 2
H-Ras	Harvey-rat sarcoma

JNK	c-Jun N-terminal kinase
kDa	kilo Dalton
MSKCC	Memorial Sloan-Kettering Cancer Center
N-terminus	amino-terminus
P53	tumor protein 53
PAK	p21-activated kinase
Par	partitioning defective
PDZ	PSD-95, Dlg-A, ZO-1
PH	Pleckstrin homology
PI3-K	phosphatidylinositol 3-kinase
PIP3	phosphatidylinositol (3,4,5)-trisphosphate
PKA	protein kinase A
PKC	protein kinase C
PR	Progesterone Receptor
Rac	Ras related C3
Ras	Rat sarcoma
RBD	Ras binding domain
Rho	Ras homologous
RhoGDI	Rho GDP dissociation inhibitor
RNA	ribonucleic acid
RNAi	RNA interference
Rnd	round
ROCK	Rho kinase
shRNA	short hairpin ribonucleic acid
siRNA	small interfering ribonucleic acid
STAT	Signal Transducer and Activator of Transcription
STEF	sif and Tiam-like exchange factor
TIAM1	T-cell invasion and metastasis gene 1
TIAM2	T-cell invasion and metastasis gene 2

Chapter 1: Introduction

Overview

Breast cancer is the second most common cancer type found in women in the United States, second only to skin cancer. Over 200,000 new cases are diagnosed each year [1], and almost 40,000 women will die each year – not from an operable tumor in the breast but from cancer having spread (metastasized) to distant organs such as the lungs, brain, or bones. In order for the cancer to metastasize, primary tumor cells must break through the basement membrane underlying the epithelial cell layer in the breast. Then they must invade the surrounding stroma and intravasate into the blood/lymphatic vessels where they must somehow survive while detached from the extracellular matrix, in addition to evading the body's immune system. Eventually, cancer cells extravasate at a distant site and grow into a metastasis. [2, 3] Elucidating the mechanisms that cancer cells use during invasion can lead to the discovery of new molecular targets for cancer therapies.

Cellular Migration and Invasion: Overview

Directional cell motility is a fundamental process essential to almost all forms of life. Similar processes to those used by single celled organisms, such as the slime mold Dictyostelium discoideum, are used by multicellular organisms for embryonic development, tissue homeostasis, immune responses, and wound healing. [4, 5] Different modes of migration build upon this basic process depending on the environmental context and the intrinsic properties of different cell types. Certain cells are able to invade through a surrounding matrix or tissue (3D migration), in addition to migrating along a surface (2D migration). [6] The complex processes of migration and invasion can be broken down into a functional set of component pathways, which include polarization, protrusion, adhesion, translocation, and retraction. [7, 8] The regulation and specific modality of each of these processes

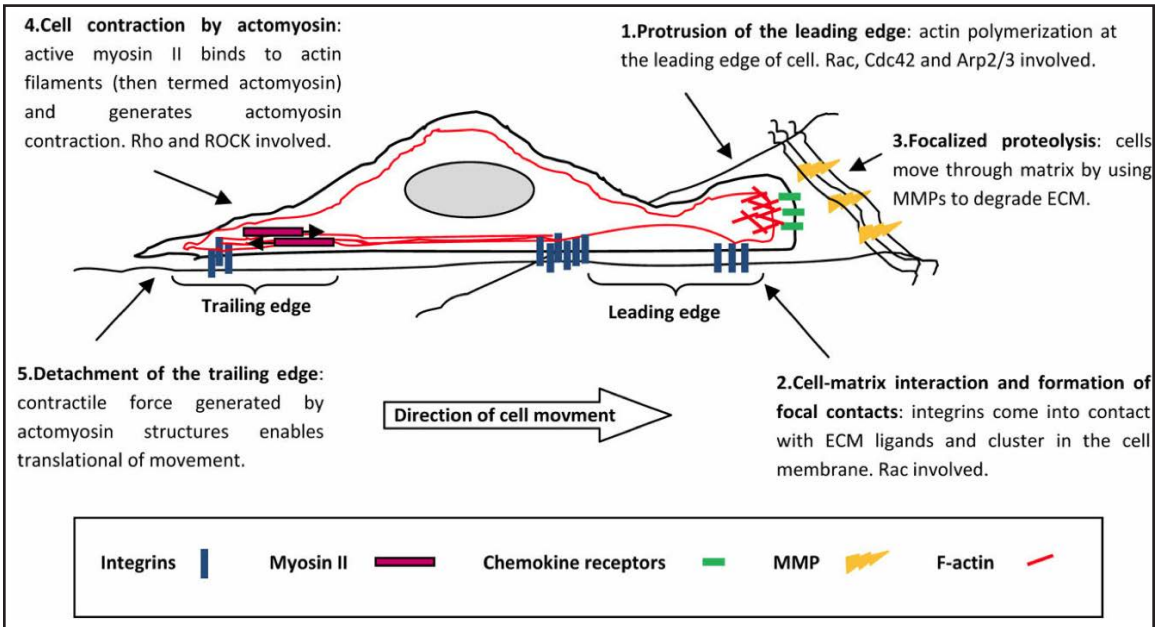

Figure 1: Cell Migration

1. lamellipodium extension at the leading edge

2. formation of new focal adhesions complexes

3. secretion of surface protease to ECM contacts and focalized proteolysis

4. cell body contraction by actomyosin complexes

5. tail detachment [9]

differs depending on whether the cells adopt one of two major categories of individual cell migration: amoeboid or mesenchymal, which can occur individually or more collectively as a group or sheet.

Mesenchymal Migration:

The process of migration can be envisioned as a repetitive cycle of polarization, forward protrusion, and retraction at the rear of the cell. [7, 9] Polarization occurs in response to a variety of extracellular stimuli, resulting in an extension of the cell body in the direction of migration. This protrusion is always accomplished by a reorganization of the actin cytoskeleton resulting in the formation of a narrow spike (filopodia) and/or a wide brush-like lamellipodia. This initial protrusion extends the cell body forward, where it can begin forming new adhesions to the extracellular matrix (ECM). [10] As these adhesions mature, the cell moves forward leaving a trailing portion of the cell body that must detach from the substrate and retract toward the nucleus. Repetition of this sequence results in persistent directional migration of a cell.

Polarization: Differences in molecular processes between the leading edge and rear of the cell result in polarized cell movement. [8] Cdc42 is often referred to as a master regulator of polarity as disruption of its activity often results in disorganization of polarity and in turn, prevents directional migration. [11-13] One way in which cell polarity is achieved is by proper positioning of the microtubule organizing center and the Golgi apparatus. This may contribute to enhanced microtubule growth toward the leading edge of the cell and facilitate efficient vesicle transport to the leading edge along microtubules in some cell types. [12, 14] Cdc42 regulates cell polarity through activation of the Par3/Par6/aPKC (atypical protein kinase C) pathway in many cell types. [15, 16] Phospholipids also play an important role in targeting the GTPases to the membrane. Upon sensing a migratory attractant, a cell will extend membrane protrusions in the direction of the chemoattractant. This "directional sensing" is initiated by the recruitment of phosphatidylinositol (PtdIns) 3-kinases of (PI3K) to the area of attraction, generating phosphatidylinositol-(3,4,5)-trisphosphate (PtdIns(3,4,5)P3 (PIP3). [17] Simultaneously, the phosphatase PTEN activated at the rear and sides of the cell, lowering PIP3 levels, [18] thereby amplifying the internal difference in PIP3 levels. [19] Localization of Cdc42 to the PIP3-rich leading edge inactivates PTEN locally, thus creating a negative feedback loop. [20] Rac is also involved at the leading edge of the cell, and can recruit and/or activate PI3K to the leading edge to maintain the lipid gradient in addition regulating actin polymerization and membrane extension. [21, 22]

Protrusion: Membrane protrusion is driven by the polymerization of actin monomers into helical filaments initiated on the sides of existing filaments and extending toward the front edge of the cell. [23] Lamellipodia formation, one form of membrane protrusion commonly seen in migrating cells, results from a highly branched actin network mediated by the activity of the Arp2/3 complex. This complex of seven subunits binds the side of actin fibers and facilitates ATP-dependent nucleation of new branches at a characteristic 70° angle to the mother filament. [24] This branching is controlled spatially by the WASP/WAVE proteins,

which interact with a wide variety of signaling molecules to activate Arp2/3. [25, 26] The rate and organization of actin polymerization is controlled by an array of regulatory proteins. Profilin binds to actin monomers, preventing random nucleation and directing them toward the barbed end. [27] Capping proteins terminate actin polymerization, confining polymerization to the plasma membrane of the leading front. [28] Cross-linking by filamin A and α-actinin stabilizes the entire actin network, while cortactin binding stabilizes actin branches and recruits additional Arp2/3 to promote cell migration. [29] Disassembly of actin filaments occurs when proteins like severin, gelsolin, and villin cleave the fiber, releasing monomers back into the cytosolic pool. [30, 31]

Filopodia represent a second type of actin-dependent protrusion seen at the leading edge of migrating cells, consisting of unbranched, aligned filaments. These filaments elongate from the barbed end, and release actin monomers from the pointed end in a treadmill fashion. [32] The tips of filopodia include proteins that prevent capping and encourage elongation; such as Ena/VASP (Vasodilator-stimulated phosphoprotein) family proteins found at high levels in the growth cones of neurons, but whose precise roles are still unclear. [33] One actin crosslinking protein, fascin, is able to hexagonally pack bundles of actin filaments together in a way that increases stiffness and supports filopodia extension. [34] Filopodia may also function as a type of cellular antennae, sensing environmental cues such as epidermal growth factor (EGF) and transport those activated receptors toward the cell body (retrograde transport). [35]

More specialized protrusive structures exist in different cell types. Highly invasive cancer cells extend invasive feet that have high levels of protease activity, termed invadopodia. [36] In breast cancer, invadopodia formation is closely linked to the aggressiveness of cells to metastasize. [37, 38] Intravital imaging has demonstrated that this phenomenon also occurs in vivo during tumor invasion. [39]

Adhesion: After polarization is established and cell membranes are extended, the cell must attach to the surroundings in order to generate the force required to move in space. The exact receptors vary between cell types but integrins are a key family of transmembrane receptors that mediate attachment of a cell to surrounding tissues and the extracellular matrix (ECM). [10] Integrins are found in all animals as heterodimers of α and β subunits and are key links between the ECM and the actin cytoskeleton. [40, 41] The degree to which different integrins bind to the ECM and how they cluster dictate the strength of cell attachment. [42] Signaling can occur bidirectionally, such that extracellular information is relayed to the cell, and the cell can determine the appropriate degree of adhesion. [10, 43] As a cell moves along a surface, some adhesion sites are dismantled while others mature into more stable focal adhesions. [44, 45] Focal adhesions were characterized by electron microscopy as plaques [46] that are closely associated with bundles of actin fibers in chick embryo fibroblasts. [47] These structures facilitate both cell signaling through proteins such as paxillin and focal adhesion kinase (FAK) [48, 49] as well as supporting the intracellular structures through proteins such as talin [50] and vinculin. [51]

Amoeboid Migration

Cells that lack the distinctive mesenchymal characteristics of stress fibers and focal adhesions can still migrate across a surface in what is referred to as amoeboid-like movement, best characterized by Dictyostelium discoideum. [52, 53] Cells using this mode of migration are typically round and rapidly extrude and contract their membrane, resulting in a blebby morphology. Mammalian cells such as lymphocytes and neutrophils migrate in this way and appear microscopically to quickly glide over surfaces within the body. [4, 54, 55] Membrane blebs are extended in the direction of migration, followed by contraction of cortical actin, pushing the cytoplasm into this new protrusion. [56] Actin then reorganizes to stabilize the cell in the new position. [57] This process occurs in the absence of Rac driven protrusions, but requires Rho acting through ROCK to promote contraction of the

actin:myosin cytoskeleton. [9] While prevalent in circulating lymphocytes and other cell types, amoeboid movement relies on much weaker cell-matrix interactions and exhibits a more diffuse cortical actin cytoskeleton [4, 58]. Largely in the absence of integrin contacts or metalloproteases (MMPs), cells can squeeze through gaps in a three dimensional (3D) ECM rather than remodel it using amoeboid movement.

Collective Cell Migration

Cells are also capable of moving in concert with one another, while maintaining cell-cell contacts. This method of migration is commonly observed in embryonic development, for example when the neural tube closes [59] or when the mammary gland forms ducts, but is also seen in cancer invasion. [60, 61] Maintaining cell contacts has the interesting effect of forming a multicellular contractile body due to a special form of cortical actin filament assembly along junctions. [62] The cells move in concert, with the cells at the front leading and cells inside the group following. [63] Whether or not cells migrate individually or as a group is likely to be related to the level of differentiation, where more differentiated cells are likely to maintain contacts and invade collectively. [64]

Cancer Cell Invasion

Cell migration that occurs in three dimensions is termed invasion. All of the processes described above not only apply to normal biology, but are also used by cancer cells to disseminate throughout the body. [65-67] Immune cells accomplish this primarily through amoeboid invasion, extending membrane blebs through the ECM, and contracting the cytoskeleton to push the cell forward, and allowing them to quickly pass through tissues. [4, 54, 55] Carcinoma, which develops from epithelial tissues, can undergo an epithelial to mesenchymal transition (EMT) in which cells begin to develop mesenchymal modes of migration. [68, 69] This requires secretion of matrix metalloproteinases (MMPs) that

remodel the ECM, facilitating a path for invasion. [70] Specific cancer-related integrins convey signals from the ECM to the cancer cell that further facilitate invasion in a Rho-GTPase dependent manner. [40, 71]

In different contexts, cancer cells are able to switch between modes of migration. [57, 72] This may be due the expression, or lack thereof, of specific integrins or other receptors that respond to a changing environment. [73] This plasticity in the type of migration is one explanation why drugs targeting one particular type of invasion may fail to stop the spread of disease. [74] For example, an individually migrating cell that can no longer degrade the ECM due to inhibition of MMPs can switch to an amoeboid mode of migration and back again as necessary. [56, 75] Similarly, collectively migrating cells can either change from sheets into strands or individual cells and back again by regulating cell-cell adhesions. [64, 66] Changes in the balance of Rho/ROCK and Rac activity levels have also been shown to be important for switching between modes of migration. [57]

Using 3D culture models, it has been shown that cancer cells are capable of switching from mesenchymal to amoeboid migration when treated with MMP or integrin antagonists [56, 76]. This has been termed a mesenchymal-amoeboid transition (MAT) [76]. This has also been proven to occur in patients and is exemplified by the failure of current MMP inhibitory drugs in the clinic [77, 78]. Cancer cells exhibit great plasticity in migration mechanisms and can undergo EMT and MAT and thereby escape anti-cancer therapies. [56, 75, 76, 79, 80] Due to their important role in cytoskeleton control, migration and invasion, Rho GTPases may control critical factors responsible for all types of cellular migration.

Interestingly, Rho GTPases are important at multiple steps of the cell migration process, in EMT, MAT, and collective migration. Increased Rho expression is common in mesen-

chymal migration of metastatic breast tumors [57, 81, 82]. The Rho effector, Rho Kinase (ROCK), is important for MAT migration [83, 84].

Rho Family GTPases

Cell migration and invasion are reliant on coordinated reorganization of the actin (and sometimes microtubule) cytoskeleton. Key regulators of these processes are Rho family GTPases that act as molecular switches to control the transduction of signals from outside the cell to downstream effectors in a spatially controlled manner.

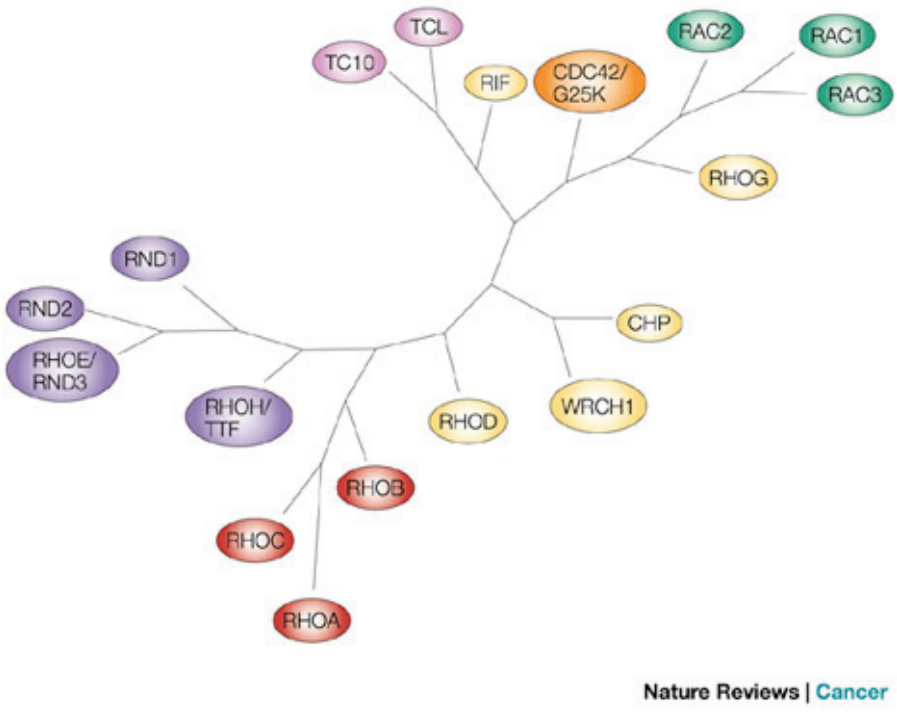

Figure 2: Rho Family Tree

The RHO proteins can be subdivided on the basis of functional, biochemical and sequence data. This phylogenetic tree has been altered to take functional and biochemical studies into account. The RND proteins and RHOH have been grouped together because of their predicted lack of GTPase activity. [85]

Introdution: Rho (Ras Homologous) proteins are a distinct family within the Ras superfamily of small GTPases (guanosine triphosphate hydrolases), sharing 30% homology with other Ras family proteins (and 40-90% homology with each other). [86, 87] Rho itself was first isolated in 1985 from the marine snail Aplysia californica, and shares 85% homology with its human ortholog. [88] In humans, there are 20 Rho family members, with conserved orthologs in many other species including yeast, plants, worms, and flies. [89] The three most well studied members of the Rho family are RhoA, Rac1, and Cdc42. [90, 91] Most members actively cycle between inactive GDP-bound and active GTP-bound states, thus functioning as molecular switches within the cell. [92] Structurally, the Rho proteins are distinct from other members of the Ras superfamily due to the insertion of a 12 amino acid "Rho insert sequence" within the GTPase domain, forming and extra alpha-helix within the structure. [93] A hypervariable domain is found at the carboxy-terminus and includes a CAAX motif, allowing for the addition of post-translational modifications such as the addition of lipids, resulting in a 21-25 kDa molecule. [94] Rho proteins are best known as regulators of cell migration and morphology through control of the actin cytoskeleton. For instance, Rho activation leads to the formation of actin:myosin filaments, focal adhesions, and integrin adhesion complexes, lending rigidity and structure to cells and providing the contractile forces necessary for migration. [95, 96] Rac promotes actin polymerization at the at the cell periphery producing lamellipodia and membrane ruffling, while active Cdc42 promotes filopodia formation – both processes associated with directed cell migration. [97] Cdc42 also plays vital roles in cell polarity, controlling apical-basal polarity in epithelial cells [12, 98], in addition to influencing the direction of cell migration and invasion. [12, 16, 99] Together, Rho proteins are major regulators of the cytoskeleton and actin-dependent processes including cell polarity and migration in addition to cell-cycle progression and gene expression. Tight regulation of these GTPases is critical for proper cell behavior, and misregulation can have serious consequences such as contributing to tumor development and metastasis. [85]

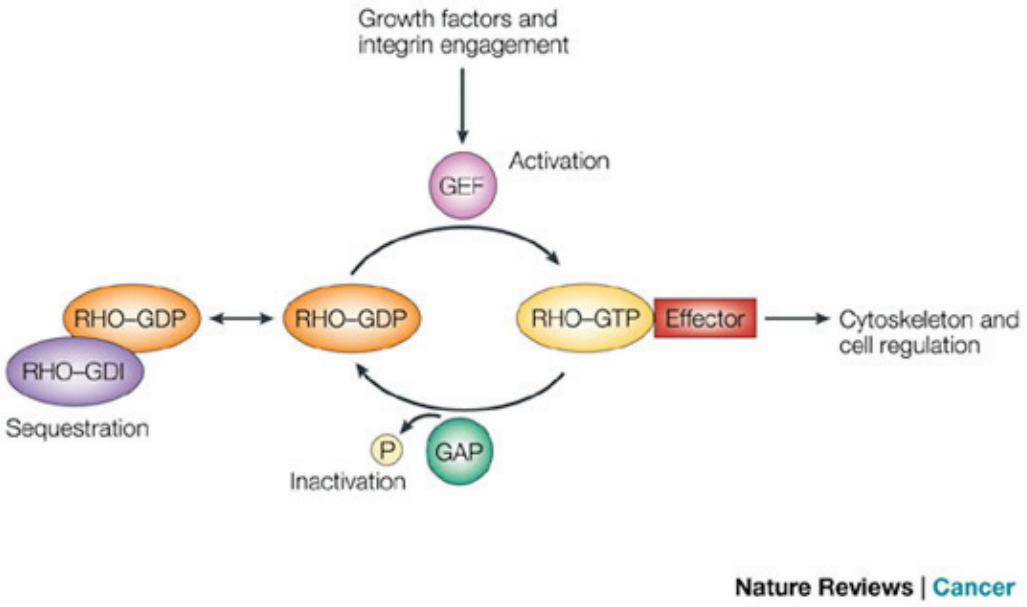

Figure 3: Regulation of Rho Family GTPases

RHO proteins can bind either GTP or GDP. When bound to GDP, they can be sequestered in the cytoplasm by RHO–GDP dissociation inhibitors (RHO–GDIs). The exchange of GDP for GTP is promoted by RHO guanine nucleotide exchange factors (RHO–GEFs), and is often associated with translocation of RHO proteins to cell membranes. GTP-bound RHO proteins interact with a range of effector proteins and modulate their ability to regulate cell behaviour. Most RHO proteins have an intrinsic ability to hydrolyse GTP to GDP and inorganic phosphate (P), which can be promoted by RHO–GTPase-activating proteins (RHO–GAPs). RND1, RND2 , RND3/RHOE and RHOH are unable to hydrolyse GTP, and their regulation is likely to be through changes in protein level or localization, not through GDP/GTP binding. [85]

Regulation: Three families of proteins regulate the molecular switch function of Rho GTPases. Guanine nucleotide exchange factors (GEFs) bind the GTPase and catalyze dissociation of GDP, allowing GTP to bind, leaving the GTPase in an active conformation. [13] GTPase activating proteins (GAPs) catalyze the inherently slow rate of hydrolysis of GTP to GDP, resulting in conformational inactivation. This regulation between active and inactive states allows GTPases to function as molecular switches. Only in the active state can GTPases interact with their downstream effector molecules. Upstream in the signaling cascade, Rho family GEFs and GAPs are themselves regulated by an extensive array of extracellular and intracellular signals. [100] The interactions between various components of the Rho GTPase signaling pathway are highly specific, allowing a wide array of upstream signals to couple to an equally diverse set of downstream effectors. The third family of Rho GTPase regulators is guanine nucleotide dissociation inhibitors (GDIs), which prevent spontaneous cycling between GDP and GTP bound states, and promote sequestration in the cytoplasm. [101-104] They bind the lipid moiety of the GDP-bound state of the GTPase and prevent signaling to downstream effector molecules. [105]

Crosstalk: GTPases can signal to one another, adding a layer of complexity in GTPase signaling biology. [106] This can occur between families; Ras for example, can regulate the activity of Rac1 through the GEFs Tiam1 and SOS1. [107] Rac1 and Cdc42 are capable of downregulating RhoA levels, demonstrating that crosstalk also occurs within the Rho family GTPases. [108] Rac was shown to mediate reactive oxygen species production to downregulate Rho activity through p190RhoGAP, resulting in membrane ruffling and increased cell spreading. [109] An interesting winner-take-all model has been proposed, using a hypothetical crosstalk between Rho Rac and Cdc42 to model the behavior of the neuronal growth cone. [110]

Functions: GTPases act as switches, regulating various functions in the cell through the binding of effector molecules. [13] Many kinases have been identified as targets of Rho GTPase regulation including ROCK [111-113], PAK [114], and PKN families; [115, 116] but in addition, scaffolds [117], adapters [118], phosphatases [119], and lipases have been found. [120, 121] This diversity of effector proteins positions Rho GTPases as key regulators of a wide variety of biological processes including cell shape, size, polarity, proliferation, transformation and differentiation. [13, 90, 122]

The best-characterized role of Rho GTPase is in regulating the actin cytoskeleton. Microinjection of recombinant Rho protein first revealed its role in promoting actin stress fiber formation in fibroblasts [96] Later, it was shown that RhoA controls cell shape through two targets, the Rho-associated protein kinase (ROCK), which can phosphorylate myosin light chain (MLC), LIM kinase, and MLC phosphatase, and mDia which promotes linear actin filament assembly. [112, 123] These proteins alter the organization and contractility of actin fibers, and thus cellular morphology. In migrating cells, asymmetric Rho activity is important to restrict membrane protrusions to the leading edge of the cell. [124]

The microtubule cytoskeleton is a network of cylindrical polymers of α- and β-tubulin dimers. Rho and Rac have been shown to play a role in microtubule stability and directional migration through p160Rho kinase and p65Pak, respectively. [125] Cdc42 controls polarity through proper microtubule spindle orientation [98] in mammals and proper bud site positioning in yeast. [12, 126] Through control of the cytoskeleton, Rho GTPases exert control over other cellular processes, including tight junction assembly [127] and transcription. [128]

Cancer progression leading to cellular invasion subverts normal pathways regulating cell migration during development. [118] For instance, PAK is upregulated in some breast can-

cers [129], and induces anchorage independent growth as well as disorganized mitotic spindles in MCF-7 cells. [130] Expression of ROCK might affect testicular tumor cell migration, contributing to metastasis. [110, 131]

Guanine Nucleotide Exchange Factors (GEFs)

Introduction: Activation of Rho family GTPases is facilitated by guanine nucleotide exchange factors (GEFs), which facilitate release of GDP, allowing GTP to bind (since the intracellular GTP concentration is around ten times higher than that of GDP). [132] GEFs respond to intracellular and extracellular cues to couple an upstream signal to the activation of the appropriate Rho GTPase at the proper time and location. In humans, approximately 80 GEFs have been identified and are classified as part of either the Dbl family, or DOCK family branches. [133]

Dbl Family: This family's namesake, Dbl (diffuse B-cell lymphoma), was identified as an oncogene based on its ability to induce focus formation in NIH-3T3 cells. [134] It harbors a catalytically essential Dbl-homology (DH) domain that shares sequence homology with the Cdc42-activating protein Cdc24 in S. cerevisiae. Genetic analysis placed Cdc24 upstream of Cdc42 in the bud assembly pathway, and this yielded the initial clue that the DH domain acts as a GEFs for Rho GTPases. [135] Since then, the Dbl family of GEFs has expanded to include approximately 70 family members in humans. This common ability to transform fibroblasts when truncated forms are overexpressed in cells has helped identify new members and expand the family. A pleckstrin homology (PH) domain invariably follows the DH domain, and is important for proper cellular localization and in vivo GEF activity. This DH-PH domain combination defines the Dbl subfamily of GEFs. [136, 137]

While GEFs have a diversity of structures and domains, the small (~200 residues) DH domain is the minimal domain required to exchange GDP for GTP in vitro. This domain

is itself helical, being comprised of multiple alpha-helices and 310-helices, and forms a structure resembling a chaise longue that interacts with the surface of the interacting GT-Pase. [138] The sequences comprising this interacting region vary among GEFs and are considered important for conferring specificity. When a Dbl-family GEF binds to a GT-Pase, a structural rearrangement occurs in the switch I and switch II regions of the GT-Pase. This alters the shape of the nucleotide-binding pocket, freeing the GDP and Mg2+ to disassociate. The GEF-bound GTPase only remains nucleotide-free until GTP binds (due to its greater abundance than GDP in the cytoplasm), releasing the GEF and allowing the now-active GTPase to bind downstream effectors. Some, but not all, GEFs acting on other members of the Ras superfamily share this general mechanism of structural remodeling to facilitate nucleotide exchange. For instance, when Sos binds to Ras the conformation of the switch II region of Ras is disrupted, releasing the metal ion and nucleotide. In contrast, some Ras GEFs are able to insert residues into the nucleotide-binding pocket to dislodge GDP, a mechanism more similar to the DOCK-family GEFs (see below).

The PH domain is found immediately c-terminal to the DH domain in most Dbl-family GEFs. Evidence exists for a variety of roles for the PH domain. [139] Some studies show that it enhances the rate of nucleotide exchange, while others suggest a role in localization at phospholipid membranes, or even orientation at those membranes. Structurally, there are a wide variety of orientations between the DH and PH domains, suggesting that this may also help to confer specificity for both the GTPase and its subcellular localization. For example, Cdc42 contacts the PH domains of Dbl, Trio, and Dbs but not that of ITSN suggesting that it is not essential in manipulating the conformation of the GTPase. [140]

Membrane localization is a key feature of Rho GTPase activation, and the PH domain has been implicated in proper membrane targeting through its capacity to bind phospholipids such as PIP3. This membrane anchoring function of the PH domain seems to either be

dispensable, or superseded by other targeting domains. [100] Whether or not the PH domain is important for proper membrane orientation or allosteric regulation of GEF activity is subject to much debate. Reports of mild increases, no effect, and mild decreases in GTPase activity have clouded the issue and no reports have included strong physiological significance. Stronger evidence exists for a role in membrane orientation, as point mutations within the PH domain of Dbs will block phospholipid binding, but do not alter the membrane localization. [133] The in vitro GEF activity is unaffected by these mutations, but the protein loses the ability to transform fibroblasts, suggesting that binding to phospholipids such as PIP3 is required for proper GEF function. PH domains are not limited to binding phospholipids, but can also bind other proteins. The PH domain of Trio interacts with filamin to properly localize the GEF to actin filaments and promote membrane ruffling in the malignant melanoma M2 cell line, while Dbl interacts with ezrin via its PH domain. [141] Despite the sometimes mysterious role that PH domains play, their consistent presence adjacent to the DH domain implies an important role in Dbl-family GEF function.

DOCK Family: The founding member of the second family of Rho GEFs is the dedicator of cytokinesis of 180 kDa (DOCK180). [142] Orthologs in flies and worms go by the names Myoblast city and Ced-5, respectively. Alternatively, this family is referred to as CZH proteins, an acronym, combining Ced-5, Dock180, and Myoblast city as CDM and Zizimin homologous proteins. [143] The DOCK family proteins lack a DH-PH domain, yet are still capable of catalyzing nucleotide exchange on Rac and Cdc42 (but not Rho) GTPases. DOCK180 (or DOCK1) was identified originally as interacting with c-Crk, and later was shown to be involved in cytoskeletal reorganization in fibroblasts. [144] There are currently 11 members of the DOCK family of GEFs. [145]

To activate Rho GEFs, DOCK proteins use the second of two DHR domains to catalyze nucleotide exchange. [142] This catalytic DHR2 domain alone has been shown to increase

the rate of GTPase activation using biochemical studies. Structural evidence points to a direct insertion mechanism used to displace the Mg2+ ion and the GDP. In contrast, the DH-PH domain disorganizes the nucleotide-binding pocket rather than directly disrupting nucleotide binding, while DOCKs can use both. Specifically, DOCK9 has been shown to require a conserved valine that disrupts Mg2+ binding in addition to inducing conformational changes that disrupt the structure of the switch I region in Cdc42. [146]

The DHR1 domain precedes the DHR2 domain in DOCK proteins and has been shown to bind phosphoinositides such as PIP3. It is dispensable for GTPase activation in vitro, but is necessary for proper targeting of DOCK180 to the plasma membrane and in vivo activation. Replacing the DHR1 domain with a PH domain is sufficient to induce cell migration in the CHO variant LR73 cells, supporting the notion that DHR1 properly localizes DOCK180 to the plasma membrane. More recent studies reveal the structural basis for this localization a pocket that binds the PIP3 lipid head group. [147, 148]

GTPase Activating Proteins (GAPs)

Introduction: Rho GTPases are capable of inactivating themselves due to their intrinsic ability to hydrolyze GTP. The rate of hydrolysis, and thus inactivation, is greatly enhanced by interaction with GTPase activating proteins (GAPs). In this way, a GAP's ability to inactivate a GTPase in a specific biological context complements the ability of GEFs to specifically control GTPase activation. [149] The first Rho GAP, p50RhoGAP, was purified from spleen extracts and shown biochemically to enhance the intrinsic rate of Rho, Rac, and Cdc42 GTP hydrolysis. [150] Since then, approximately 70 human Rho GAPs have been identified. All these proteins share a conserved approximately 170 amino acid domain known as the RhoGAP domain (also sometimes referred to as the BH domain), that defines the family and is catalytically active. While there is little sequence similarity between

Rho GAPs and Ras GAPs, they appear to share a similar 3D structure as well as a similar mechanism of activity. [149]

The Rho GAP domain consists of 9 α-helices in a loop structure with a key arginine residue that is evolutionarily conserved. [151] This "arginine-finger" is capable of inserting into the active site of GTPases, while the rest of the structure stabilizes the switch I, switch II, and P-loop. Crystal structure models suggest that RhoGAP does not participate in the hydrolysis reaction chemically, but stabilizes the transition state structure of GTP, resulting in efficient cleavage of the terminal phosphate by H2O and leaving GDP-bound. [152] Structural studies have yet to address exactly how substrate specificity is achieved. The interaction between the GAP domain of p190RhoGAP, with different chimeras of RhoA and Cdc42, showed that residues outside the catalytic domain do affect specificity. [153] Further studies have shown that the presence of different lipids or phosphorylation status of the GAP can alter specificity of p190RhoGAP for different GTPases, but these modifications are not found in the conserved regions. [154, 155] Additional work remains to confirm the specificity of GAPs to different GTPases in a physiological context.

Rho GTPases in Cancer

In cancer, Rho GTPase dependent signaling pathways may become disregulated. Unlike the Ras proteins, which are commonly mutated in many types of human cancer, Rho GTPases mutants are very rare and have only recently been described for Rac1 in melanoma. [156] Instead, they are often overexpressed as compared to paired normal tissue, especially in breast cancer. [81, 157] Prominent examples include RhoC overexpression in inflammatory breast cancer (IBC) and Rac1b overexpression in breast and colorectal tumors. [82, 157, 158]

A few examples of mutated regulators have been reported in cancer. In 10% of renal cell carcinomas (RCC), an activating mutant of the Rac-specific GEF Tiam-1 has been identified that causes focus formation using in vitro cell culture studies [159]. Truncated forms of the GEFs Ect2, Dbl, and other family GEFs are able to transform fibroblasts in culture, although they have not been found in human cancers. [137, 160, 161] ErbB receptors in breast cancer cell lines can activate the Rac GEF P-Rex1. The expression of P-Rex1 has also been shown to correlate with ErbB2 and ER expression. [162] Recently, the Rho GEFs Vav2 and Vav3 were implicated in transcriptional control of proteins that promoted tumorigenesis and lung-specific metastasis of breast cancer, identifying potential targets for cancer therapy and solidifying importance of GEFs in human tumor biology. [163, 164]

Deletions or decreased expression levels of the DLC-1 and DLC-2 Rho GAPs have been linked to increased GTPase activity in breast and hepatocellular carcinomas, implicating a role for these proteins as tumor suppressors. Loss of the related protein DLC-3 has been shown to contribute to oncogenesis by disrupting for adherens junctions and enhancing an epithelial to mesenchymal transition. [165] In addition, ARHGAP8 mutations have been discovered in colorectal and breast cancers. [166] Any mutations in GEFs or GAPs can shift the balance of normal GTPase activity, promoting oncogenesis and metastasis. Therefore, a systematic analysis of all the GEFs and GAPs would provide a clearer picture of how Rho GTPase activation affects cellular migration and invasion.

Chapter 2: Materials and Methods

Cell Culture

Cell Lines and Culture Conditions

Breast Cell Lines

MDA-MB-231 cells were acquired from ATCC (catalog #HTB-26) and grown in Leibovitz's L-15 Medium (Invitrogen, catalog #11415-114) supplemented with 10% fetal bovine serum (FBS) (BenchMark, Lot #A27A00X) and a mixture of penicillin (100 U/mL) and streptomycin (100 µg/mL) antibiotics (Invitrogen, catalog #15140-163). Cells were grown in 100% air humidified incubator at 37°C. Cells were passaged by rinsing once with phosphate buffered saline (PBS) (MSKCC Media Facility), treating with Trypsin-EDTA 0.05% (Invitrogen, catalog #25300-062) and split 1:4 after reaching 80% confluence, approximately every 2-3 days.

Hs578t cells were obtained from ATCC (catalog #HTB-126). Cells were grown in DMEM supplemented with FBS (Omega Scientific, Lot #104021) and a mixture of penicillin (100 U/mL) and streptomycin (100 µg/mL) antibiotics (Invitrogen). Cells were grown at 5% CO2 in a humidified incubator at 37°C. Cells were passaged by rinsing once with PBS, treating with Trypsin-EDTA 0.05% and split 1:4 after reaching 80% confluence, approximately every 2-3 days.

SkBr7 cells were provided by Dr. F. Giancotti (MSKCC) and grown in Roswell Park Memorial Institute medium 1640 (RPMI1640) (MSKCC Media Facility) supplemented with 10% FBS (Omega Scientific, Lot #104021), 10 µM Non Essential Amino Acids (NEAA) (Invitrogen, catalog #11140-050) and a mixture of penicillin (100 U/mL) and streptomycin (100 µg/mL) antibiotics (Invitrogen). Cells were grown at 5% CO2 in a humidified incuba-

tor at 37°C. Cells were passaged by rinsing once with PBS, treating with Trypsin-EDTA 0.05% and split 1:4 after reaching 80% confluence, approximately every 4 days.

SkBr3 cells were obtained from ATCC (catalog #HTB-30) and grown in Dulbecco's Modified Eagle's Medium/Ham's Nutrient Mixture F-12 (DME/F12) supplemented with 10% FBS (Omega Scientific, Lot #104021), 10 μM Non Essential Amino Acids (NEAA) (Invitrogen, catalog #11140-050) and a mixture of penicillin (100 U/mL) and streptomycin (100 μg/mL) antibiotics (Invitrogen). Cells were grown at 5% CO2 in a humidified incubator at 37°C. Cells were passaged by rinsing once with PBS, treating with Trypsin-EDTA 0.05% and split 1:4 after reaching 80% confluence, approximately every 4 days.

T47D cells were obtained from ATCC (catalog #HTB-133) and grown in DME/F12 supplemented with 10% FBS (Omega Scientific, Lot #104021), 10 μM NEAA and a mixture of penicillin (100 U/mL) and streptomycin (100 μg/mL) antibiotics. Cells were grown at 5% CO2 in a humidified incubator at 37°C. Cells were passaged by rinsing once with PBS, treating with Trypsin-EDTA 0.05% and split 1:4 after reaching 80% confluence, approximately every 4 days.

MCF-7 cells were obtained from ATCC (catalog #HTB-22). Cells were grown in DMEM supplemented with FBS (Omega Scientific, Lot #104021), 10 μM NEAA, and a mixture of penicillin (100 U/mL) and streptomycin (100 μg/mL) antibiotics. Cells were grown at 5% CO2 in a humidified incubator at 37°C. Cells were passaged by rinsing once with PBS, treating with Trypsin-EDTA 0.05% and split 1:4 after reaching 80% confluence, approximately every 2-3 days.

MCF-10a cells were obtained from ATCC (catalog #CRl-10317) and grown in DME/F12 supplemented with 5% horse serum (Invitrogen, catalog #11965-118), 20 μg/mL epidermal

growth factor (EGF) (Peprotech; Catalog # 100-15), 5 µg/mL hydrocortizone (Sigma; catalog# H-0888), 1 µg/mL cholera toxin (Sigma; Catalog # C-8052),10 µg/mL insulin (Sigma, Catalog # I-1882) and a mixture of penicillin (100 U/mL) and streptomycin (100 µg/mL) antibiotics (Invitrogen). The serum, EGF, hydrocortisone, cholera toxin, and insulin were premixed in 10 mL of DME/F12 and filtered through a 0.2 µ filter. Cells were grown at 5% CO2 in a humidified incubator at 37°C. Cells were passaged by rinsing once with PBS, treating with Trypsin-EDTA 0.05% and split 1:4 after reaching 70% confluence, approximately every 2-3 days.

HMEC cells were obtained from Lonza (catalog #CC-2551). Cells were grown in Mammary Epithelial Basal Medium (MEBM) with BulletKit defined supplements (catalog# CC-3150). Cells were incubated at 37°C in a humid atmosphere of 5% CO2/95% air. Upon reaching 60% confluence (approximately 3-4 days), cells were passaged by rinsing twice with PBS, treating with Trypsin-EDTA 0.05% for up to 8 minutes, and then quenching with and equal volume Defined Trypsin Inhibitor (Invitrogen, catalog# R-007-100). Cells were pelleted in a clinical centrifuge at (175 x g), re-suspended in fresh media and re-plated at a 1:3 ratio.

BT-474 cells were obtained from ATCC (catalog #HTB-20). Cells were grown in RPMI1640 (MSKCC Media Facility) supplemented with 10% FBS (Omega Scientific, Lot #104021), 10 µM Non Essential Amino Acids NEAA and a mixture of penicillin (100 U/mL) and streptomycin (100 µg/mL) antibiotics. Cells were cultured at 5% CO2 in a humidified incubator at 37°C. Cells were passaged by rinsing once with PBS, treating with Trypsin-EDTA 0.05% and split 1:4 after reaching 80% confluence, approximately every 4 days.

Pancreatic Cell Lines

HPDE-E6/E7 human pancreatic duct epithelial cells (HPDE) were provided from Dr. M. Resh Lab (MSKCC), and grown in keratinocyte serum-free medium pre-supplemented with epidermal growth factor (EGF) and bovine pituitary extract (Invitrogen, catalog# 17005-075). Cells were grown at 5% CO2 in a humidified incubator at 37°C. Cells were passaged by rinsing once with PBS, treating with Trypsin-EDTA 0.05% and split 1:4 after reaching 90% confluence, approximately every 2-3 days.

MiaPaCa2 cells were provided by Dr. M. Resh (MSKCC) and grown in DMEM supplemented with 10% FBS, and a mixture of penicillin (100 U/mL) and streptomycin (100 µg/mL) antibiotics. Cells were incubated at 37°C in a humid atmosphere of 5% CO2/95% air. Cells were passaged by rinsing once with PBS, treating with Trypsin-EDTA 0.05% and split 1:4 after reaching 70% confluence, approximately every 2-3 days.

AsPc1 cells were provided by Dr. M. Resh (MSKCC) and grown in DMEM supplemented with 10% FBS, and a mixture of penicillin (100 U/mL) and streptomycin (100 µg/mL) antibiotics. Cells were incubated at 37°C in a humid atmosphere of 5% CO2/95% air. Cells were passaged by rinsing once with PBS, treating with Trypsin-EDTA 0.05% and split 1:4 after reaching 70% confluence, approximately every 2-3 days.

Panc 05.04 cells were provided by Dr. M. Resh (MSKCC) and grown in RPMI1640 supplemented with 15% FBS, insulin (20 U/mL), and a mixture of penicillin (100 U/mL) and streptomycin (100 µg/mL) antibiotics. Cells were incubated at 37°C in a humid atmosphere of 5% CO2/95% air. Cells were passaged by rinsing once with PBS, treating with Trypsin-EDTA 0.05% and split 1:4 after reaching 70% confluence, approximately every 2-3 days.

Other Cell Lines

HEK293T cells were obtained from (ATCC) (catalog #CRL-11268). Cells were grown in Dulbecco's Modified Eagle Medium (DMEM) (Invitrogen, catalog #11995-065) supplemented with 10% FBS (Omega Scientific, Lot #104021) and a mixture of penicillin (100 U/mL) and streptomycin (100 µg/mL) antibiotics (Invitrogen). Cells were grown at 5% CO2 in a humidified incubator at 37°C. Cells were passaged by rinsing once with PBS, treating with Trypsin-EDTA 0.05% and split 1:8 after reaching 80% confluency, approximately every 2-3 days.

Transfections with siRNA and cDNA

Transfection of HEK293T cells with plasmid DNA

2.5x105 cells were seeded in each well of a 6-well cell tissue-culture dish (Nunc, catalog # 140685) and allowed to adhere overnight resulting in approximately 35% confluence the following day. Lipofectamine LTX with Plus reagent (Invitrogen, catalog #15338-100) was mixed with DNA in a 1:1:3 ratio (LTX:Plus:DNA) (v/v/w) typically using 3 µg DNA per the manufacturers instructions in a volume of 200 µL Opti-MEM Reduced-Serum Medium (Invitrogen, catalog #31985-070). The transfection mixture was added dropwise to 2 mL of fresh antibiotic-free media in the well and incubated for 3 hours before replacement with fresh complete growth media including antibiotics.

Transfection of MDA-MB-231 cells with siRNA

2.5 x 105 cells were seeded in each well of a 6-well cell culture dish and allowed to adhere overnight resulting in approximately 30% confluence the following day, when the medium is changed to antibiotic-free (2mL/well). Equal volumes (5 µL) of siRNA (20 µM) and Dharmafect-1 (Dharmacon, catalog# T-2001-03) were independently mixed with 100 µL Opti-Mem in separate 0.6 mL micro-centrifuge tubes and incubated for 5 minutes at room temperature. The contents of the two tubes (210 µL) were mixed gently by pipetting and incubated for 15 minutes at room temperature, and then added dropwise to each well for a final concentration of 50 nM. After overnight incubation (16 hours), the medium was replaced with complete growth media.

Virus Production and Purification

One day prior to transfection, 1.5 x 106 HEK 293T cells were seeded in T-25 cm flasks (Nunc, catalog# 136196) coated with fibronectin (Sigma, catalog# F-0895). Plasmids encoding VSV-G with appropriate gag-pol (pCPG for retrovirus, pDeltaR8.9 for lentivirus) were mixed with the required viral plasmid at a 1:1:3 (µg), respectively. Transfection proceeded as above, using Lipofectamine LTX and Plus reagent, except that after 3-hours the medium and incubator conditions were changed to match the growth requirements for the cells to be infected (indicated above). The medium was collected daily for three days, pooled, centrifuged at 2500 x g for 5 minutes and passed through a 0.45µm filter (Sarstedt). For retroviral gene expression, purified viral supernatants were stored at -80°C in 1 mL aliquots. Purified lentiviral shRNA viral supernatant was concentrated by centrifugation at 28,000 x g (Sorvall RC6 Plus, SS-34 rotor) at 4°C for two hours. The resulting virus pellet was resuspended in 1 mL PBS and stored at -80°C in 100 µL aliquots.

Infection

2.5 x 105 cells were seeded in each well of a 6-well cell culture dish and allowed to adhere overnight resulting in approximately 30% confluence the following day. Viral supernatant or pellets were diluted in each well to 2 mL using antibiotic-free medium supplemented with 8 µg/mL polybrene (Sigma, catalog# H9268). Plates were centrifuged at 900 x g for 30 minutes at room temperature, then the media containing virus was discarded and replaced with fresh complete medium. Antibiotic selection began two days post-infection using 2 µg/mL puromycin (Sigma, catalog# P8833) and continued indefinitely. Control cells died completely after 3 days in selective media.

Table 1: siRNA Duplexes used in this study.

Target	Duplex	Target Sequence
RGNEF	1	GCAAGGAUGCCAAAGAUAA
RGNEF	2	GUGCGUGAAUUAACAGUAU
RGNEF	3	GAUAUUAAACUCUUCCGGA
RGNEF	4	GACUAGCCCUCGGAAUAAA
Tiam2	1	GAACUUCAGGCGUCACAUA
Tiam2	2	CGACCUAAAUUCUGUUCUA
Tiam2	3	GUGUAAGGAUCGCCUGGUA
Tiam2	4	UAAGAGAGCCGUCAUACUG
Tiam2	Plus-11	GAGCACUUCUCCCGGGAAA
Tiam2	A59	GCCUGGUACCUCUUAAGAA
Tiam2	A60	CCAACAUUGUUAAGGUGAU
Tiam2	A61	CCACUGGAGAAAACGUGUA
Cdc42	1	GGAGAACCAUAUACUCUUG
Cdc42	2	GAUUACGACCGCUGAGUUA
Cdc42	3	GAUGACCCCUCUACUAUUG
Cdc42	4	CGGAAUAUGUACCGACUGU
ITSN2	1	GAUCAAACGUGACAAGUUG
ITSN2	2	GACAGGAGCUUCUCAAUCA
ITSN2	3	CCAAACAUGUGGGCUAUUA
ITSN2	4	AAACUCAGCUGGCUACUAU
Dbs	1	AAACAGAGCUGCCCAAUGA
Dbs	2	CGACAUCGCUUUCAAAUUC
Dbs	3	UCAAGGAAAUGCUGAAAUA
Dbs	4	CAACAGGCCUUCACAACAA
Fgd6	1	GCUCAAAGAUGCCUUAAUA
Fgd6	2	GAAUUCCGAGUCUAAAGUA
Fgd6	3	GCUCGUCUGUUACGCCAAA
Fgd6	4	GAUUGAAAGUGUAGAACGU
DOCK5	1	AGAACUAUCUAAUUCGUUG
DOCK5	2	GUAACGGGAUGCCCAAGGA
DOCK5	3	GAGUGGCAGUGAUGGAUAU
DOCK5	4	UAUCAUACAUGGGAAGGUG

Table 2: Short hairpin shRNA used in this study.

Name	Clone ID	Target Sequence	Hairpin Sequence
Tiam2 sh-10	TRCN0000107210	GCCCTACTAAAGACATC-GAAA	5'-CCGG-GCCCTACTAAAGA-CATCGAAA-CTCGAG-TTTCGAT-GTCTTTAGTAGGGC-TTTTTG-3'
Tiam2 sh-11	TRCN0000107211	CCACTTCAGAATGAGA-CCTTT	5'-CCGG-CCACTTCAGAATGAGA-CCTTT-CTCGAG-AAAGGTCT-CATTCTGAAGTGG-TTTTTG-3'
Tiam2 sh-12	TRCN0000107212	CCTTTCTCACTTTA-AGAGTAA	5'-CCGG-CCTTTCTCACTTTA-AGAGTAA-CTCGAG-TTACTCT-TAAAGTGAGAAAGG-TTTTTG-3'
Tiam2 sh-13	TRCN0000107213	CCCTTGACAGTCAGTCT-GAAA	5'-CCGG-CCCTTGACAGT-CAGTCTGAAA-CTCGAG-TTTCAGACTGACTGTCAAGGG-TTTTTG-3'
Tiam2 sh-14	TRCN0000107214	CCTTTATTACGCGGAC-CACTT	5'-CCGG-CCTTTATTACGCGGAC-CACTT-CTCGAG-AAGTGGTCC-GCGTAATAAAGG-TTTTTG-3'
pLKO.1	TRCN0000208001	CCGGACACTCGAG-CACTTTTTG	N/A

Tumor growth and Metastasis

Modified Boyden Chamber Transwell Invasion Assay

BD BioCoat Matrigel Invasion Chambers (24-well, 8-µm) (BD Biosciences, catalog# 354480) were rehydrated with 500 µL additive-free L-15 media in the upper and lower chambers for 2 hours prior to the desired start time. MDA-MB-231 cells were trypsinized in 400 µL trypsin for 5 minutes followed by the addition of 1 mL complete media and agitation by pipetting to disrupt cell aggregates. A 50 µL aliquot of cells was counted using a Coulter counter (Beckman). Cells were pelleted in a clinical centrifuged for 4 minutes at 175 x g, and re-suspended in enough serum-free media to achieve a concentration of 4 x 105 cells/mL.

The medium remaining in the upper chamber of the transwell insert was carefully aspirated using a glass Pasteur pipette, leaving the hydrated Matrigel undisturbed. Inserts were placed into a single well of the provided 24-well plate after the addition of 750 µL of complete medium. Into the top chamber, 500 µL of the re-suspended cells were pipetted, resulting in 2 x 105 cells total. The inserts were inspected for the presence of bubbles (removed by pipetting), and then the complete plate was incubated overnight.

After 16 hours, the medium was carefully aspirated from both sides of the insert using a Pasteur pipette, being careful not to touch the lower surface. Two cotton-tipped swabs (Fisher, catalog# 23-400-119) were used to completely remove any remaining Matrigel from the inner surface of the insert. Inserts were fixed for 10 minutes in neat methanol, stained for 15 minutes (1% methylene blue, 1% sodium borate (w/v) in water), rinsed twice in water and allowed to dry at room temperature.

Imaging and quantification of invasion membranes

Cursory scans of the inserts were made by using a flatbed scanner and visually inspected for artifacts. For accurate quantification, membranes were scanned using the 5x phase-contrast objective of a Zeiss Axiovert 200 equipped with a motorized stage controlled by Axiovision v4.7 software. Mosaic images of the inserts were aligned and stitched together automatically using the same software resulting in a single image of the entire insert (approximately 9000 pixels2). Quantification was performed using Metamorph software to first convert the image to black and white using a single empirically determined threshold value which yields an image where the area of an invaded cell is black and the background is white. Then, the ratio of black-to-total pixels is calculated. A high number indicates more invasion than a lower number. The amount of invasion is normalized by expression as a percentage of control, which allows comparison between experiments.

Wound-Healing Scratch Assay

Cells are seeded in 6-well dishes at 2.5 x 105 for siRNA treatment, and 5 x 105 for stable lines and allowed to reach confluence (usually after 3-4 days). In a tissue culture hood, the cells are scratched using a P-10 pipette tip (0.5 μm) vertically across the entire diameter of the well. The medium is then exchanged to remove floating debris. Cells are returned to the incubator overnight, or imaged by time-lapse microscopy using a Zeiss Axiovert 200 equipped with a motorized stage and XL-3 incubator at 37% and appropriate CO2 levels. The width of the wound was measured at zero and 18 hours using a 10x phase objective on an Axiovert 200 microscope with Axiovision acquisition software.

Tumor Colony Formation Assay – Soft Agar

MDA-MB-231 cells stably expressing shRNA were counted using a coulter counter and 2 x 104 were suspended in 350 μL warm complete medium containing 0.4% bacto-agar.

The total volume was carefully layered onto a bed of 350 µL 0.6% soft agar in the center 8 wells of a 24-well plate (Nunc). The outer wells were filled with sterile distilled water to avoid edge effects. Medium was changed twice weekly. After 3 weeks, plates were stained with MTT ([3-(4,5-dimethylthiazol-2-yl)- 2,5-diphenyltetrazolium bromide) and colonies larger than 0.5 µm were quantified using a Gelcount automated colony counter scanner (Oxford Optronix).

FACS cell cycle analysis

Trypsinized cells were fixed in 70% ethanol at 4°C overnight. Cells were washed twice with PBS, stained with a mixture of 0.2 mg/ml propidium iodide (Sigma, catalog# P4170), 0.2 mg/ml RNAase A (Qiagen, catalog# 19101), and 0.1% Triton X-100 (Sigma, catalog# T8787). Samples were analyzed on a FACSCalibur (BD Biosciences) instrument by the MSKCC flow cytometry core facility.

Molecular Biology

Table 3: DNA constructs shRNA used in this study.

Insert Name	Source	Vector
STEF-FL	M. Hoshino	pBabe-HA
STEF-ΔN	M. Hoshino	pBabe-HA
STEF-PHnTSS	M. Hoshino	pBabe-HA
Tiam1	Open Biosystems	pCR-XL-TOPO
Tiam2	Open Biosystems	pCR-XL-TOPO
Tiam2	J. Smith	pBabe-HA
Tiam2-AB	J. Smitih	pBabe-HA
Tiam2-CD	J. Smith	pBabe-HA

DNA agarose gel electrophoresis

0.8% agarose gels were prepared by mixing 800 mg agarose (Sigma) in 100 mL TAE (40 mM Tris-acetate, 1 mM EDTA pH 8) and boiling in a microwave oven. Ethidium bromide (Sigma) was then added for a final concentration of 500 ng/mL and the gel was allowed to polymerize for 45 minutes. 8x DNA loading buffer consisted of 50% glycerol (v/v), 0.1% bromophenol blue (w/v), and 0.1% xylene cyanol (w/v) and was mixed with DNA samples to achieve 1x final loading dye concentration. Gels were run for approximately 1 hour at 120 V in TAE buffer with 1 ng/mL ethidium bromide until adequate separation was achieved and the bands revealed using a UV transilluminator.

Site Directed Mutagenesis

Mutagenesis of cDNA was performed using overlap-extension two-step polymerase chain reaction (PCR) using Phusion high-fidelity DNA polymerase (Finnzyme, catalog# F-530L). Overlapping primers (50 pmol) (Integrated DNA Technologies) with the desired mutations were designed to bidirectionally amplify the necessary fragment of template DNA (1 ng) with a complimentary specific primer matching the opposite end of the desired region. Samples were placed on an Eppendorf Mastercycler Gradient and cycled 30 times with the following parameters: 10 seconds at 98°C, 30 seconds at 55-75°C annealing, 60 seconds at 72°C (with 30 second initial 98°C denaturation and final 10 minute 72°C elongation). The full PCR reaction was loaded onto a 1% agarose gel, separated by electrophoresis (125 V, 45 mins), and purified using a QIAquick Gel Extraction Kit (Qiagen, catalog# 28706) following manufacturers directions using 20 µL sterile water for elution.

A second round of PCR was performed using 5 µL of each PCR product from the first-round reactions as template. The outermost primer sets are used in the same conditions as the previous reaction resulting in a full-length product harboring the desired mutations.

After purification as above and eluting in 30 μL sterile water, the fragment was directly cloned into a shuttle vector for sequencing using a Zero Blunt® TOPO PCR Cloning Kit (Invitrogen, catalog# K2830-20). The sequence was verified (MSKCC sequencing facility) and then the insert was sub-cloned into the desired vector.

Sub-cloning was performed by digesting 15 μL of mini-prepped plasmid DNA in the Topo vector with appropriate restriction enzymes (New England Biolabs). The destination vector was similarly digested and both were separated via agarose gel electrophoresis, gel purified, and eluted in 20 μL sterile water. The insert and vector were ligated using 10 μL Mighty Mix DNA Ligation Kit (TaKaRa, catalog# 6023) mixed with 7 μL insert and 3 μL vector for 1 hour at 18 °C. After ligation, 10 μL of the reaction were used to transform 50 μL of Subcloning Efficiency DH5α competent E. coli (Invitrogen, catalog# 18265-017).

Plasmid DNA Purification & Quantification

Plasmid DNA was purified from E. coli using one of two methods. Small amounts (approximately 12 μg) were purified from 3 mL culture using the QIAprep Spin Miniprep Kit (Qiagen, catalog# 27106). Large amounts (approximately 650 μg) were purified from a 250 mL culture using the QIAfilter Plasmid Maxi Kit (Qiagen, catalog# 12263). DNA was eluted in TE buffer and stored at 4°C. Quantification (A260) and quality (A260/A280) were determined by UV spectroscopy using a NanoDrop 2000.

Quantitative PCR

Total cellular RNA was isolated from cells in each well of a 6-well dish using the RNAeasy Mini kit (Qiagen, catalog# 74104) and QIAshredder columns (Qiagen, catalog# 79656) following manufacturer instructions. SuperScript III One-Step RT-PCR kit (Invitrogen, catalog# 12574-026) was used to perform reverse transcription-PCR using 200 ng RNA

primed by random hexamers. Taqman reagents were used to perform quantitative PCR using an Applied Biosystems 7500 Real-time PCR instrument in 384-well format (samples loaded in triplicate). TaqMan probes used were: Hs99999905_m1 amplifies GAPDH, Hs00608460_m1 amplifies Tiam2 (long and short), and Hs01076261_m1 amplifies Tiam2 (long only).

Sequencing MDA-MB-231 endogenous Tiam2

Total cellular RNA was isolated as above and reverse transcribed by the Genomics Core Lab (GCL) at MSKCC. Nine primer pairs were designed by Dr. Agnes Viale (GCL) to amplify nine approximately 1000 bp of overlapping fragments of the Tiam2 transcript. Fragments were amplified by PCR [98° 30 sec; 30x 98°C 10 sec, 64°C 30 sec, 72°C 1 min; 70°C 10 min, 4°C hold] and separated on a 1% agarose gel. Fragments of the predicted size were directly sequenced by the MSKCC sequencing facility and SNPs identified by comparison to reference sequence NM_012454.3.

Table 4: Primer Pairs for Tiam2 Sequencing

Pair Name	Primer Name	Primer Sequence
Set 1	Set 1 Top	CTGACGGAAGCACTAAAGGCAAT
	Set 1 Bottom	TGGTGACGGATCTGCGCCT
Set 2	Set 2 Top	AGAGTGACATCCTGAGCGATGAA
	Set 2 Bottom	CTTATTTTCCTTTTACTATACAGCTTGG
Set 3	Set 3 Top	GGCTCTGTGTATGAATGACAAGG
	Set 3 Bottom	CCAGCGTTTTGATGAGCACTC
Set 4	Set 4 Top	AACGCTGGGGAAGCTGGAT
	Set 4 Bottom	TTCTATGTTCTCAGTGTTGGTCCT
Set 5	Set 5 Top	GACTACTTTGACAGTCGCTCTGA
	Set 5 Bottom	TTCTCAAGATTCTGCTCCCA
Set 6	Set 6 Top	CAGAAGACAGCATAGTGCAGTCTG
	Set 6 Bottom	GATCCCTACAGTAACTCCGTGA
Set 7	Set 7 Top	GCATCTTGTCTGTTTCCTCTTTCCA
	Set 7 Bottom	AGGAGGGGGCAGCAGACTCTT
Set 8	Set 8 Top	AGGTGGATGAGCGTCAGCATC
	Set 8 Bottom	CCAAAAAGTGACTCCATCTCATCT
Set 9	Set 9 Top	TCATCCAGGAGCTTGTGGACA
	Set 9 Bottom	TCAGAAGCTCTCCCATCGAAAGT

Protein Biochemistry

Cell Lysate Preparation

Cells were rinse once in ice-cold PBS and lysed by scraping in ice-cold 100 µL buffer containing 150 mM NaCl, 50 mM Tris-base pH 8, 1% NP-40, 50 mM NaF, 0.1% SDS, 0.5% sodium deoxycholate (Sigma), and Complete Protease Inhibitor cocktail (Roche, catalog# 11-836-153-001). Lysates were cleared by centrifugation at 28,000 x g for 5 minutes at 4°C. Protein concentration was determined using the DC Protein Assay Kit II (Bio-Rad, catalog# 500-0112) and a Synergy 2 plate reader (BioTek) in 96-well format. For samples that are probed with phospho-specific antibodies, the lysis buffer was supplemented with β-Glycerophosphate (to 10 mM) and sodium orthovanadate (to 100 µM). After quantification, the soluble fraction was mixed with 6x LSB protein sample buffer (50 mM Tris-HCl pH 6.8, 10% (v/v) glycerol, 2% (w/v) SDS, 100 mM DTT, 100 mM β-mercaptoethanol, 0.1% (w/v) bromophenol blue).

Western blot analysis

Lysates were loaded onto 3-8% NuPAGE Tris-Acetate gel system (Invitrogen) using Tris-Acetate SDS Running Buffer and electrophoresed at 150 V for 60 minutes at room temperature. Following separation, gels were transferred onto nitrocellulose membrane (Whatman) in a solution of NuPAGE transfer buffer (Invitrogen, catalog# NP00061) supplemented with 10% methanol for 1 hour at 4°C under constant 400 mA current. Membranes were briefly washed in water, followed by blocking with TBS (Fisher, catalog# BP2471-1) containing 0.1% Tween-20 (Sigma, catalog# P1379) and 1% (w/v) dry milk. Primary antibodies were incubated overnight at 4°C with TBS containing 0.1% Tween-20 (TBS-T) on a rocking platform. Three washes in TBS-T (5 minutes each) preceded incubation with HRP-conjugated secondary antibodies of appropriate species for 45 minutes at room temperature on an orbital shaker. Three more five minute TBS-T washes followed, and then

a one minute rinse in pure distilled water to remove detergent. Proteins were revealed using ECL Western Blotting Detection Reagents (GE Healthcare, catalog# RPN2209) for all proteins except Tiam2, which required SuperSignal West Dura extended duration substrate (Thermo Scientific, catalog# 34076) for 1 minute and then exposing to Amersham Hyperfilm (GE Healthcare, catalog# 28906837).

GTPase Pulldown

The E. coli strain BL21 DE3 pLysS transformed with the plasmid pGEX-PAK CRIB was grown overnight at 37°C in 100 ml Lysogeny broth (LB) containing 100 µg/mL ampicillin and 25 µg/mL chloramphenicol (Amp/Chlor) inside a shaking incubator. The next day, 50 mL of the culture was added to 450 mL LB and grown for 2 hours at 30°C. To induce protein production, isopropyl β-D-1-thiogalactopyranoside (IPTG) was added to a final concentration of 0.5 mM for 5 hours. The bacteria was pelleted by centrifugation at 4700 x g at 4°C in a conical tube (Corning, catalog# 430776), and supernatant removed by careful decanting. Pellets were stored at -80°C after snap freezing in liquid nitrogen.

Pellets were thawed on ice and resuspended by vigorous pipetting in 20 mL GTLB I buffer (50 mM Tris pH 8.0, 40 mM EDTA pH 8.0, 25% sucrose, 1 mM PMSF, Complete Protease Inhibitors). Lysis was accomplished by addition of 8 mL GLTB II buffer (50 mM Tris pH 8.0, 100 mM MgCl2, 0.2% Triton X-100, 1 mM PMSF, Complete Protease Inhibitors) and incubaton at 4°C for 10 minutes with rotation. Genomic DNA was sheared by sonication in a ice water bath using short (3-5 second) pulses separated by 30 seconds of rest to allow cooling until the solution was no longer viscous but before becoming opaque. Lysates were clarified by centrifugation in an Oak Ridge Tube (Nalgene, catalog# 3119-0050) at 12,000 x g at 4°C for 45 minutes. The supernatant was carefully pipetted without disturbing the pellet into a clean 50 mL conical tube containing 1 mL glutathione agarose beads (Sigma, catalog# G4510) (50% slurry in water) and rotated at 4°C for 1 hour to bind GST-PAK

CRIB. Beads were then washed four times in 5 mL wash buffer (50 mM Tris pH 7.6, 50 mM NaCl, 5 mM MgCl2, 1 mM PMSF, Complete Protease Inhibitors) and resuspended in 1 mL wash buffer supplemented with 25% glycerol. 100 µL aliquots were stored at -80°C.

Stably transfected MDA-MB-231 cells were seeded at 2.5 x 105 cells/well in 6-well dishes, and starved in serum-free media for 48 hours. Cells were treated with 100 ng/mL EGF in pre-warmed serum-free medium for 4 minutes and then immediately rinsed with ice-cold TBS on ice followed by addition of 500 µL lysis buffer (50 mM Tris pH 7.6, 1% Triton X-100, 0.5% Na-DOC, 0.1% SDS, 500 mM NaCl, 50 mM MgCl2, 1 mM PMSF, Complete protease inhibitors). Cells were gently scraped and lysates were cleared by centrifugation at 28,000 x g for 5 minutes at 4°C. A 25 µL aliquot is removed and 6x LSB added to serve as 5% input. The remainder of the lysate was added to a 5 µL aliquot of the previously prepared GST-PAK CRIB beads and incubated on a rotator at 4°C for 40 minutes. The beads were washed four times with 1 mL wash buffer (50 mM Tris pH 7.6, 1% Triton X-100, 500 mM NaCl, 50 mM MgCl2, 1 mM PMSF, Complete Protease Inhibitors) on ice, and then pelleted at 900 x g at 4°C for 2 minutes. Finally, 25 µL 2x LSB was added to the beads and then boiled for 5 minutes and analyzed by western blot using a 4-12% Bis-Tris gel using MES running buffer (Invitrogen, catalog# NP0002). [167]

Table 5: Antibodies used in this study All primary antibodies used for western blot analysis and immunofluorescence microscopy are listed with working concentrations. In some cases the concentration is not known, and the working dilution is given. Poly: polyclonal. WB: western blot.

Antibody	Host	Clone	Source	Catalog #	Stock (µg/mL)	WB Dilution (µg/mL)
α-tubulin	rat	YL1/2	Serotec	MCA77S	n/a	0.736111111
HA	rat	3F10	Roche	1867423	100	0.1
Cdc42	mouse	44	BD Transduction	610929	250	0.25
RhoA/C	rabbit	poly	Santa Cruz	sc-179	200	1
Rac	mouse	23A8	GeneTex	GTX13048	50	0.1
β-actin	mouse	AC-74	Sigma	A5316	1700	0.085
ITSN2	mouse	poly	Abnova	H00050618-A01	n/a	1:1000
Tiam1	rabbit	poly	Santa Cruz	sc-872	200	0.2
Dock5	rabbit	poly	Hall Lab	n/a		1:1000
Tiam2	rabbit	poly	Sigma Prestige	HPA013903	110	0.073
Fam13a	rabbit	poly	Sigma Prestige	HPA038109	250	0.25
Dbs	mouse	poly	Abnova	H00023263-M01	1000	0.5

Mouse Xenograft

All animals were maintained under the care and supervision of the MSKCC Research Animal Resource Center (RARC) and all work adhered to the proper IACUC protocols.

Tumor Cell Injections

Virgin Female NOD.CB17-Prkdcscid/NcrCrl (NOD/SCID) mice were used for orthotopic tumor injection at 5 weeks old (Charles River, strain code 394). MDA-MB-231 cells stably expressing Tiam2 shRNA or non-targeting control were grown in 15 cm plates (Nunc). Next, cells were trypsinized and pelleted at 125 x g for 5 minutes in a conical tube. Cells were resuspended in 5 mL PBS, counted using a Coulter counter, pelleted again, and resuspended in enough cold sterile PBS to reach 4 x 107 cells/mL. Mice were anesthetized using 100 mg/mL ketamine in sterile PBS, allowing the mammary fat pad to be exposed via incision with sterile scissors. Immediately prior to injection, an equal volume of Matrigel was added to the cells and 40 μL of the resulting mixture was injected bilaterally into the posterior fat pad using a 20G needle resulting in 2 injections per mouse of 8 x 105 cells per mammary fat pad. The wound was closed using 7 mm metal clips (Alzet, catalog# 0009972), and the mice were monitored until regaining consciousness and again after 24 hours.

Tumor Proliferation

Mice were monitored weekly for the presence of tumors by palpation. After 11 weeks, animals were sacrificed by asphyxiation under CO2 for 5 minutes and the tumors were dissected, photographed, and weighed. Additionally, the lungs were dissected to inspect for evidence of metastasis. A small portion of the tumor was separated using a scalpel and used to generate tumor derived cell lines. The lungs and remainder of the tumor were rinsed in PBS, fixed overnight in 4% PFA (paraformaldehyde) in PBS on a rotator at 4°C, then washed twice again in PBS and stored in 70% ethanol at 4°C.

Tumor Derived Cell Lines

A small portion of the tumor (approximately 0.2 g) was minced in a tissue culture hood using sterile scalpels in a 10 cm tissue culture dish (Nunc) and transferred to a 50 mL conical tube. Tissues were digested in 5 mL DMEM containing 15 units Collagenase 3 (Worthington Biochemical, catalog# CLS-3) and 20 units Liberase (Roche, catalog# 05401119001) for 3 hours at 37°C in a humidified incubator. Digested tissue was pipetted vigorously, then pressed through a 40 μm cell strainer (BD Falcon, catalog# 352340) with a cell scraper (Costar, catalog# 3008) into a 10 cm dish. Complete DMEM was added to a volume of 10 mL and the cells incubated overnight at 37°C in a humid atmosphere of 5% CO2. Medium was exchanged daily for 3 days at which time cells were cultured as MDA-MB-231 cells and switched to complete L-15 media with appropriate culture conditions.

Chapter 3: RNAi Screens to Identify Rho GEFs and GAPs Required for Breast Cancer cell Invasion

Overview

Metastatic spreading of cancer cells from the site of formation into the surrounding tissue and the rest of the body is the major cause of cancer-related deaths. Understanding the invasive process that cancer cells use to disseminate into the body is critical in designing new therapies to prevent metastasis. Rho GTPases play a central role in regulating the cytoskeletal reorganization necessary for cancer cells to successfully intravasate from the primary tumor into the circulatory system, eventually extravasating into a new metastatic niche. The aim of this project was to elucidate the upstream regulators that mediate Rho-family dependent invasion, and to gain mechanistic insight into the process of invasion. A cell culture system allows for straightforward manipulation of the molecular regulators of Rho GTPases and provides a relatively straightforward assay to evaluate the invasive capacity of different cell types. In this study, a modified Boyden chamber system is used to model breast cancer invasion to identify which Rho family GEFs and GAPs are necessary for invasion.

MDA-MB-231 Cells model breast cancer cell invasion

MDA-MB-231 cells were isolated from an epithelial breast adenocarcinoma in 1973 from the pleural effusion of a 51-year-old Caucasian female at MD Anderson Cancer Center. [168] These cells are basal-type triple-negative (ER/PR/Her2) and harbor an activating K-Ras mutation. Furthermore, they are highly invasive both in vitro and in vivo, making them a suitable model in which to perform a loss-of-function screen for regulators of invasion. [169, 170] In contrast, most other breast cancer cell lines form tumors when studied in vivo, but do not exhibit invasive behavior in vitro. For these reasons, and because they

can be efficiently transfected with siRNA, I chose this cell line to perform a siRNA based screen to study the role of Rho family GTPases and their associated GEF and GAP regulators in breast cancer cell invasion.

Screening of GTPases

The Rho family small GTPases are major regulators of the actin cytoskeleton. The three best studied members, RhoA, Rac1, and Cdc42, control actin rearrangement that mediates changes in cell shape, size, polarity, and migratory capacity. [13, 85, 90] To explore whether these GTPases are required for MDA-MB-231 cells to maintain invasiveness, RNAi was used to deplete endogenous proteins and the effects on invasion through Matrigel determined using a modified Boyden chamber. Cells were transfected overnight at low density with siRNA SMARTpools targeting RhoA, RhoC, Rac1, or Cdc42. After 96 hours, cells were loaded on top of a layer of Matrigel in serum-free medium inside an invasion chamber and allowed to invade toward the lower chamber, which was filled with medium containing serum as a chemoattractant. After 16 hours, cells that had invaded through the chamber were fixed, stained, and the amount of invasion determined qualitatively by scanning, or quantitatively by microscopy (see materials and methods).

Rho: Depletion of RhoA protein by the siRNA SMARTpool reduced the ability of cells to invade through Matrigel to 25% of the level of the siGLO control (Figure 4). Western blot analysis revealed that the RNAi successfully lowered the levels of endogenous RhoA protein (Figure 4, Panel B). Cells treated with the siRNA SMARTpool targeting RhoC reduced invasiveness only modestly to 75% of control levels. Unfortunately, the level of RhoC protein remaining after treatment with siRNA could not be determined since unlike RhoA, no antibody is available specifically for this isoform. Surprisingly, depletion of RhoC appears to reduce the level RhoA. This observation could indicate that the RhoA antibody cross-reacts with RhoC, or that the RhoC siRNA SMARTpool also targets RhoA due to

the high level of sequence identity in the corresponding mRNAs. Curiously, transfection with RhoA siRNA SMARTpool caused a moderate depletion of Cdc42 (and vice versa) as demonstrated by western blot (Figure 4, Panel B). One explanation for this may be linked to RhoGDI, which interacts with all Rho GTPases. [171] Overexpression of one GTPase has been reported to result in degradation of other GTPases by competing for a limited amount of RhoGDI. However, this could not account for the results observed after depletion of a GTPase. Perhaps the decrease in GTPase levels was due to an off-target effect of the siRNA, or other factors that affect the relative levels of Rho family GTPases.

Rac: Transfection of MDA-MB-231 cells with a siRNA SMARTpool targeting Rac1 did not significantly reduce the number of cells that invaded through Matrigel. However, western blots showed no change in the level of total endogenous Rac protein (Figure 4). Repeat experiments with different siRNA reagents were also unable to effectively reduce Rac levels. The study of Rac is further confounded by the lack of antibodies specific for each of the three known isoforms.

Cdc42: Depletion of Cdc42 protein by a siRNA SMARTpool reduced the ability of MDA-MB-231 cells to invade through Matrigel to <5% of the level of siGLO control (Figure 4). Western blot analysis revealed that protein levels were strongly reduced compared to the siGLO control (Figure 4, Panel B). This clear reduction in both protein level and number of invaded cells suggests that Cdc42 may play an important role in controlling invasion in MDA-MB-231 cells. To test whether this phenotype is due to the specific depletion of Cdc42, each of the siRNA duplexes comprising the SMARTpool was individually transfected into cells and then assayed for invasiveness and protein expression (Figure 5). All four of the individual duplexes caused a significant reduction in the number of invading cells in addition to nearly complete depletion of endogenous protein. All four duplexes, each targeting a unique sequence in Cdc42 mRNA, reduced both protein levels and num-

ber of cells invaded, supporting a role for Cdc42 in MDA-MB-231 cell invasion. Since the Cdc42 phenotype is robust, it was used in subsequent experiments as a positive control for inhibition of invasion when screening for GEFs and GAPs that potentially regulate invasion in MDA-MB-231 cells.

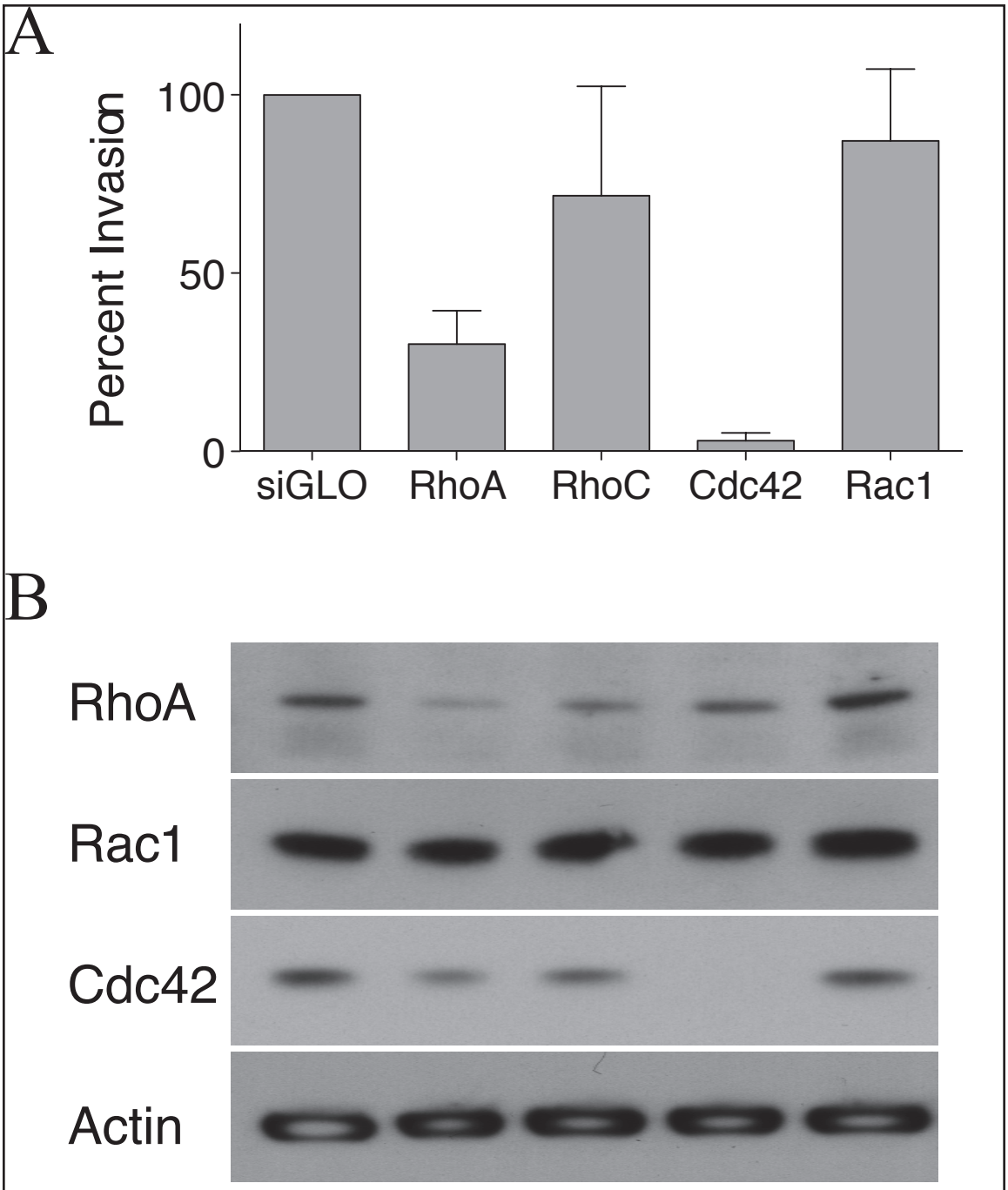

Figure 4: Rho GTPase depletion inhibit invasion

MDA-MB-231 cells were transfected with indicated SMARTpool siRNA or siGLO positive control. (A) Quantitation of scanned invasion filters expressed as a percentage of siGLO control. (C) siRNA depleted MDA-MB-231 cells were lysed analyzed by western blot with the indicated antibodies. Left to right, loaded samples are siGLO, RhoA, RhoC, Cdc42, and Rac1.

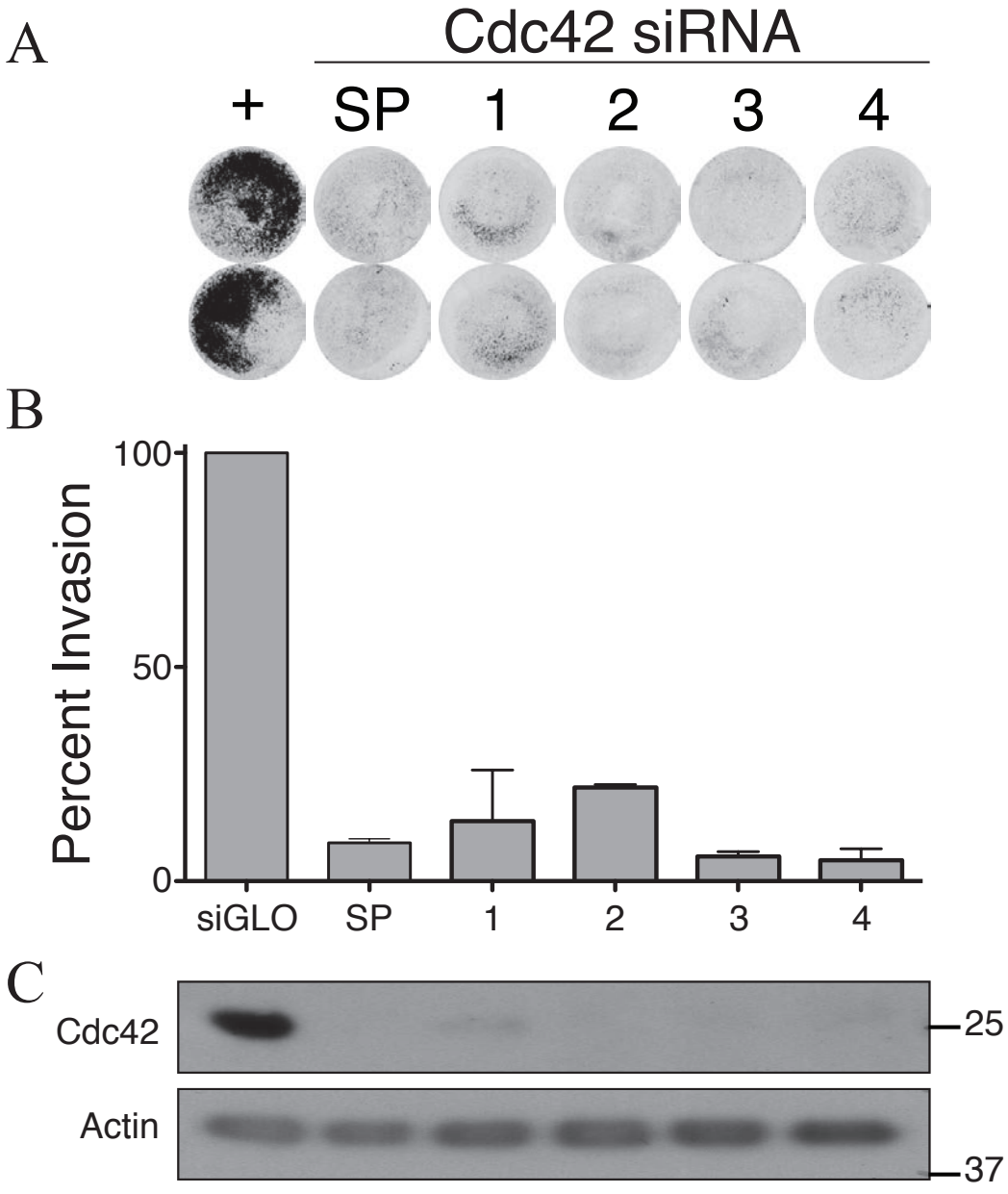

Figure 5: Cdc42 depletion inhibits invasion

MDA-MB-231 cells were transfected with indicated siRNAs and control (+) siGLO. (A) Invasion filter scans of MDA-MB-231 cells after invasion through matrigel for 16 hours. Filters were fixed and stained with methylene blue. (B) Quantification of 3 invasion experiments. (C) siRNA depleted MDA-MB-231 cells were lysed analyzed by western blot with the indicated antibodies.

Table 6: GEF siRNAs screened in this study

#	Name	Accession #	Alternative Name(s)
1	SWAP70	NM_015055	
2	SGEF	NM_015595	ARHGEF26
3	PREX1	NM_020820	
4	GEFT	NM_133483	p63 RhoGEF
5	ARHGEF16	NM_014448	NBR, neuroblastoma
6	ARHGEF10L	NM_018125	GrinchGEF
7	FGD6	XM_370702	
8	DNMBP	NM_015221	Tuba
9	MCF2	NM_005369	Dbl
10	MCF2L	NM_024979	Dbs, ARHGEF14
11	DOCK4	NM_014705	
12	DOCK5	NM_024940	
13	DOCK6	NM_020812	
14	DOCK7	NM_033407	
15	DOCK8	NM_203447	
16	NGEF	NM_019850	Ephexin
17	FGD2	NM_173558	
18	SPATA13	NM_153023	Asef2
19	MCF2L2	NM_015078	
20	DEF6	NM_022047	IBP
21	FGD4	NM_139241	Frabin
22	ARHGEF19	NM_153213	
23	FGD3	NM_033086	
24	DOCK10	XM_371595	
25	PLEKHG5	NM_020631	
26	DOCK9	NM_015296	
27	AKAP13	NM_006738	Lbc
28	LOC351864	XM_302177	*removed*
29	ECT2	NM_018098	
30	FARP1	NM_005766	
31	FARP2	XM_376193	CDEP
32	ABR	NM_001092	FRG
33	ALS2	NM_020919	
34	ARHGEF3	NM_019555	Alsin
35	ARHGEF4	NM_015320	Asef
36	ARHGEF10	NM_014629	
37	ARHGEF15	NM_173728	Vsm-RhoGEF

#	Name	Accession #	Alternative Name(s)
38	BCR	NM_004327	
39	PLEKHG2	NM_022835	Clg
40	DOCK1	NM_001380	DOCK180
41	DOCK2	NM_004946	
42	DOCK3	NM_004947	
43	PLEKHG6	NM_018173	
44	NET1	NM_005863	
45	ARHGEF39	NM_032818	
46	ARHGEF38	NM_017700	
47	ITSN1	NM_003024	Intersectin1
48	ITSN2	NM_006277	Intersectin2
49	ARHGEF12	NM_015313	Larg
50	ARHGEF2	NM_004723	GEF-H1
51	Obscurin	XM_290923	
52	ARHGEF18	NM_015318	p114-RhoGEF
53	ARHGEF1	NM_004706	p115-RhoGEF
54	ARHGEF17	NM_014786	p116-RhoGEF
55	ARHGEF11	NM_014784	PDZ-RhoGEF
56	ARHGEF9	XM_377014	Collybistin, h-PEM2
57	ARHGEF6	NM_004840	α-PIX
58	ARHGEF7	NM_003899	β-PIX
59	RASGRF1	NM_002891	
60	RASGRF2	NM_006909	
61	SOS1	NM_005633	
62	SOS2	NM_006939	
63	TIAM1	NM_003253	
64	TIAM2	NM_012454	
65	ARHGEF5	NM_005435	TIM
66	TRIO	NM_007118	
67	VAV1	NM_005428	
68	VAV2	NM_003371	
69	VAV3	NM_006113	
70	FGD5	XM_371619	
71	PLEKHG1	XM_027307	
72	RGNEF	XM_371755	p190-RhoGEF
73	ARHGEF40	XM_370737	SOLO
74	PLEKHG4B	NM_052909	
75	PLEKHG7	NM_001004330	

#	Name	Accession #	Alternative Name(s)
76	LOC401147	XM_376334	*removed*
77	ECT2L	XM_294019	
78	DOCK11	NM_144658	
79	FGD1	NM_004463	
80	KALRN	NM_003947	Duet
81	PLEKHG4	NM_015432	
82	PLEKHG3	NM_015549	

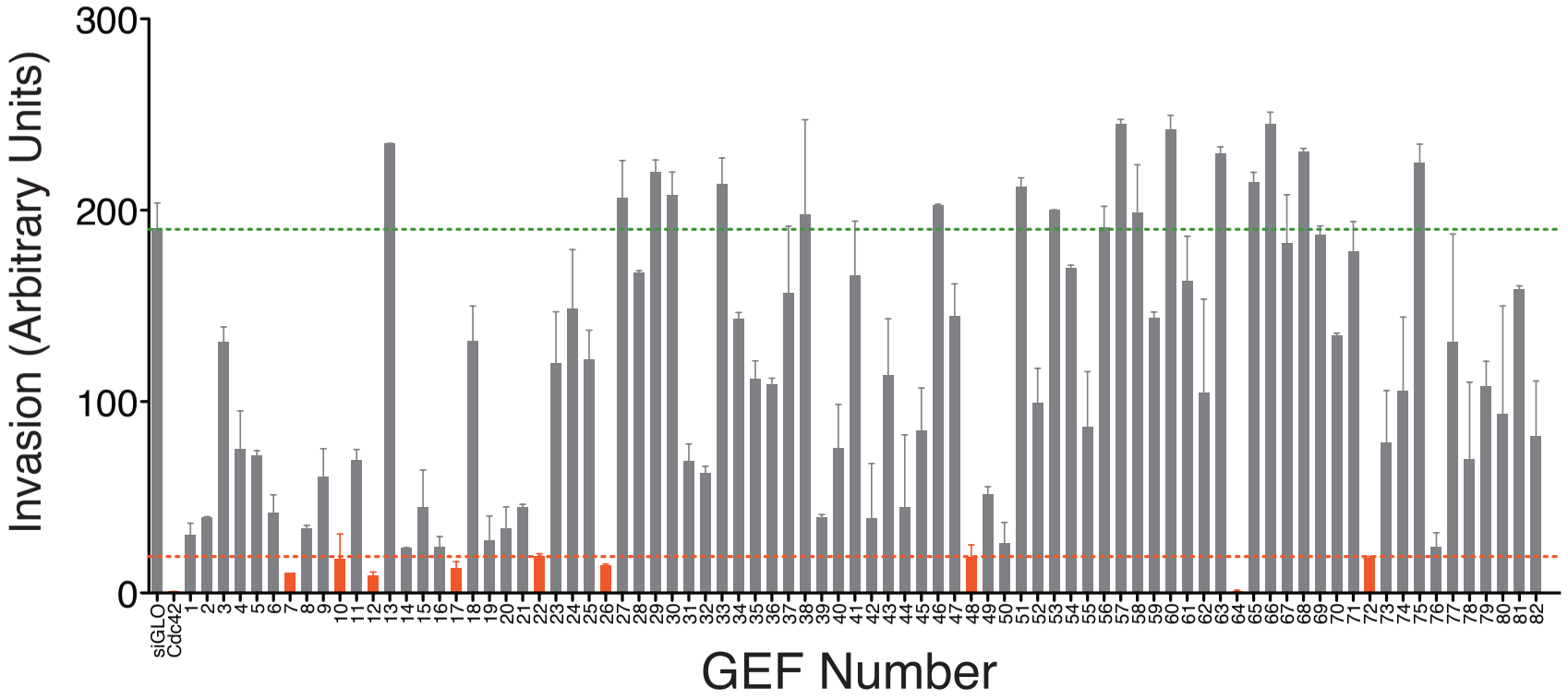

Figure 6: GEF Screen Results

MDA-MB-231 cells were transfected with indicated siRNA (see Table of GEFs) in addition to Cdc42 (positive) and siGLO (negative) controls. (A) Quantitation of scanned invasion filters. Red line is threshold to consider as a hit, Green line is the siGLO control for full invasion.

Screening of GEFs

To identify regulators of Rho family GTPases required for invasion, I screened a library of siRNA SMARTpools targeting the 82 known human GEFs. Each SMARTpool was transfected into MDA-MB-231 cells and were incubated for 4 days, before being assayed for invasive capacity using a modified Boyden chamber coated with Matrigel. Cdc42 was used as a positive control and siGLO was used both as a negative control and as a marker of transfection efficiency (Figure 6). To select candidates that have a strong effect on invasion, the threshold for an "inhibition of invasion" phenotype was set at 10% of siGLO control (double the invasion of the Cdc42 positive control), which identified nine potential candidates: Tiam2, Dbs, DOCK4, Fgd6, Fgd2, Fgd4, RGNEF, ITSN2, and ARHGEF19. These initial candidates were subjected to a second round of screening to confirm the initial result.

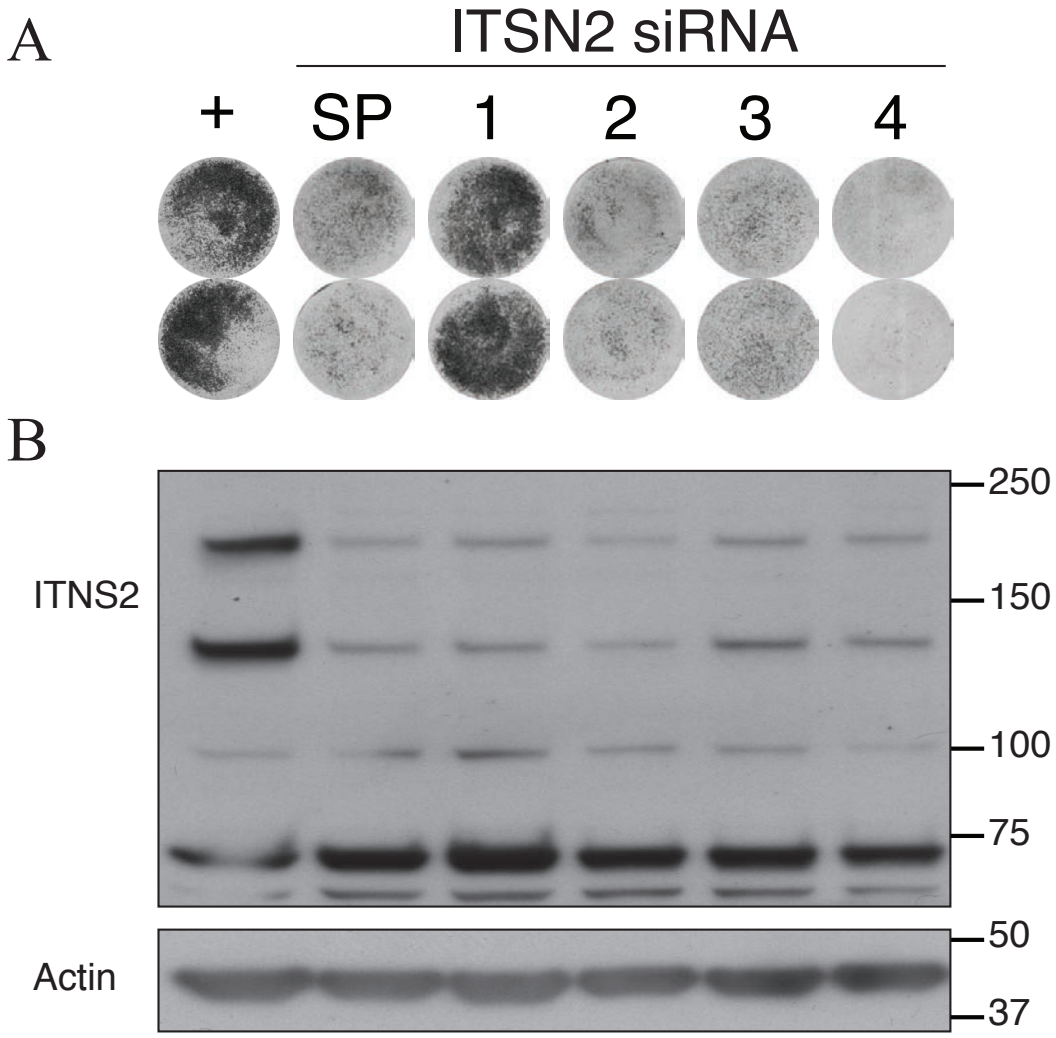

Figure 7: GEF Screen Confirmation – ITSN2

MDA-MB-231 cells were transfected with indicated siRNAs and control (+) siGLO. (A) Representative invasion filter scans of MDA-MB-231 cells after invasion through Matrigel for 16 hours. Filters were fixed and stained with methylene blue before scanning. (B) siRNA depleted MDA-MB-231 cells were lysed analyzed by western blot with the indicated antibodies.

ITSN2: The siRNA SMARTpool #48, targeting Intersectin 2 (ITSN2), strongly inhibited invasion in the initial GEF screen. To confirm the specificity of this result, the four individual duplexes comprising the SMARTpool were individually transfected into MDA-MB-231 cells (Figure 7). Three duplexes (#2, #3, and #4) were able to strongly inhibit invasion, while treatment with duplex #1 showed no difference from the control siGLO. Western blot analysis revealed that all four duplexes reduced the level of the 140 and 180 kDa isoforms of ITSN2 to similar levels. Concurrent work by a colleague also cast doubt on the specificity of this siRNA, raising additional concerns that these effects may not be due to specific effects of ITSN2 protein. Due to a lack of correlation between protein level and invasiveness, in addition to the above concerns and the availability of more promising candidates, further investigation of this protein was discontinued.

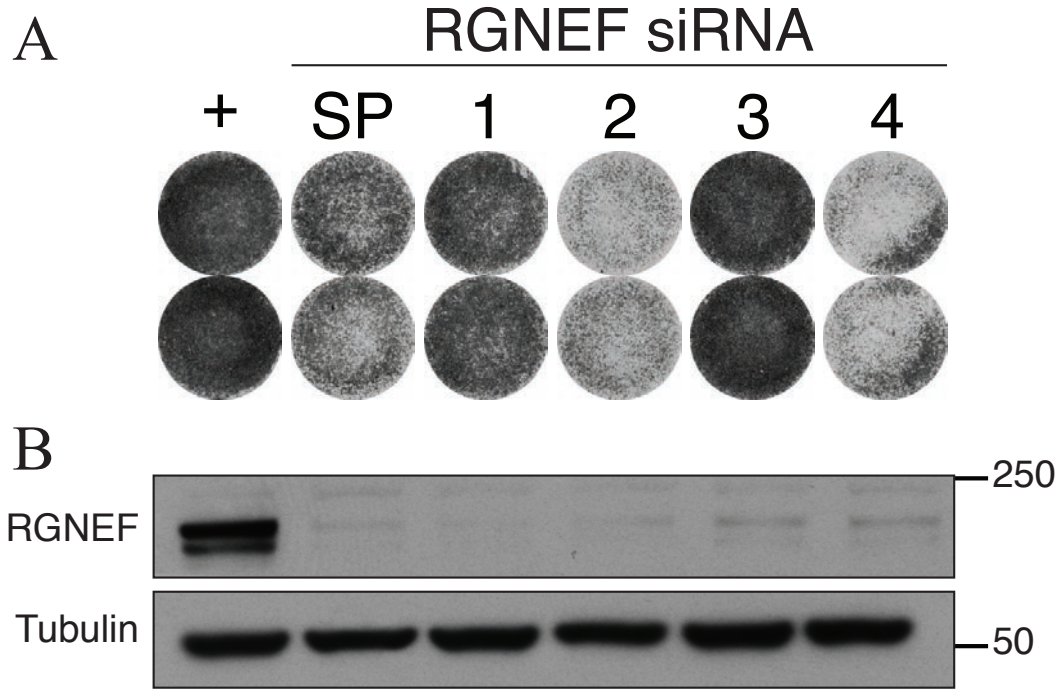

Figure 8: GEF Screen Confirmation – RGNEF

MDA-MB-231 cells were transfected with indicated siRNAs and control (+) siGLO. (A) Representative invasion filter scans of MDA-MB-231 cells after invasion through Matrigel for 16 hours. Filters were fixed and stained with methylene blue before scanning. (B) siRNA depleted MDA-MB-231 cells were lysed analyzed by western blot with the indicated antibodies.

RGNEF: The siRNA SMARTpool #72, targeting RGNEF, inhibited invasion in the initial GEF screen. To confirm the specificity of this result, the four individual siRNA duplexes comprising the SMARTpool were individually transfected into MDA-MB-231 cells (Figure 8). Western blot analysis showed that all four duplexes were able to deplete the endogenous 192 kDa protein almost completely. However, only duplexes #2 and #4 were able to inhibit invasion to a level similar to the SMARTpool. Duplexes #1 and #3 showed a level of invasion similar to siGLO control. Since the protein levels did not correlate with inhibition of invasion, this candidate was deemed a false positive and excluded from further investigation.

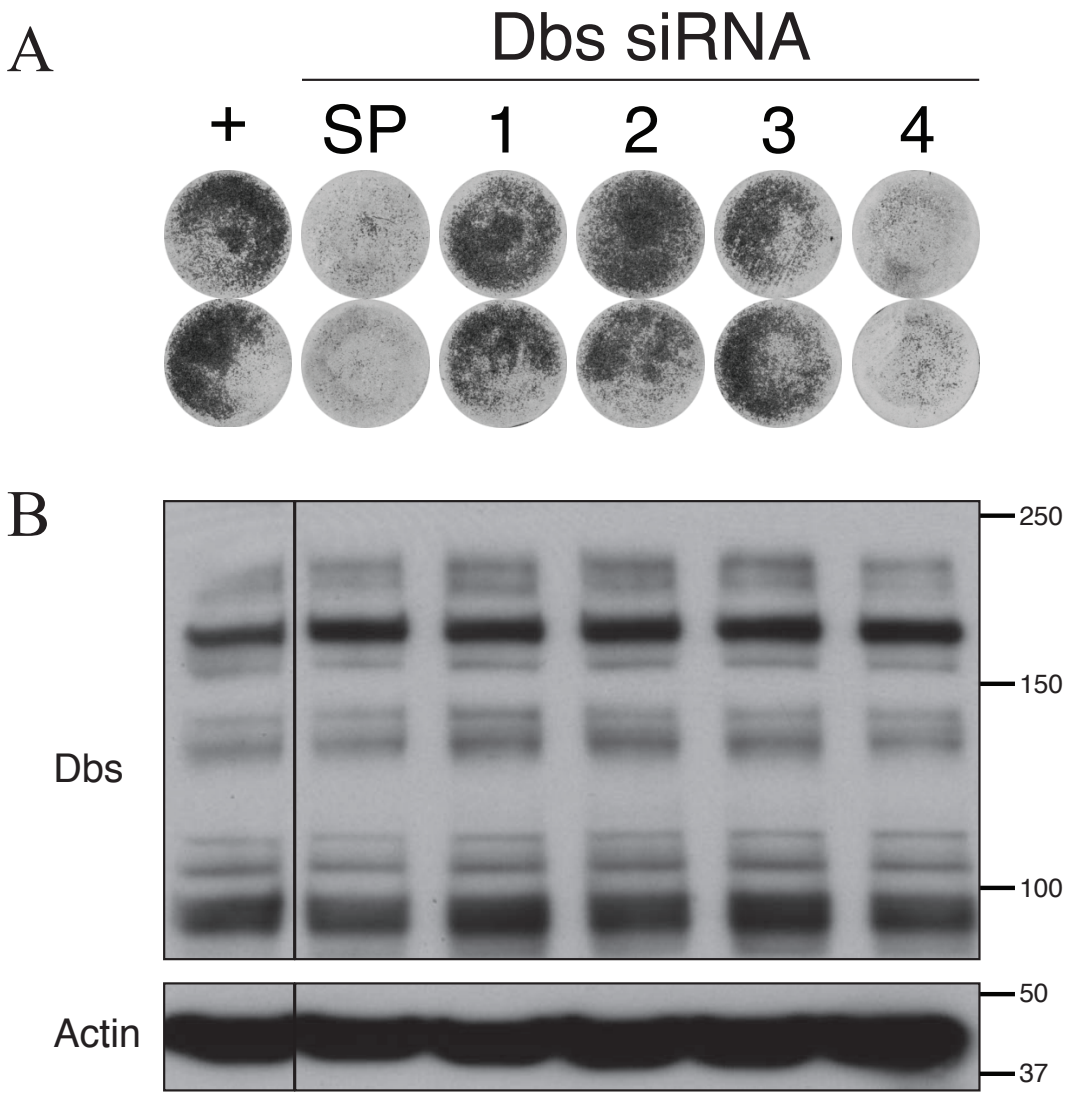

Figure 9: GEF Screen Confirmation – Dbs

MDA-MB-231 cells were transfected with indicated siRNAs and control (+) siGLO. (A) Invasion filter scans of MDA-MB-231 cells after invasion through Matrigel for 16 hours. Filters were fixed and stained with methylene blue before scanning. (B) siRNA depleted MDA-MB-231 cells were lysed analyzed by western blot with the indicated antibodies.

Dbs: The siRNA SMARTpool #10, targeting Dbs (MCF2L) strongly inhibited invasion in the initial GEF screen. To confirm the specificity of this result, the four individual siRNA duplexes comprising the SMARTpool were transfected into MDA-MB-231 cells (Figure 9). Only duplex #4 was able to inhibit invasion to a level similar to the SMARTpool, while the other duplexes (#1, #2, #3) showed a level of invasion similar to siGLO control. Western blot analysis failed to reveal any protein band of the predicted size (128 kDa), and showed no differences in staining pattern. The inhibition of invasion by duplex #4 was could be a nonspecific effect although it is possible that the antibody was not sensitive enough, or the level of expression was undetectable. Since no antibody was available to correlate protein knockdown to the invasion phenotype and three duplexes had no effect on invasion, this candidate was excluded from further pursuit.

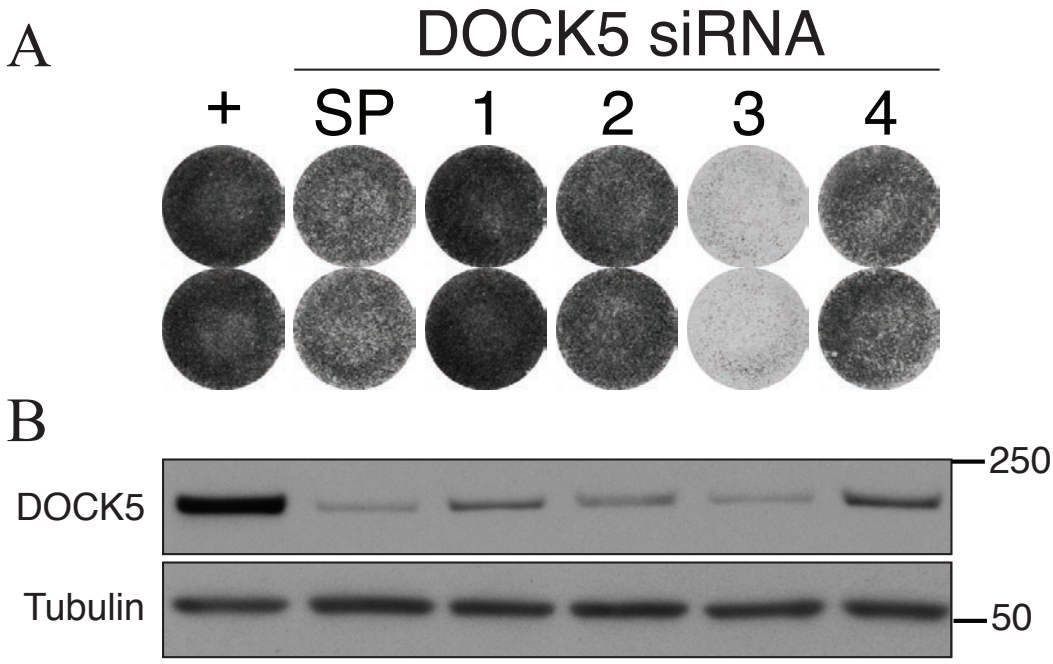

Figure 10: GEF Screen Confirmation – DOCK5

MDA-MB-231 cells were transfected with indicated siRNAs and control (+) siGLO. (A) Representative invasion filter scans of MDA-MB-231 cells after invasion through Matrigel for 16 hours. Filters were fixed and stained with methylene blue before scanning. (B) siRNA depleted MDA-MB-231 cells were lysed analyzed by western blot with the indicated antibodies.

DOCK5: The siRNA SMARTpool #12, targeting DOCK5, strongly inhibited invasion in the original screen. To confirm the specificity of this result, the four individual siRNA duplexes comprising the SMARTpool were individually transfected into MDA-MB-231 cells (Figure 10). Western blot analysis revealed that all four duplexes were able to deplete the endogenous 215 kDa protein to varying degrees. Of the four duplexes, only one (#3) strongly inhibited invasion. Also, the SMARTpool siRNA only slightly reduced invasion despite effective protein depletion. These data could suggest that a very strong knockdown of the protein is necessary to induce a phenotype, or that the effect of duplex 3 is non-specific. Since the protein levels did not correlate with the inhibition of invasion, and three duplexes had only a weak effect on invasion, DOCK5 was excluded from further investigation.

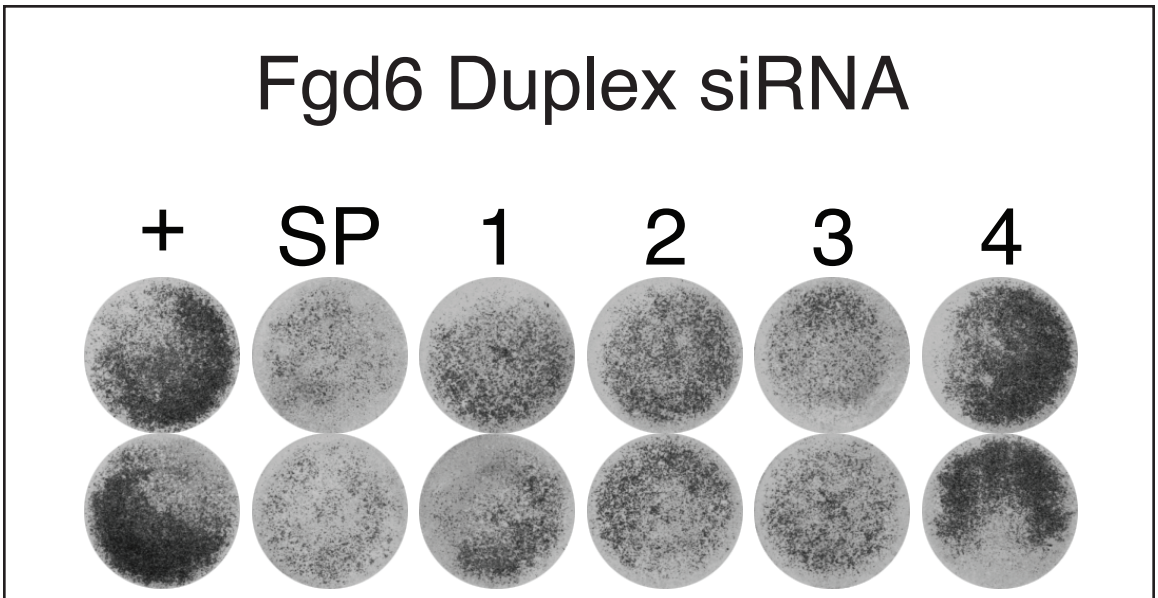

Figure 11: GEF Screen Confirmation – Fgd6

MDA-MB-231 cells were transfected with indicated siRNAs and control (+) siGLO. Invasion filter scans of MDA-MB-231 cells after invasion through Matrigel for 16 hours. Filters were fixed and stained with methylene blue before scanning.

Fgd6: The siRNA SMARTpool #7, targeting Fgd6, was able to inhibit invasion by ~90% in the original screen. To confirm the specificity of this result, the four individual siRNA duplexes comprising the SMARTpool were individually transfected into MDA-MB-231 cells (Figure 11). Duplex #4 had no effect on invasion, while duplexes #1-3 showed a modest inhibition of invasion. None were as effective as the SMARTpool reagent. Unfortunately, no antibody was commercially available to detect Fgd6 preventing the determination of protein expression level. Since only the SMARTpool reagent is able to robustly inhibit invasion, this candidate was excluded from further investigation.

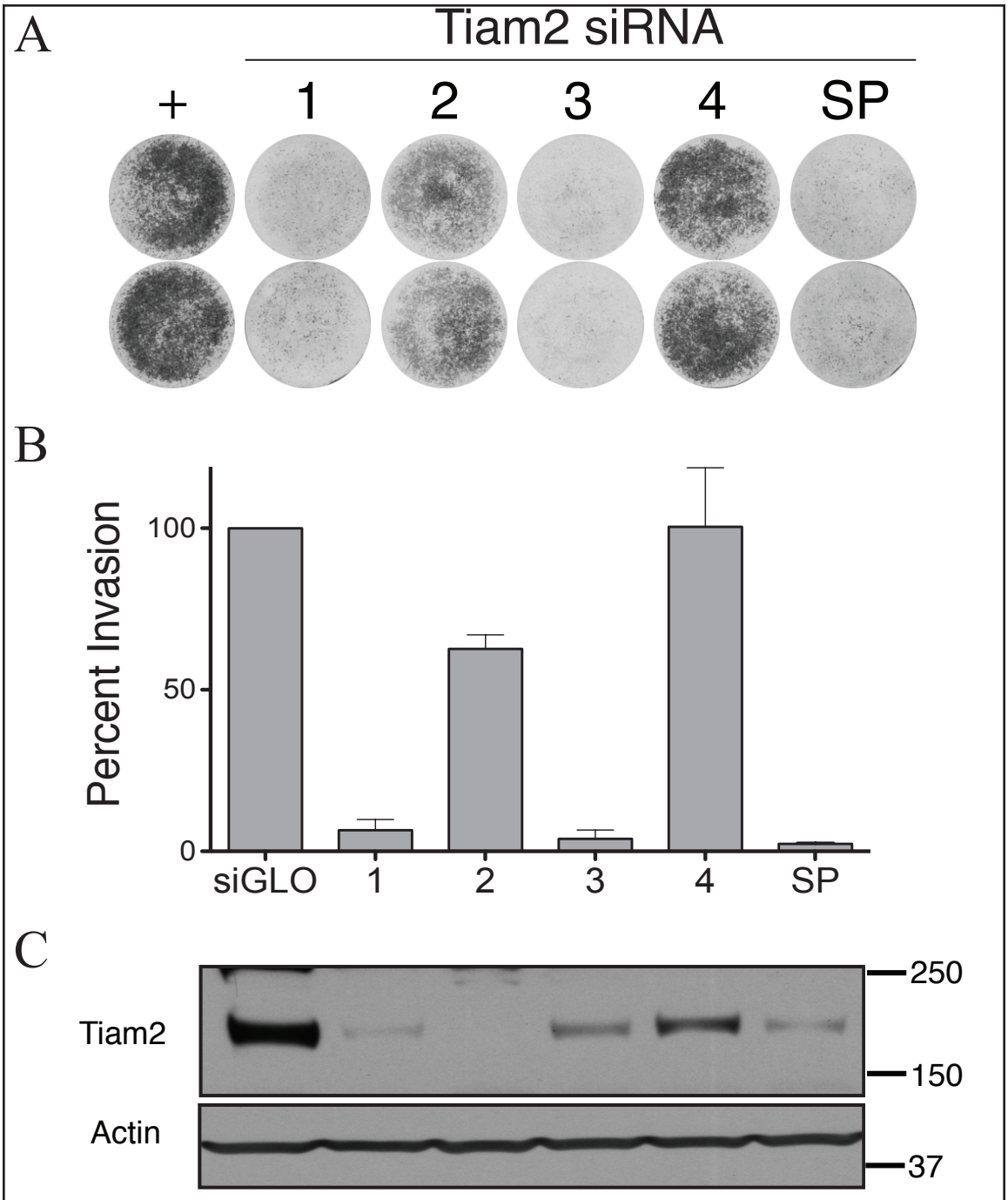

Figure 12: GEF Screen Confirmation – Tiam2

MDA-MB-231 cells were transfected with indicated siRNAs and control (+) siGLO. (A) Representative invasion filter scans of MDA-MB-231 cells after invasion through Matrigel for 16 hours. Filters were fixed and stained with methylene blue before scanning. (B) Quantification of 3 invasion experiments. (C) siRNA depleted MDA-MB-231 cells were lysed analyzed by western blot with the indicated antibodies.

Table 7: Rho GAPs screened in this study.

Number	Group	Name	Accession #	Alternative Name(s)
1	1A	7H3	NM_033025	SYDE1
2	2A	ARHGAP1	NM_004308	
3	2B	ARHGAP10	NM_024605	GRAF2
4	1B	ARHGAP11A	NM_014783	
5	1C	ARHGAP12	NM_018287	
6	1C	ARHGAP15	NM_018460	
7	1D	ARHGAP17	NM_018054	RICH1
8	2C	ARHGAP18	NM_033515	
9	2D	ARHGAP19	NM_032900	
10	2E	ARHGAP20	NM_020809	
11	2F	ARHGAP21	NM_020824	
12	2G	ARHGAP22	NM_021226	
13	2F	ARHGAP23	XM_290799	
14	2G	ARHGAP24	NM_031305	
15	2G	ARHGAP25	NM_014882	
16	2B	ARHGAP26	NM_015071	GRAF
17	2C	ARHGAP28	NM_030672	
18	1D	ARHGAP4	NM_001666	
19	2I	ARHGAP5	NM_001173	
20	1E	ARHGAP6	NM_001174	
21	2A	ARHGAP8	NM_001017526	
22	1C	ARHGAP9	NM_032496	
23	2J	BNIP2	NM_004330	
24	2C	C5ORF5	NM_016603	
25	1F	CDGAP	NM_020754	
26	2K	CENTD1	NM_015230	ARAP2
27	2K	CENTD2	NM_015242	ARAP1
28	2K	CENTD3	NM_022481	ARAP3
29	2L	CHN1	NM_001822	Chimaerin-1
30	2L	CHN2	NM_004067	Chimaerin-2
31	1G	DEPDC1	NM_017779	
32	1G	DEPDC1B	NM_018369	
33	2M	DLC1	NM_006094	STARD12, p112-RhoGAP
34	1H	FKSG42	NM_032032	
35	1I	SYDE2	XM_086186	
36	1J	ARHGAP36	NM_144967	
37	2B	FLJ32810	XM_370651	*removed*
38	2H	GMIP	NM_016573	
39	2I	GRLF1	NM_004491	p190-RhoGAP

Number	Group	Name	Accession #	Alternative Name(s)
40	2H	HA-1	NM_012292	
41	2N	INPP5B	NM_005540	
42	1K	ARHGAP44	NM_014859	
43	1L	ARHGAP39	NM_025251	
44	1M	ARHGAP27	NM_199282	
45	1M	ARHGAP30	NM_181720	
46	1N	LOC285101	XM_210411	*removed*
47	1O	ARHGAP40	XM_293123	
48	1P	Fam13a	XM_371697	
49	2O	MYO9A	NM_006901	
50	2O	MYO9B	NM_004145	
51	2N	OCRL	NM_000276	INPP5F
52	2B	OPHN1	NM_002547	
53	2H	PARG1	NM_004815	ARHGAP29
54	2P	PIK3R1	NM_181504	p85-alpha
55	2P	PIK3R2	NM_005027	p85-beta
56	1Q	RACGAP1	NM_013277	Mgc-RacGAP
57	1R	RALBP1	NM_006788	
58	1S	RICS	NM_014715	GRIT, p200-RhoGAP
59	1D	SH3BP1	NM_018957	
60	1T	SNX26	NM_052948	TCGAP
61	1U	SRGAP1	NM_020762	
62	1U	SRGAP2	NM_015326	
63	1U	SRGAP3	NM_014850	
64	2M	STARD13	NM_052851	DLC2
65	2M	STARD8	NM_014725	DLC3
66	1V	TAGAP	NM_054114	

Tiam2: The siRNA SMARTpool #64, targeting Tiam2, inhibited invasion by more than 95% of control. To confirm the specificity of this result, the four individual siRNA duplexes comprising the SMARTpool were individually transfected into MDA-MB-231 cells (Figure 12). Two of the four duplexes (#1 and #3) inhibited invasion to the same level as the SMARTpool. Duplex #2 inhibited invasion to nearly 50% of control, while duplex #4 was similar to siGLO control. Western blots analysis showed that duplexes #1 and #3 reduced Tiam2 protein levels to a similar level as the SMARTpool. Duplex #4 was least effective at reducing protein levels, which correlates to the lack of inhibition of invasion. Curiously, duplex #2 was the most effective at reducing Tiam2 protein levels while only moderately inhibiting invasion. These data were encouraging, although the levels of protein depleted did not correlate perfectly with the extent of invasion. Thus, although duplex #2 showed the lowest level of protein after transfection, it induced a modest phenotype; nevertheless, since Tiam2 depletion was broadly associated with inhibition of invasion, this candidate was subjected to further investigation.

Fgd2, Fgd4, and ARHGEF19 antibodies were not available, and these candidates were not pursued further.

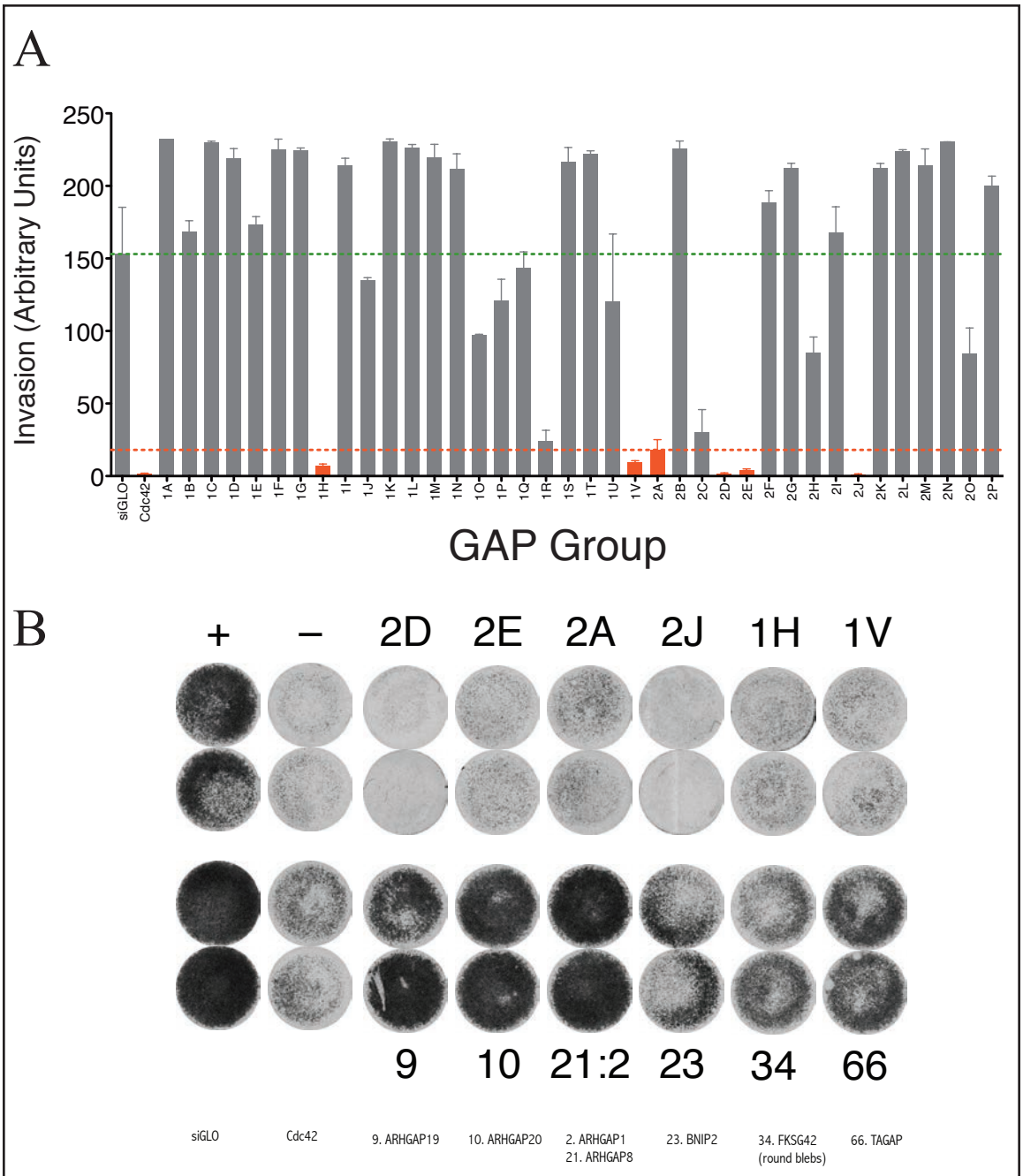

Figure 13: GAP Screen Results

MDA-MB-231 cells were transfected with indicated group of siRNAs (see Table of GAPs) with and control (–) Cdc42 and (+) siGLO. (A) Quantitation of scanned invasion filters. Red line is threshold to consider as a hit, Green line is the siGLO control for full invasion. (B) Potential hits were repeated, and the invasion filters fixed and stained with methylene blue and scanned.

Screening of GAPs

To identify negative regulators of Rho family GTPases that might influence invasion, I screened a library of siRNA SMARTpools targeting the 66 known human GAPs in MDA-MB-231 cells. This screen was essentially performed as described for the GEFs, except that SMARTpools targeting related proteins were grouped together based on homology, prior to transfection to reduce the likelihood of false negative results due to functional redundancy. The transfection concentration of siRNAs was maintained at 50 nM, resulting in lower concentration of each individual siRNA. Seven potential candidates: ARHGAP19, ARHGAP20, ARHGAP1 + ARHGAP8, BNIP2, FKSG42, and TAGAP reduced the level of invasion to 10% or less of the control level (Figure 13). These candidates were prioritized based on published literature and the availability of reagents. The initial candidates were subjected to a second round of screening to confirm the initial result. The results of the repeated screen revealed that none of the hits were reproducible.

Discussion

The work presented in this chapter utilized siRNA-based screening methods to identify Rho family GTPases, and their positive and negative regulators, which regulate breast cancer cell invasion.

GTPases

Surprisingly, depletion of Rac1, which is thought to be important for membrane protrusion, had no effect on invasion in this cell line (Figure 4). One reason for this could be functional redundancy among the three Rac isoforms. This poses a problem experimentally, as current antibodies are unable to distinguish between endogenous Rac1 and Rac3. Even though Rac 2 is normally expressed only in hematopoietic cells, it could potentially be expressed in cancer cells due to aberrant gene regulation. Quantitative RT-PCR could be used to determine which isoforms of Rac are expressed at the mRNA level in MDA-MB-231 cells, but protein stability and turnover may cause the protein levels to be different from that of the message. It may be possible to study the effects of Rac on invasion by depleting all isoforms of Rac, either by using multiple siRNAs or a single siRNA targeting all isoforms. The results of this approach may be difficult to interpret if incomplete knockdown was achieved, although qRT-PCR might offer some insight. Alternatively, a dominant negative Rac mutant (N17) could have been expressed which would have interfered with the function of all Rac isoforms. Finally, MDA-MB-231 cells may utilize a Rac-independent method of cell invasion, or may be capable of switching between methods of invasion that would not be detected using the Boyden chamber assay.

Depletion of RhoA reduced the invasive capacity of MDA-MB-231 cells moderately (25% of control levels)(Figure 4). This result was not confirmed with multiple siRNAs, but would be consistent with the known functions of RhoA in cell migration. [90, 92, 125] RhoA is

known to regulate cell contractility and membrane protrusion important for amoeboid cell migration. It is also important for mesenchymal migration where it controls the retraction of the trailing edge of the cell body. [13, 122, 172] The level of invasion observed could be explained by functional redundancy between Rho isoforms, incomplete depletion of RhoA protein, or the existence of redundant mechanisms of invasion. Similar strategies as proposed for the study of Rac (see above) could also be used here to further elucidate the role of Rho in MDA-MB-231 cell invasion.

Cdc42 depletion strongly reduced the invasive capacity of MDA-MB-231 cells using multiple siRNA reagents (Figure 5). [12, 16, 99, 114, 173] Cdc42 activation induces filopodia formation, which can initiate cell migration. Cdc42 regulates actin polymerization through its effector protein N-WASP/WASP, which in turn activates Arp2/3 to stimulate actin branching and increased polarization. Cdc42 controls polarity during cell migration through recruitment of the Par3/Par6/aPKC complex. [174-176] Activation of this complex has been show to induce membrane ruffling by Rac and Cdc42 activation at the leading edge through binding of PDZ and CRIB motifs. [175] Interfering with either polarization or cytoskeleton reorganization could prevent cell migration in the modified Boyden chamber assay.

Since RhoA and Cdc42 were identified as regulators of cell invasion, and other GTPases may also contribute, I set out to identify the specific GEFs that activate Rho family GTPases in this context.

GEF Screen

In order to study how Rho Family GTPases affect breast cancer cell invasion, I screened a library of SMARTpool siRNAs using a modified Boyden chamber assay. Because GEFs

are activators of GTPase function, and active GTPases promote migration, the screen was designed to identify genes that would interfere with, rather than promote, invasion.

Since GEF activity could potentially affect cell proliferation as well as invasion, the invasion assay was optimized for the minimal time to invade, 16 hours, to reduce the contribution of proliferation to the observed phenotype. This is less than the 28-hour doubling time for MDA-MB-231 cells, so the contribution of daughter cells invading through Matrigel should be minimal but, but not completely avoided. One limitation of this screen is that it cannot distinguish between methods of cellular invasion. It is known that some cancer cells can sometimes switch between mesenchymal and amoeboid modes of invasion, so if depleting a GEF caused cells to switch invasion types it would not be recognized in this end-point assay. [74] The method of cellular invasion could be studied using time-lapse microscopy.

Another weakness, as mentioned earlier in the case of Cdc42, is that disruption of cell polarity could inhibit directional cell invasion. Without the ability to persistently sense direction, cells would fail to migrate directionally, and would therefore appear not to invade. This would increase the number of candidate GEFs that regulate invasion, but since either phenotype is of equal interest this was not felt to be a problem at this stage.

GEF Screen Results

The first step after identifying potential candidates in the GEF screen was to confirm that inhibition of invasion was specifically related to depletion of the indicated protein. The primary method used to improve confidence that siRNA effects are specific is to use multiple siRNA duplexes that target non-overlapping regions of the mRNA sequence. [177] The observed phenotype should correspond to the level of protein knockdown achieved, keeping in mind that certain proteins may require a minimal threshold level to be reached

before any phenotype is revealed. [178] RNAi prediction algorithms suggest that unique siRNA duplexes are unlikely to have similar off-target effects even when targeted against the same protein. Mixtures of siRNAs at low concentrations should allow for robust depletion of the specific target protein and mitigate off-target effects. This was the rationale for using SMARTpool mixtures of siRNAs in the original screen of Rho GEFs.

Transfection of individual siRNA duplexes comprising the SMARTpool for each of the GEF candidates allowed us to correlate protein level with the amount of invasion. Candidates were excluded from consideration when western blot analysis revealed no clear correlation between the level of protein present and the amount of residual invasion. For a complex phenotype like invasion, the use of siRNA SMARTpools in the initial round of screening may not be ideal. Such a complex phenotype may be sensitive to the disruption of many cellular processes, such that multiple siRNAs could increase the chance that an off-target effect would yield a false positive.

In addition, the duplex nature of siRNA results in both the targeting strand and the guide strand being incorporated into the silencing complex, potentially increasing the possibility of off-target effects. Chemical modifications to the guide strand have been shown to reduce the number of off target effects by interfering with its proper binding to the RISC complex. [179] This technology was only beginning to be offered commercially during the time when the library was purchased. Another concern when introducing exogenous siRNA duplexes is that they may interfere with the endogenously expressed small RNA molecules that regulate gene expression. In this case, transfection of siRNA can disrupt endogenous microRNAs from the RISC complex, resulting in re-expression of previously degraded transcripts.[180] For this reason, it is important to transfect cells at the lowest siRNA concentration that achieves sufficient target protein depletion.

GAP Screen

After identifying one potential positive regulator of Rho GTPase signaling in breast cancer cells, I investigated the role of Rho GAPs in cancer invasion. One consideration when performing the GAP screen using the siRNA SMARTpool library was to try and limit the number of false negatives identified as compared to the GEF screen. To avoid the possibility that structurally related GAPs might be functionally redundant, I grouped highly related GAPs together before transfection (Table 7). By grouping related GAP siRNAs such that related proteins were simultaneously depleted, I aimed to increase the chances of successfully identifying positive regulators of GTPase signaling. Since a system was already in place to screen for molecules that inhibit invasion, the same modified Boyden chamber assay used in the GEF screen was used to screen a library of 66 known GAPs.

In retrospect, this protocol may not have been ideal for identifying GAPs involved in invasion. Rho GAPs inhibit signaling through Rho family GTPases, which are positive regulators of cell migration. It is more likely that a reduction in GAP levels would increase the activity of GTPases, resulting in promotion of an invasive phenotype. This would not have been detectable using the current assay conditions. However, inactivation of GTPases could disturb cell polarity, which would have caused cells to migrate randomly instead of directionally. The modified Boyden chamber assay cannot distinguish between these phenotypes and should still yield candidates involved in cell polarization. Additionally, aberrant regulation of any type could cause cells to lose the ability to invade due to the importance of a precise balance of GTPase activity both spatially and temporally.

More candidates may have been identified had a more weakly invasive cell type been used. Alternatively, if fewer MDA-MB-231 cells were used in the invasion assay after transfection with siRNAs targeting GAPs, it might be possible to detect an increase in invading cells.

There are at least three potential reasons for the low number of GEFs and GAPs identified in this screen. First, invasion in MDA-MB-231 cells may not require any Rho family GEF or GAP function, though this is highly unlikely given the strong effect that Cdc42 depletion has on cell invasion. Second, functional redundancy between closely related homologues could have resulted in false negatives from the screen. An attempt was made to avoid this in the GAP screen but without success. Third, and most likely, is that the level of knock-down achieved was insufficient to interfere with protein function. These libraries of siRNA SMARTpools were not validated, so the duplexes were predicted but not proven to target the indicated proteins. Nonetheless, this screen identified Tiam2 as potential regulator of invasion (Figure 12).

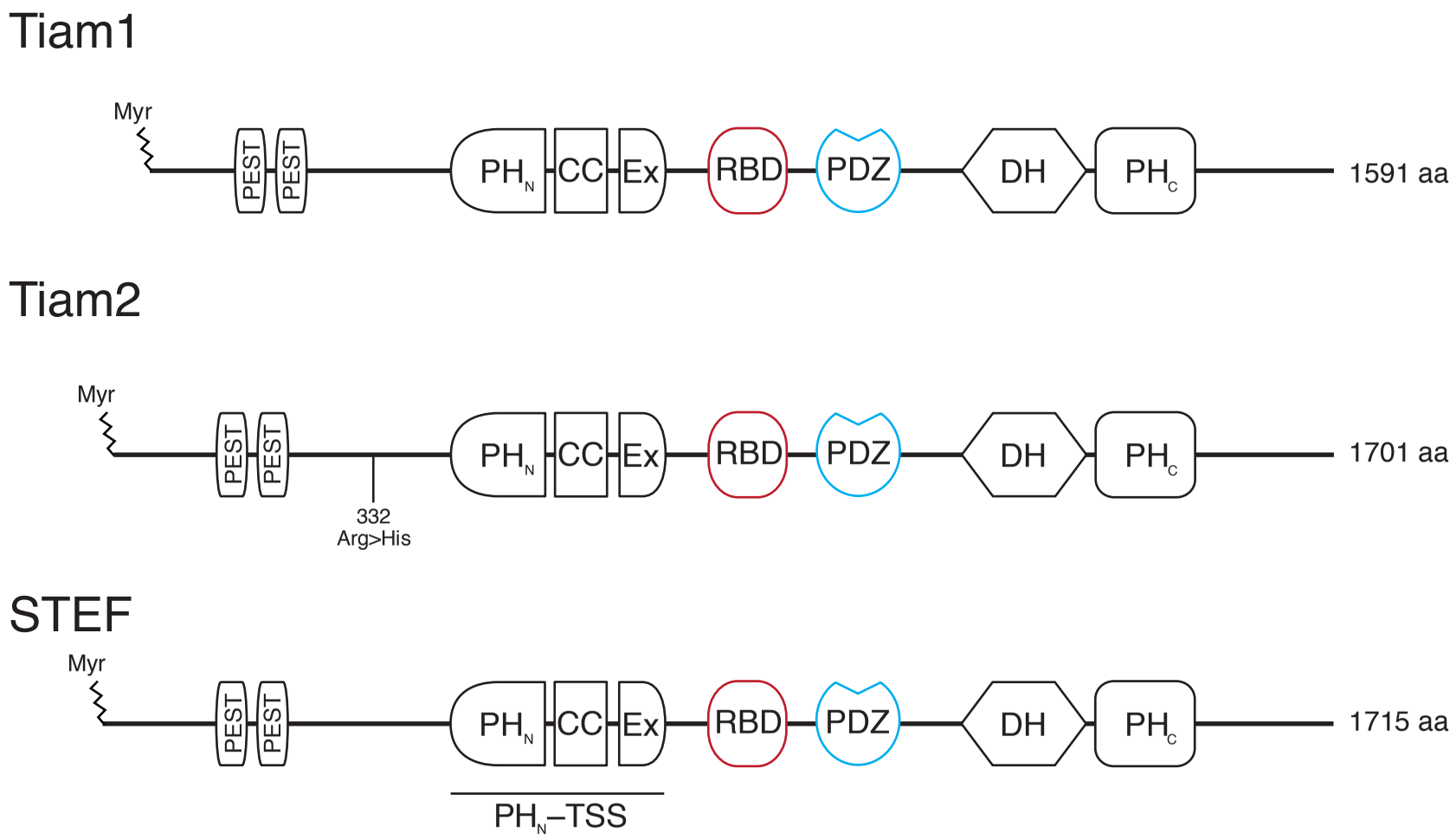

Figure 14: Tiam Family Structural Domains

Domain Structure of Tiam family proteins. Myr: myristoylation site. PEST: degradation signal. PHN-CC-Ex: PH, Coil-Coiled and Extra domain. RBD: Ras binding domain. PDZ: PSD-95/DlgA/ZO-1 domain. DH: Dbl homology domain. PH: Pleckstrin Homology

Chapter 4: Tiam2 Invasion and Growth

The data presented in Chapter 3 suggest that Tiam2 is required for MDA-MB-231 cell invasion. This finding was further pursued through studies of both invasion and proliferation in multiple breast cancer cell lines in addition to an animal model of tumor growth. These studies aimed to characterize the wider role of Tiam2 in breast cancer progression.

Tiam1 (T-cell lymphoma invasion and metastasis) was first identified in a genetic screen for factors that could increase the invasiveness of a lymphoma cell line using Moloney murine leukemia virus insertion.[181] Five years later, Tiam2 was identified using a degenerative PCR-screen by homology to Tiam1 and the DH-PH domain was shown to catalyze nucleotide exchange on Rac, but not Cdc42 or RhoA in a biochemical assay. [182] The mouse ortholog of Tiam2 is referred to as SIF or TIAM1-like exchange factor (STEF) where SIF is the name of the drosophila ortholog. This sub-family of proteins belongs to the Dbl family of GEFs due to the presence of characteristic DH-PH domains. All three proteins are similar in size (~190 kDa) and share a well-conserved domain organization. In addition to the GEF domain, an amino-terminal PH domain lies adjacent to a "coiled-coil and extra region" (PHN-CC-Ex), which is conserved across all family members. Crystal structures reveal that the PHN-CC-Ex domain folds into a single globular domain and this is important for binding to membranes in addition to important signaling partners such as Par3. [183] Other important domains include a PSD-95/DlgA/ZO-1 (PDZ) domain and a Ras binding domain (RBD) in addition to two PEST degradation signals and a myristoylation site at its N terminus. Since MDA-MB-231 cells express oncogenic Ras, Tiam2 may be a potentially interesting candidate that links Ras and Rac signaling pathways.

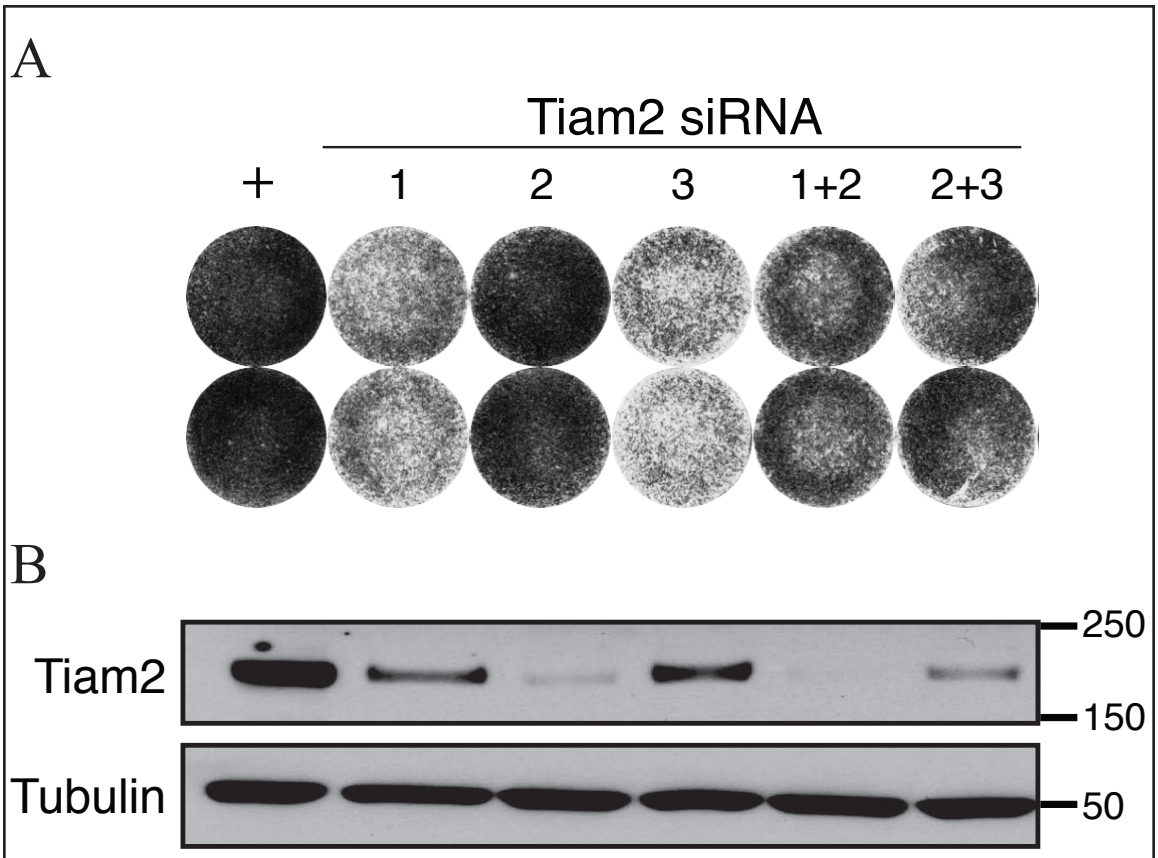

Figure 15: Tiam2 siRNA inhibits invasion in MDA-MB-231 cells

MDA-MB-231 cells were transfected with indicated siRNAs and control (+) siGLO. (A) Invasion filter scans of MDA-MB-231 cells after invasion through Matrigel for 16 hours. Filters were fixed and stained with methylene blue. (B) siRNA depleted MDA-MB-231 cells were lysed analyzed by western blot with the indicated antibodies.

Depletion of Tiam2 using siRNA

The data presented in Chapter 3 suggest that Tiam2 expression is necessary for MDA-MB-231 cells to invade through Matrigel. The observation that Tiam2 si-2 can strongly reduce the protein level while only minimally inhibiting invasion is inconsistent with the results using si-1 and si-3 (Figure 12). This could indicate that the invasion inhibition effects of si-1 and si-3 are off-target, or that si-2 has an off-target effect that somehow bypasses the need for Tiam2 in invasion. To directly test this hypothesis, the individual duplexes si-1 and si-3 were mixed with si-2 in equimolar ratios and transfected into MDA-MB-231 cells. The dominant phenotype after mixing should indicate whether or not si-2 is sufficient for cells to regain the ability to invade in the absence of Tiam2. Co-depletion reduces the protein level but cells are capable of invasion at levels close to that of control siGLO (Figure 15). This suggests that si-2 is likely to have an off-target effect that permits invasion independently of Tiam2 protein level. With this in mind, further experiments utilizing si-1 or si-3 siRNA reagents were used to examine the effect of Tiam2 depletion on invasion.

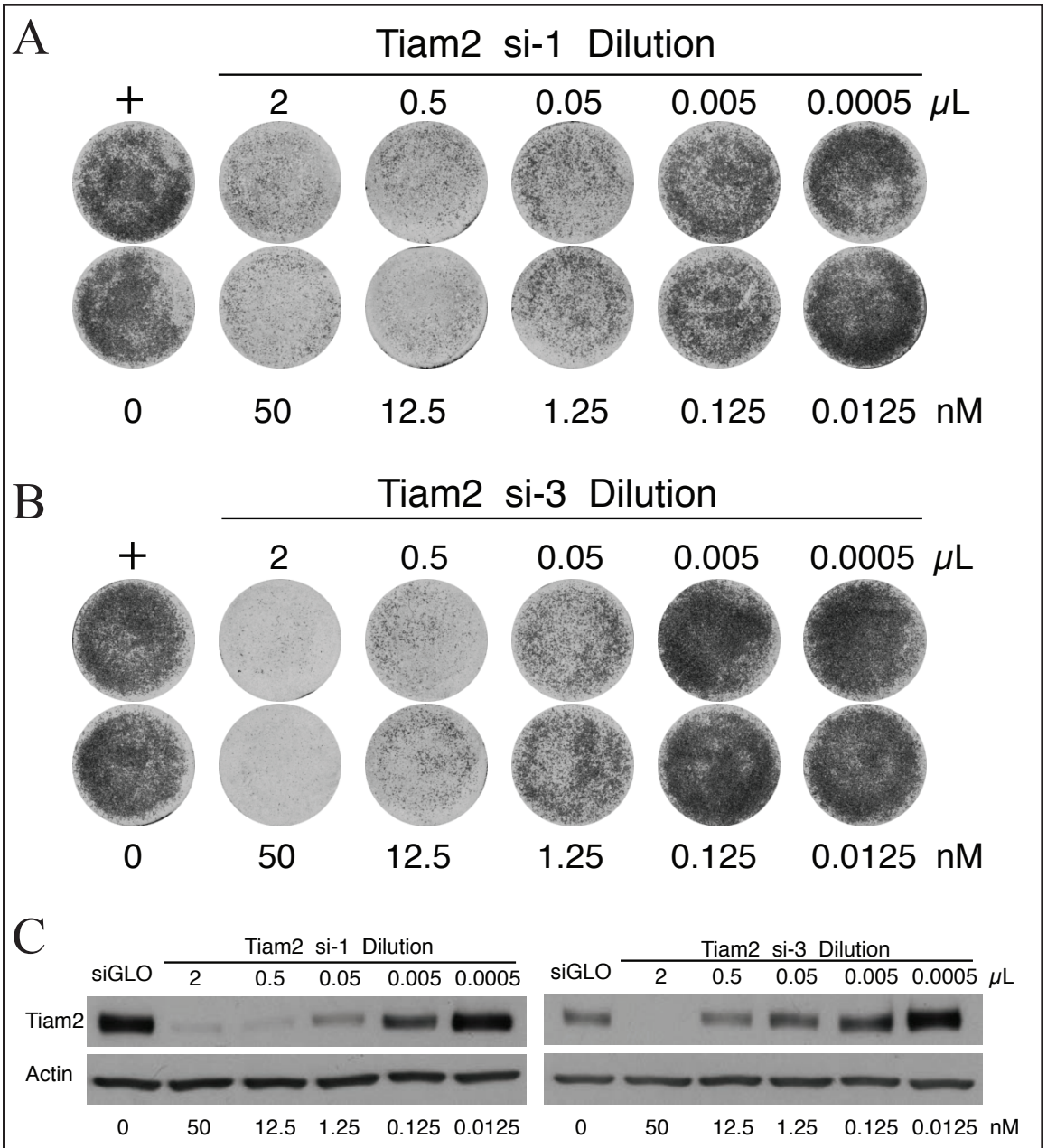

Figure 16: Dilution of Tiam2 siRNA

MDA-MB-231 cells were transfected with indicated dilution of either Tiam2 si-1 or si-3. (A, B) Invasion filter scans of cells after invasion through Matrigel for 16 hours. Filters were fixed and stained with methylene blue. (C) siRNA depleted MDA-MB-231 cells were lysed analyzed by western blot with the indicated antibodies.

To further investigate the hypothesis that siRNA depletion of Tiam2 inhibits invasion, an attempt was made to test the relationship between Tiam2 expression and invasiveness more directly. The two duplexes that best depleted Tiam2 protein levels, si-1 and si-3, were individually transfected into MDA-MB-231 cells at different concentrations between 50 nM and 0.0125 nM. To maintain a consistent total siRNA concentration of 50 nM, the balance was made up with siGLO or a non-targeting siRNA. Tiam2 si-1 (Figure 16, panel A) shows that 12.5 nM siRNA is sufficient to inhibit invasion to the same level as 50 nM. A concentration of 1.25 nM was able to partially inhibit invasion, whereas cells transfected with lower concentrations behaved similarly to control cells. Tiam2 si-3 (Figure 16, panel B) shows an strong inhibition of invasion at 50 nM and 12.5 nM, with modest inhibition even at concentrations as low as 1.25 nM. Western blot analysis (Figure 16, panel C) reveals the level of Tiam2 appears to have a direct relationship to the number of cells able to invade through Matrigel. This supports the notion that Tiam2 protein is necessary for invasion, with the caveat that dilution of the siRNA duplexes would also dilute any off-target effects. The fact that such low levels of siRNA are still able to suppress invasion and effectively lower Tiam2 levels implies that the effect is specific, because the contribution of off-target effects of siRNA are thought to disappear more quickly than the specific effect (this is the principle behind using SMARTpool siRNA). Due to variability in the invasion assay, it is difficult to draw an exact link between invasion efficiency and protein levels, but should be considered a good approximation.

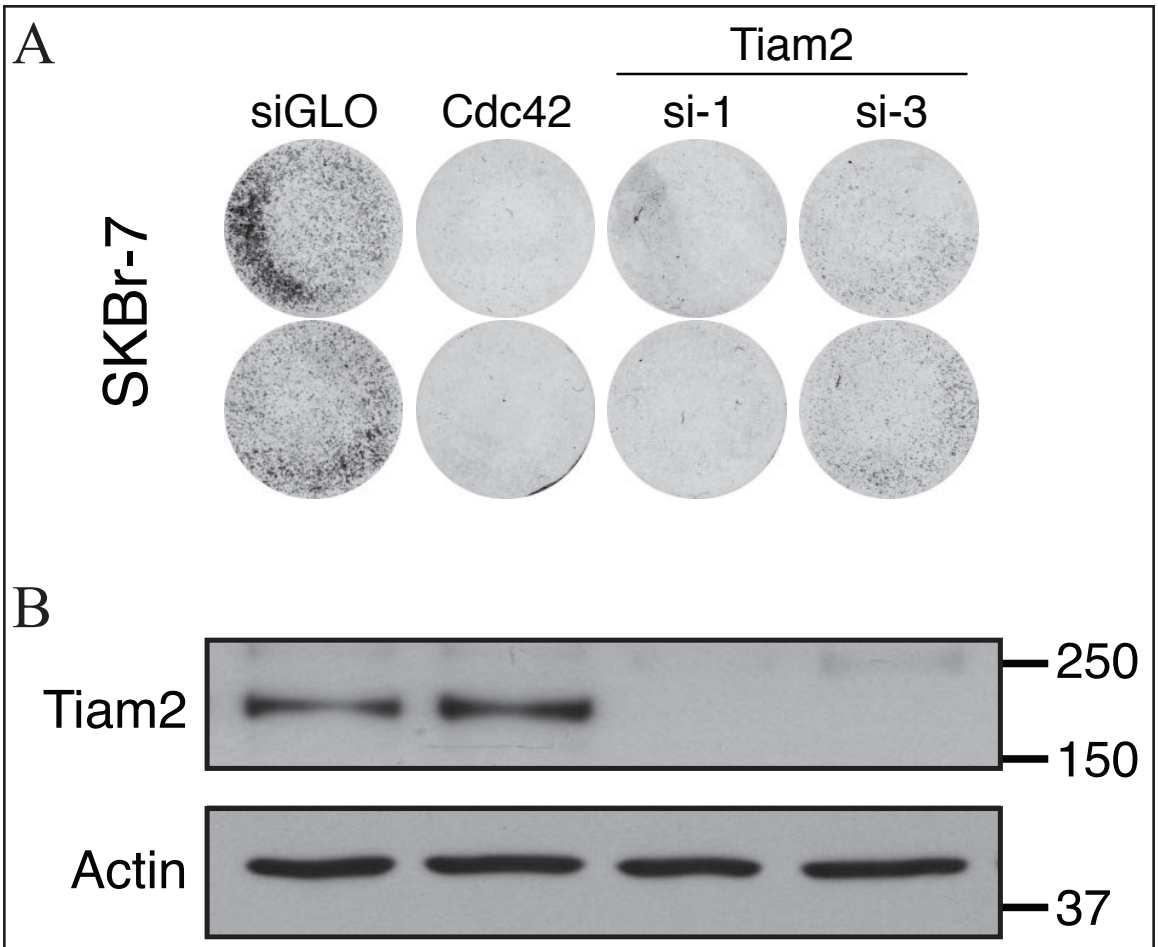

Figure 17: Tiam2 siRNA inhibits invasion in SkBr7 Cells

SKBr-7 cells were transfected with indicated siRNA. (A) Invasion filter scans of cells after invasion through Matrigel for 16 hours. Filters were fixed and stained with methylene blue. (B) siRNA depleted SKBr-7 cells were lysed analyzed by western blot with the indicated antibodies.

To support a wider role for Tiam2 in invasion, another breast cancer cell line, SkBr7, was transfected with Tiam2 duplexes si-1 and si-3 and assayed for invasion (Figure 17). This cell line is less invasive than MDA-MB-231, as judged by the lighter staining of the siGLO control (Figure 17, panel A), however, they do reproducibly invade. Depletion of Tiam2 by si-1 and si-3 reduced the ability of SkBr7 cells to invade through Matrigel to levels similar to that of Cdc42. Western blot analysis revealed that both siRNA duplexes strongly reduce the level of Tiam2 protein in SkBr7 cells (Figure 17, panel B), supporting a wider role for Tiam2 in breast cancer cell invasion.

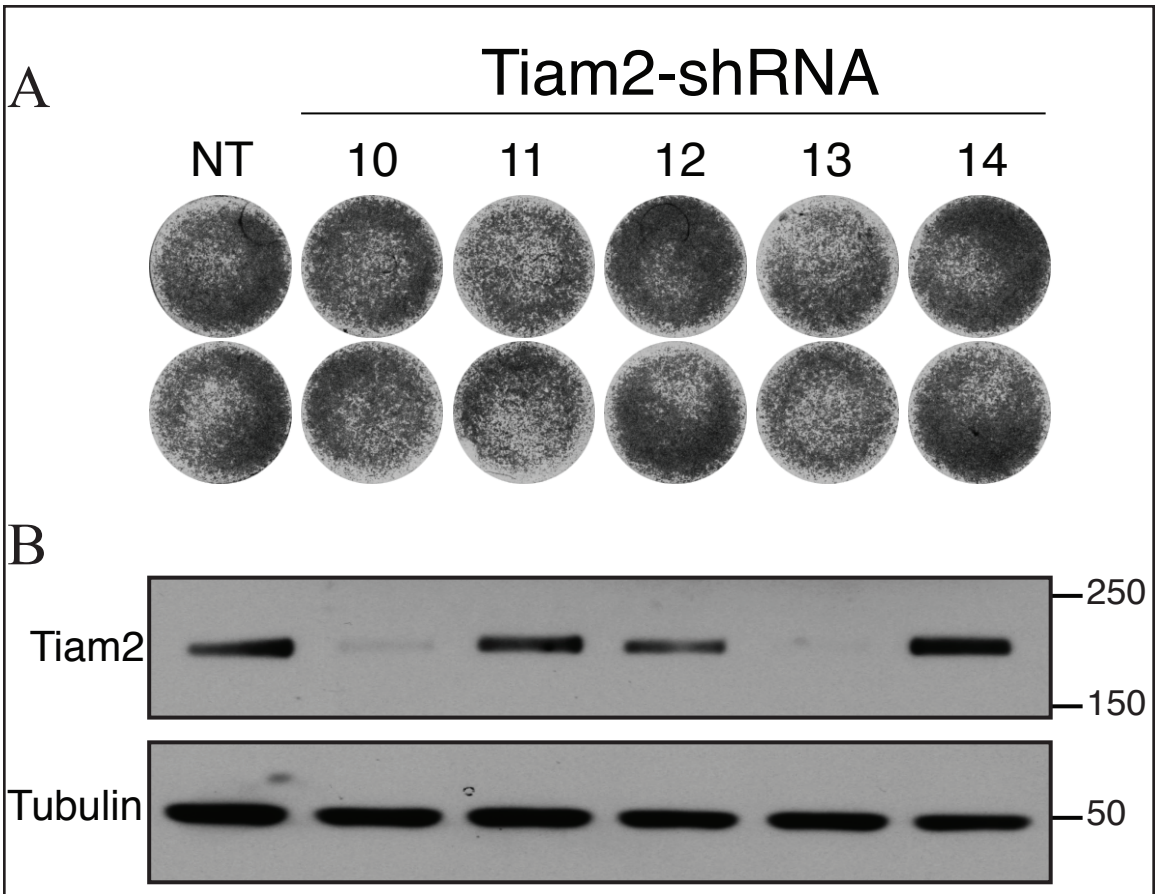

Figure 18: Tiam2 shRNA does not inhibit invasion in MDA-MB-231 cells

MDA-MB-231 cells were stably infected with indicated shRNA targeting Tiam2 or non-targeting control pLKO.1. (A) Invasion filter scans of MDA-MB-231 cells after invasion through Matrigel for 16 hours. Filters were fixed and stained with methylene blue. (B) Stable cells were lysed and analyzed by western blot with the indicated antibodies.

Depletion of Tiam2 using shRNA

Thus far, only chemically synthesized duplex siRNAs have been used to deplete Tiam2 mRNA, and in turn its translated protein product. In order to increase confidence in the observed inhibition of invasion in MDA-MB-231 cells, small hairpin RNAs (shRNA) were utilized as an alternate method to deplete Tiam2 protein. Five different plasmids containing hairpins targeted against Tiam2 were obtained and virus produced by transfection into HEK293T cells along with VSV-G and Gag/Pol. The viral particles were purified from the growth media and used to infect MDA-MB-231 cells. A stable cell line was generated after puromycin selection for 2 weeks. These stable cell lines were then assayed for invasion using the modified Boyden chamber. Cell lines expressing hairpins against Tiam2 were able to invade through Matrigel to the same extent as cells expressing control pLKO.1 non-targeting hairpin (Figure 18, panel A). Protein levels were determined by western blot and this revealed that hairpins sh-10 and sh-13 strongly depleted Tiam2 protein. Hairpin sh-12 reduced Tiam2 levels only modestly, and sh-11 and sh-14 were similar to the control non-targeting hairpin (Figure 18, panel B). This result conflicts with the data obtained with siRNA, and raises doubt that Tiam2 plays a role in MDA-MB-231 cell invasion.

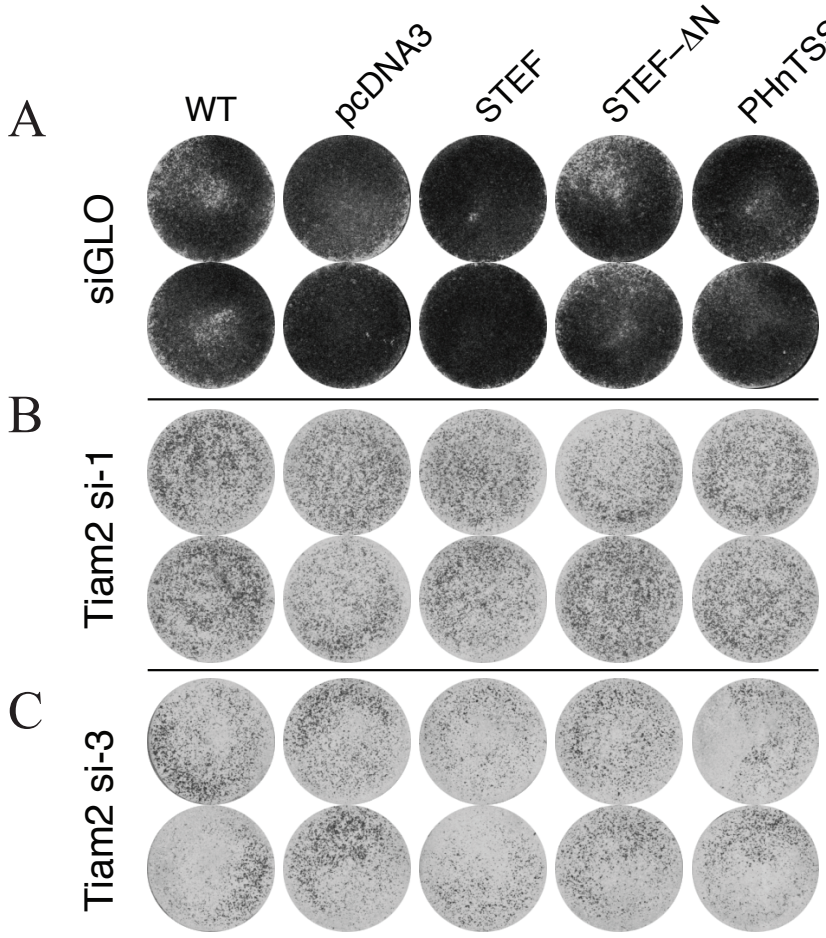

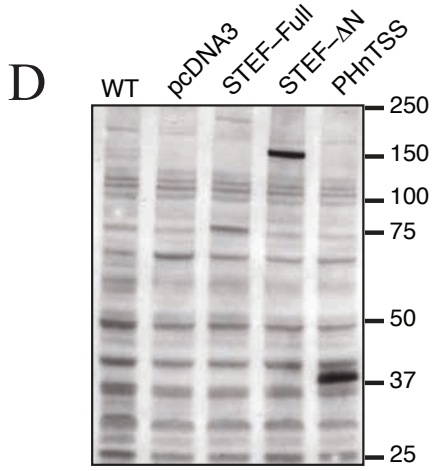

E

```
Tiam2 si-1
mouse   G AAC TTC CGG CGC CAC ATA
human   G AAC TTC AGG CGT CAC ATA


Tiam2 si-3
mouse   G TGT AAG GAC CGG CTA GTA
human   G TGT AAG GAT CGC CTG GTA
```

Figure 19: STEF cannot rescue invasion lost by Tiam2 siRNA

MDA-MB-231 cells stably expressing the indicated plasmids were treated with siRNA targeted against Tiam2 si-1, si-3, or control siGLO. (A-C) Invasion filter scans of MDA-MB-231 cells after invasion through Matrigel for 16 hours. Filters were fixed and stained with methylene blue. (D) Stable cells were lysed and analyzed by western blot with anti-HA antibody. (E) Aligned mouse STEF and human Tiam2 sequences in regions targeted by siRNA. Differences indicated in red.

Rescue of Invasion by STEF expression

To directly assess whether the defect in invasion seen with siRNA is due to specifically depleting Tiam2 or to an off-target effect, an attempt was made to rescue invasion of MDA-MB-231 cells using the mouse ortholog of Tiam2, STEF. Mouse STEF harbors sequence variations compared to human Tiam2 that should render it insensitive to the siRNA (Figure 19, panel E). The laboratory of M. Hoshino graciously provided three expression plasmids for: full-length STEF, STEF with an N-terminal deletion (ΔN), and a short internal fragment containing the PH, coil-coiled, and Ex domains (PHNTSS). These three HA-tagged constructs, along with a pcDNA3 control, were stably expressed in MDA-MB-231 cells after selection with puromycin. Each stable cell line was transfected with siGLO, Tiam2 si-1, or Tiam2 si-3 duplex siRNA and assayed for invasion using a modified Boyden chamber assay. All the cell lines maintained the ability of the parental MDA-MB-231 line to invade (Figure 19, panel A). In all cell lines, however, transfection of Tiam2 si-1 and si-3 siRNA still strongly decreased the number of cells that were able to invade through Matrigel (Figure 19, panels B and C). Western blots were used to determine the expression level of the HA-tagged STEF constructs (Figure 19, panel D). Full-length STEF expressed very weakly at ~190 kDa. The N-terminal truncation expressed at levels similar to the PHnTSS construct at ~150 kDa and ~40 kDa, respectively. Human Tiam2 and mouse STEF antibodies are not cross-reactive, making it difficult to determine if STEF is expressed at levels similar to endogenous Tiam2. Expression of STEF at a lower level than endogenous Tiam2 could be an explanation for the failure to rescue invasion. It was not determined whether or not the 2–3 base pair differences were sufficient to render STEF resistant to Tiam2 si-1 or si-3 due to the availability of reagents to perform a similar experiment with human Tiam2 (see below). Although this data does not support a specific role for Tiam2, it is possible that mouse STEF protein was not expressed at high enough levels or, less likely, that it is functionally unable to compensate for loss of the human protein.

Rescue of Invasion by siRNA resistant human Tiam2

To address the concern that mouse STEF may not be able to rescue the function of human Tiam2 protein, a rescue experiment was performed using siRNA-resistant human Tiam2. A plasmid containing the cDNA for full-length human Tiam2 was obtained from Open Biosystems and mutations were introduced to create mismatches between it and siRNAs si-1 and si-3 (rendering the mRNA resistant to degradation) without altering the encoded amino acids (Figure 20, panels D & E). Mutagenesis was performed using PCR, and confirmed by Sanger sequencing. Tiam2-AB was designed to be resistant to si-3, and Tiam2-CD resistant to si-1. These sequences were sub-cloned into the pBabe retroviral expression vector and transfected into HEK293T cells along with VSV-G and Gag/Pol plasmids. The resulting viral particles were purified and used to infect MDA-MB-231 cells. Stable cell lines emerged after selection for 8 days in puromycin.

The stable cell lines were each transfected with Tiam2 si-1, Tiam2 si-3, Cdc42 SMARTpool, and siGLO control alongside an untransfected control and assayed for invasiveness (Figure 20, panels A-C). Tiam2 si-1, si-3 and Cdc42 SMARTpool were all equally effective at reducing the number of cells that invaded through Matrigel in all cell lines. Western blot analysis showed that Tiam2-AB was resistant to depletion by Tiam2 si-3 with three mismatched bases, but still sensitive to depletion by si-1 (Figure 20, panels C & E). Surprisingly, Tiam2-CD was only partially resistant to degradation by Tiam2 si-1 with four mismatched bases (Figure 20, panels B & D), and still fully sensitive to si-3 depletion. Tiam2 protein was not fully resistant in the Tiam2-CD cell line, but no increase in the number of invading cells was observed as compared to untransfected and to siGLO control treated cells. Even though western blot analysis shows that the Tiam2-AB cell line was fully resistant to Tiam2 siRNA depletion, no increase in invaded cells was observed. These results show that siRNA-resistant Tiam2 is unable to rescue the invasion defect caused by

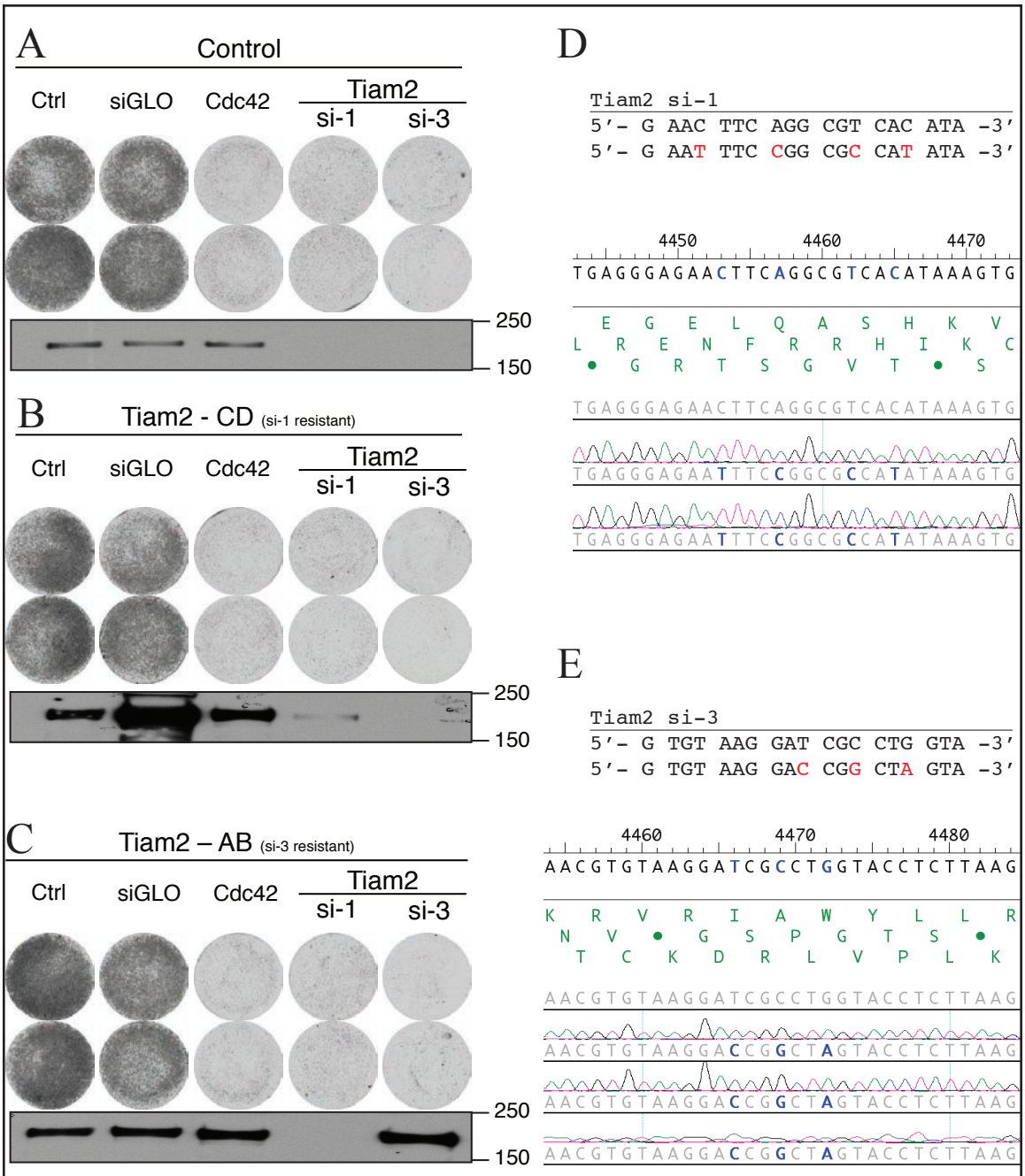

Figure 20: Human Tiam2 cannot rescue invasion lost by Tiam2 siRNA

MDA-MB-231 cells stably expressing the indicated plasmids or control (pBabe empty vector) were treated with siRNA targeted against Tiam2 si-1, si-3, using siGLO and Cdc42 as positive and negative controls, respectively, as well as untreated cells. (A-C) Invasion filter scans of MDA-MB-231 cells after invasion through Matrigel for 16 hours. Filters were fixed and stained with methylene blue. Transfected cells were analyzed by western blot using anti-Tiam2 antibody. (D & E) Tiam2 sequences targeted by si-1 and si-3. Mutations created are indicated in red. Sanger Sequencing was performed to confirm the mutated Tiam2 sequences.

Tiam2 si-1 and si-3 siRNA. This data suggests that Tiam2 is not involved in invasion, and that the previous results represented a false positive effect of two distinct siRNAs. The level of siRNA-resistant Tiam2 protein expression was expressed at higher levels than endogenous Tiam2, ruling out an expression problem in the rescue experiments. A final alternative explanation for the failure of these wild-type Tiam2 plasmids to rescue the invasion phenotype could be that endogenous Tiam2 is mutated in a way that alters its function.

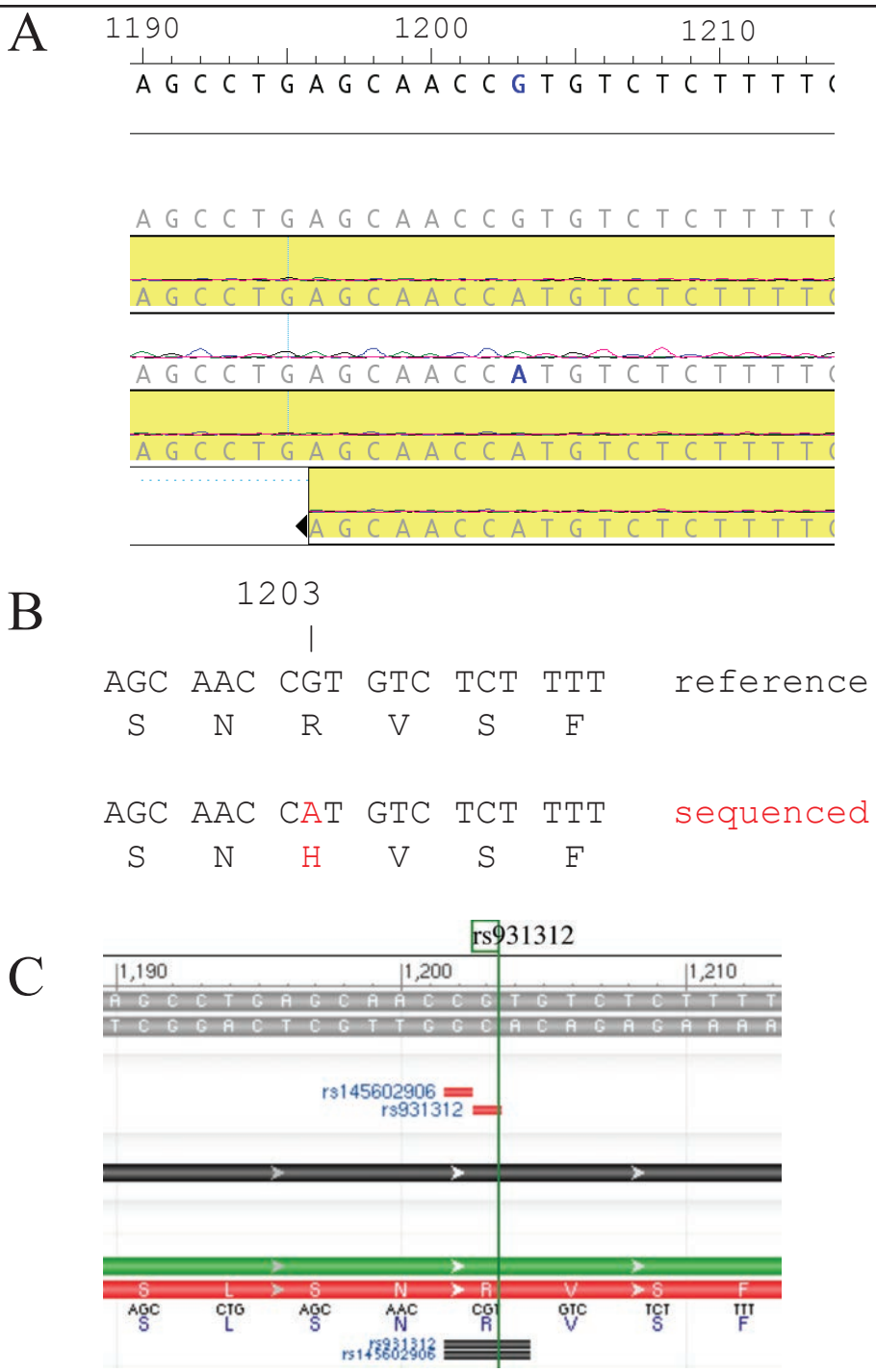

Figure 21: Sequencing of Tiam2 from MDA-MB-231 cells

RNA was isolated from MDA-MB-231 cells and a library of expressed cDNA fragments was generated by reverse transcription. (A) Sanger sequencing of the Tiam2 reverse-transcribed mRNA. (B) Reference NM_123454.3 sequence aligned with the sequence of Tiam2 isolated from MDA-MB-231 cells indicating the translated proteins. Differences are indicated in red. (C) Database dbSNP search revealed a known SNP rs931312 matches the observed mutation.

Sequencing of genomic Tiam2 in MDA-MB-231 cells

To determine whether MDA-MB-231 cells might harbor a mutation in Tiam2, mRNA was purified from MDA-MB-231 cells and subjected to reverse transcription. PCR primer pairs were designed (with the help of Agnes Viale, MSKCC GCL) to amplify ~1000 bp fragments of Tiam2 which were then sequenced and assembled to achieve full coverage of the expressed Tiam2. The sequencing results revealed one difference between the reference sequence NM_012454.3 and endogenous Tiam2 from MDA-MB-231 cells (Figure 21, panel A). This mutation is G to A at position 1203 in the reference sequence. At the protein level, this results in substitution of arginine to histidine at position 332 (Figure 21, panel B). Both histidine and arginine are basic residues, making this a conservative substitution. The database dbSNP identifies this mutation as SNP rs931312 (Figure 21, panel C), indicating that this is a recognized genetic variation. The remainder of the Tiam2 sequence exactly matched the reference sequence. Position 332 is located in a region devoid of any known functionally folded domain. The conservative nature of this mutation and the lack of any association between the reported SNP and any pathology suggested that this mutation was unlikely to significantly alter the function of Tiam2, so it was pursued no further. Only a rescue experiment showing functional rescue of invasion after incorporating this change into the siRNA-resistant Tiam2 expressed would conclusively rule-out the possibility that Tiam2 is involved in MDA-MB-231 invasion.

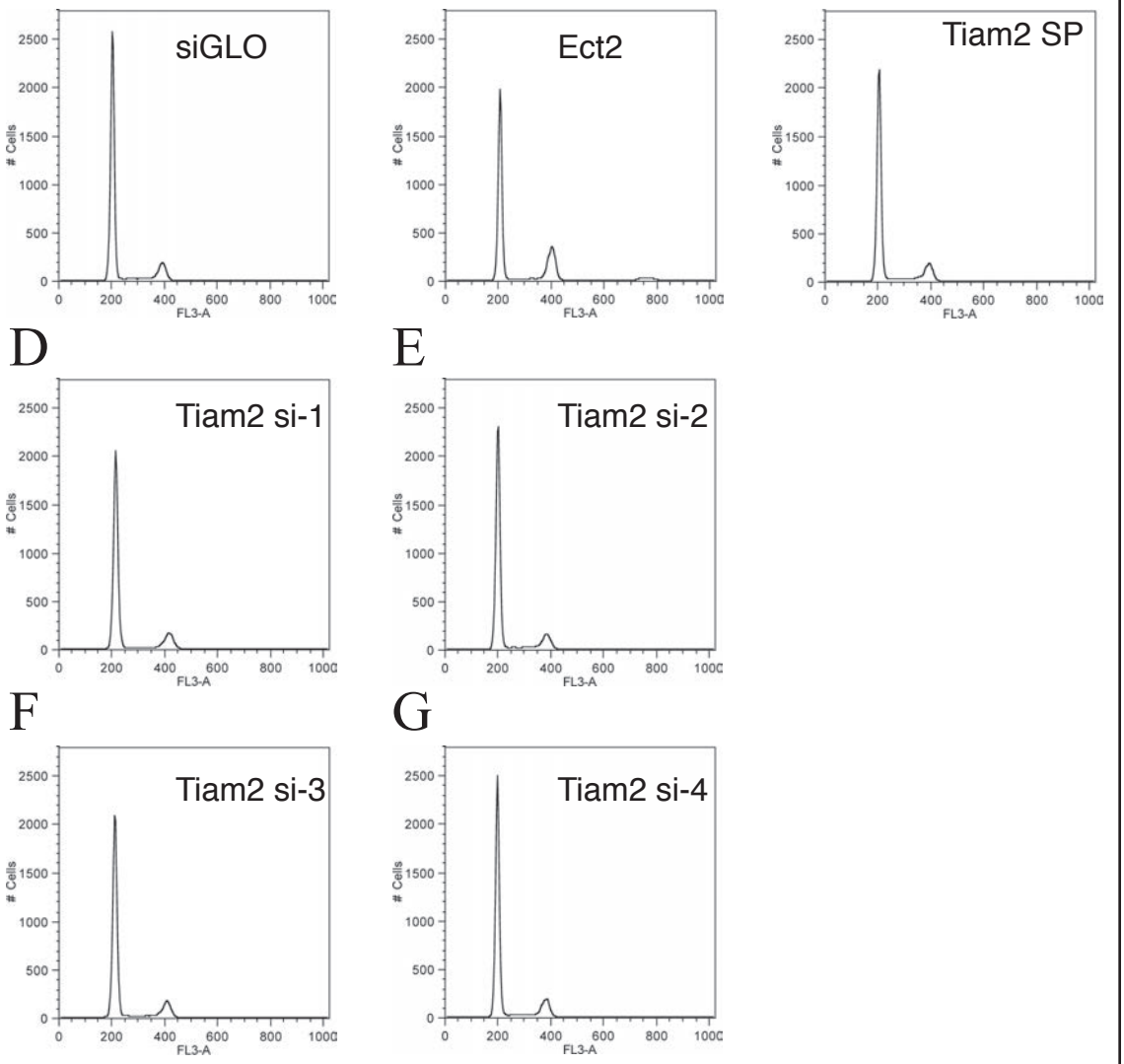

H

	%G1	%S	%G2	%<G1	%>G2
siGLO	60.9	19.3	12.0	0.8	6.3
Ect2	62.7	9.1	21.8	0.7	6.4
Tiam2 SP	65.3	16.3	13.2	0.9	3.6
Tiam2 si-1	75.0	8.2	11.3	1.9	2.8
Tiam2 si-2	65.3	16.1	11.5	1.9	3.9
Tiam2 si-3	70.0	13.0	11.2	3.0	3.2
Tiam2 si-4	65.5	15.8	12.4	1.8	4.5

Figure 22: Tiam2 affects cell-cycle progression

MDA-MB-231 cells were transfected with indicated siRNAs using Ect2 as a control for inhibition of cell cycle. (A-G) Cell-cycle plots of cells stained with propidium iodide to quantify DNA. (H) Quantification of the cell-cycle plots.

Effect of Tiam2 on Cell Proliferation

During the course of these studies, Tiam2-depleted cells were found to proliferate more slowly than controls. Since a possible role for Tiam2 in cell proliferation would be significant with respect to breast cancer, this possibility was examined directly. The siRNA SMARTpool or individual duplexes targeting Tiam2 were transfected into MDA-MB-231 cells along with control siGLO or Ect2 SMARTpool as negative and positive controls, respectively. Depletion of Ect2 blocks cytokinesis, which increases the number of multinucleated cells (%>G2). Four days after siRNA transfection, cells were fixed, stained with propidium iodide, and analyzed by FACS for DNA content. Compared to siGLO control, Ect2 treated cells showed an increase in %G2 cells and a decrease in %S phase cells (Figure 22, panels A & B). Tiam2 SP, si-2, and si-4 showed a slight increase in %G1 cells, and a slight decrease in %S phase, but no other appreciable differences (Figure 22, panels C, E, & H). Tiam2 si-1 and si-3, however, showed a modest decrease in %G2 cells and a stronger decrease in %S phase cells, which is strongest in si-1 treated cells (Figure 22, panels D & F). These results are quantified and tabulated in Figure 22, panel H. This data, along with the fact that si-1 and si-3 strongly deplete Tiam2 protein, suggests that Tiam2 may play a role in cell proliferation.

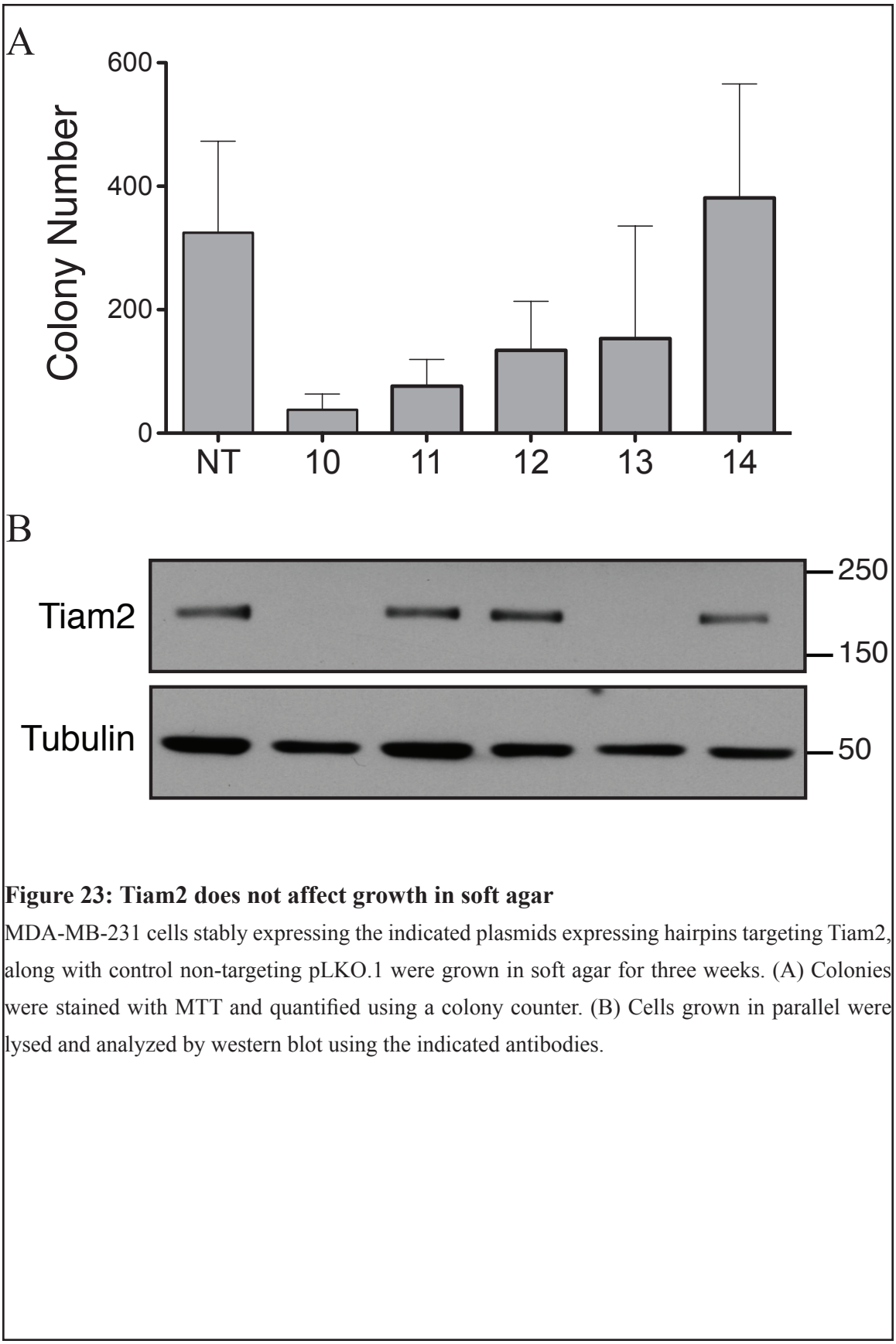

Figure 23: Tiam2 does not affect growth in soft agar

MDA-MB-231 cells stably expressing the indicated plasmids expressing hairpins targeting Tiam2, along with control non-targeting pLKO.1 were grown in soft agar for three weeks. (A) Colonies were stained with MTT and quantified using a colony counter. (B) Cells grown in parallel were lysed and analyzed by western blot using the indicated antibodies.

Effect of Tiam2 on Colony Formation in Soft Agar

To determine whether Tiam2 plays a role in anchorage-independent growth, I performed a soft agar colony formation assay. MDA-MB-231 cells stably expressing shRNA targeted against Tiam2 were grown in soft agar for three weeks (Figure 23). Samples were stained with MTT (3-(4,5-Dimethylthiazol-2-yl)-2,5-diphenyltetrazolium bromide), scanned, and counted using a colony counter. Western blot analysis revealed that sh-10 and sh-13 were the only two hairpins that effectively depleted Tiam2 protein levels. Hairpin sh-10 most strongly inhibited colony formation, and sh-13 also reduced colony formation compared to controls. However, hairpins sh-11 and sh-12 also inhibited colony formation, but without depleting of Tiam2 protein. The lack of correlation between colony number and the level of Tiam2 protein expressed suggests that Tiam2 does not play a role in anchorage-independent growth.

Effect of Tiam2 on Tumor formation in Mice

All the assays performed thus far have studied the behavior of cells using in vitro assays. To determine whether Tiam2 plays a role in tumor formation more directly, we employed an orthotopic xenograft model of tumor formation. MDA-MB-231 cells stably expressing hairpins Tiam2 sh-10 and sh-13, which were previously shown to strongly reduce the level of Tiam2 protein, were mixed with Matrigel and bilaterally injected into the mammary fat pads of NOD/SCID mice (Q. Chang & M. Berishaj, J. Bromberg Lab, MSKCC). Tumors were palpated weekly, and after 11 weeks the mice were sacrificed and the tumors were dissected and weighed (Figure 24, panel A). Tumors expressing sh-10 weighed approximately 40% less than tumors expressing non-targeting control shRNA vector pLKO.1. Western blot analysis of harvested tumor tissue shows that 3 of the 4 tumors had increased expression of Tiam2 compared to control tumors (Figure 24, panel B). This is surprising as tumor cells not only regained Tiam2 expression, but also up-regulated the protein in half the tumors analyzed. Tumors expressing sh-13, on the other hand, weighed 200% more than tumors expressing control shRNA (Figure 24, panel A). Western blots showed that Tiam2 was largely absent in all sh-13 expressing tumors (including one mammary metastasis), presumably due to stable expression of the shRNA (Figure 24, panel B). These results suggest a role for Tiam2 in tumor suppression, since the sh-10 tumors were smaller and showed higher Tiam2 expression than controls, while the inverse was true for sh-13 tumors.

To determine if Tiam2 overexpression can suppress tumor formation, similar orthotopic xenograft experiments were performed using Tiam2 overexpressing MDA-MB-231 cells. The cell lines Tiam2-AB and Tiam2-DC were originally generated to perform the siRNA rescue experiments (Figure 24, panel C). Prior to injection, the level of Tiam2 expression in each of the cell lines was determined by western blot. The Tiam2-AB cell line showed in-

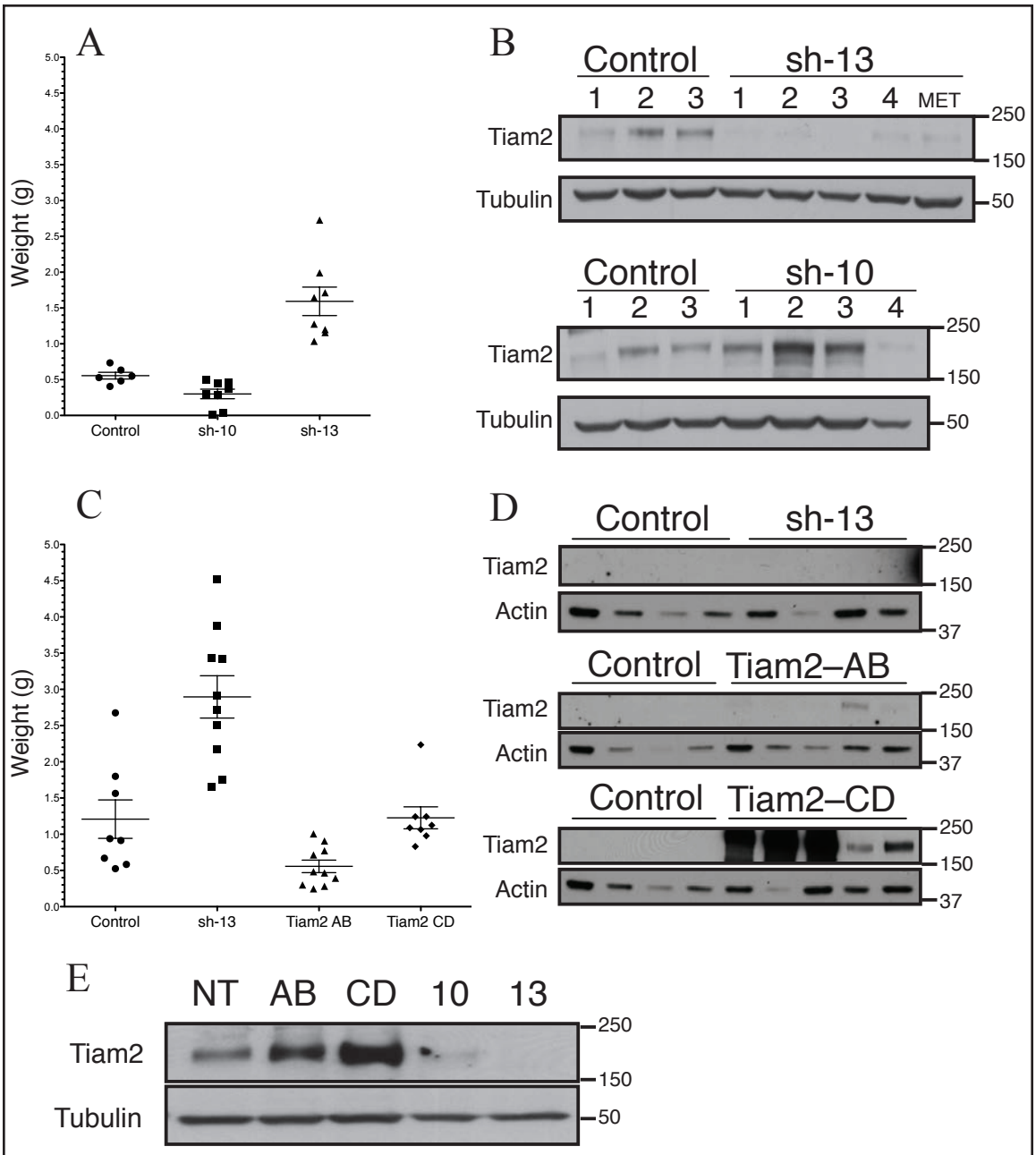

Figure 24: Effect of Tiam2 expression in Xenografts

NOD/SCID mouse mammary fat pads were bilaterally injected with MDA-MB-231 cells stably expressing the indicated plasmids and tumors were grown for 11 weeks. (A, C) Dissected tumors were weighed. (B, D) Tumor fragments were lysed and analyzed by western blot using the antibodies indicated. (E) Before injection, expression of the indicated constructs was confirmed by western blot using the antibodies indicated.

creased Tiam2 levels compared to control, and the expression in the CD cell line was even further elevated (Figure 24, panel E). Cell lines expressing sh-10 and sh-13 both expressed very low levels of Tiam2. Unfortunately, the Tiam2 sh-10 cell line became contaminated in cell culture during expansion so it was destroyed. The four remaining cell lines were bilaterally injected into the mammary fat pad of NOD/SCID mice as before, and allowed to grow for 11 weeks. Tumors expressing sh-13 grew to more than double the size of control tumors, consistent with the previous experiment (Figure 24, panel C). Tumors expressing Tiam2-AB were half the weight of control tumors, but Tiam2-CD expressing cells formed tumors that were the same weight as control. Western blot analysis showed that control tumors had lost expression of Tiam2, with levels similar to sh-13 tumors (Figure 24, panel D). Similarly, only one of the five Tiam2-AB tumor samples showed any appreciable Tiam2 protein. The Tiam2-CD cell line, however, showed strong Tiam2 expression in three of the five tumors, with moderate expression in the other two. If Tiam2 was important for tumor formation or proliferation in this mouse model, the protein levels should correlate with the weight of the tumor. These data show no correlation between Tiam2 protein levels and tumor size, suggesting that Tiam2 expression does not influence tumor formation or growth.

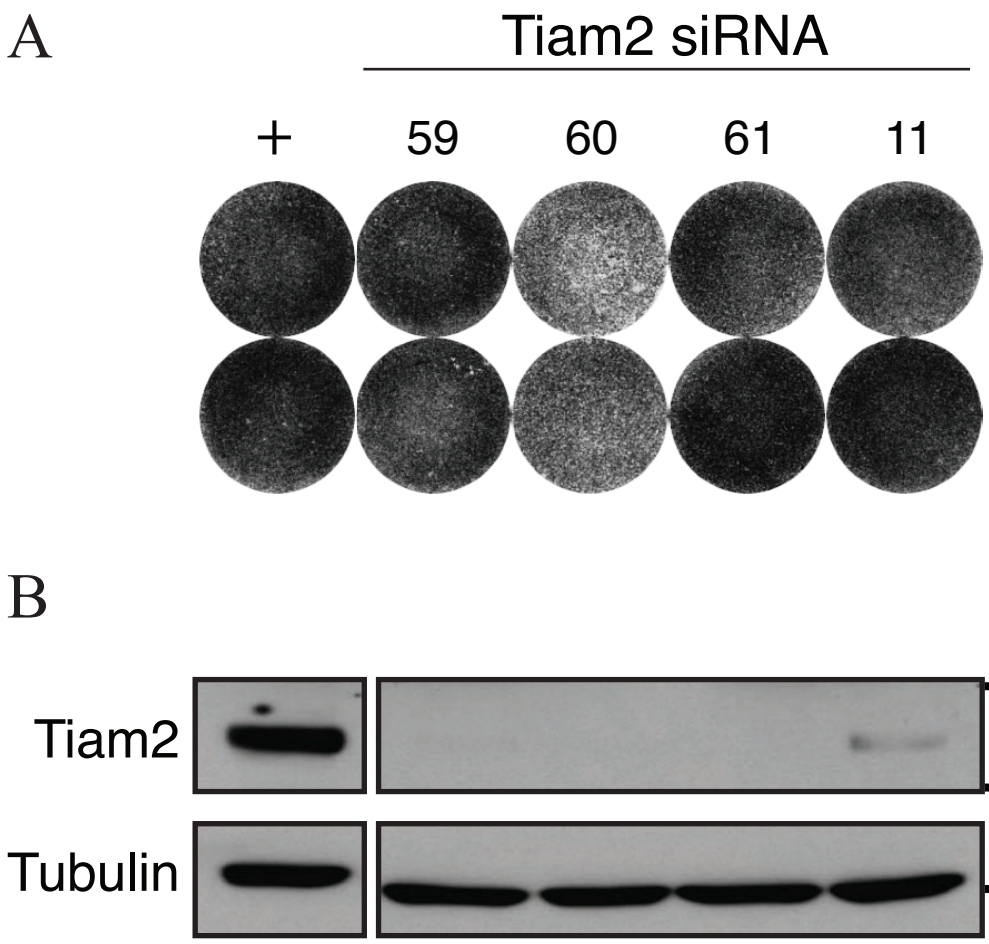

Figure 25: Expanded panel of Tiam2 siRNA

MDA-MB-231 cells were transfected with indicated siRNAs and control (+) siGLO. (A) Invasion filter scans of MDA-MB-231 cells after invasion through Matrigel for 16 hours. Filters were fixed and stained with methylene blue. (B) siRNA depleted MDA-MB-231 cells were lysed analyzed by western blot with Tiam2 (top) and Tubulin (bottom) antibodies.

Expanded panel of siRNA targeting Tiam2 and Invasion

Taken together, the data presented so far fails to offer a clear picture of whether or not Tiam2 depletion or overexpression has any specific effect on MDA-MB-231 cell invasion or proliferation. To clarify whether Tiam2 depletion affects invasion, four additional siRNAs were designed using a different targeting algorithm. Ambion SilencerSelect siRNA numbers 59, 60, 61, and Dharmacon OnTarget-Plus number 11 all effectively deplete Tiam2 protein (as evidenced by western blot) but have little effect on the ability of MDA-MB-231 cells to invade (Figure 25).

Discussion

Tiam2 siRNA Experiments

Tiam2 emerged as a likely candidate in a siRNA screen for regulators of invasion in MDA-MB-231 cells. In order to validate this result, the RNAi data was further tested as follows. While many of the candidate molecules could be excluded from consideration at an early stage, Tiam2 required closer consideration. Two siRNA duplexes (Tiam2 si-1 and si-3) were capable of depleting the protein and inhibiting invasion, while si-4 did not deplete Tiam2 protein nor did it inhibit invasion. Of some concern, duplex si-2 strongly reduced Tiam2 protein levels but showed only a modest inhibition of invasion. Four additional siRNAs that successfully reduced Tiam2 protein levels but did not interfere with MDA-MB-231 cell invasion, indicated that the effects of si-1 and si-3 on invasion were most likely unrelated to Tiam2 levels (Figure 25).

Tiam2 shRNA Experiments

Chemically synthesized siRNA can be easily transfected into cells to specifically reduce protein levels, but the knockdown achieved is transient. Sustained gene silencing can be achieved by vector based encoding of short hairpin RNA (shRNA), which is continually processed into siRNA within the cell to deplete protein levels [184]. Only two of the five shRNAs used in the study were able to successfully sustain Tiam2 knockdown in MDA-MB-231 cells. Neither hairpin, however, was able to inhibit the ability of cells to invade through Matrigel, reducing confidence that the effects of Tiam2 observed with siRNA were specific. Additionally, the soft agar assays showed wide variation in the number of colonies formed with any of the hairpins, indicating that Tiam2 was unlikely to play a role in anchorage independent growth.

The hairpin nature of the shRNA creates some risks for recombination, however, so care must be taken both when using molecular biology to manipulate plasmids containing the hairpins as well as monitoring the cellular expression and interpreting results. Often the hairpins are encoded by viral plasmids, allowing integration into the genome along with an antibiotic resistance gene allowing for straightforward creation of stable lines. One caveat to this approach is that the antibiotic resistance gene may be retained while recombination destroys the hairpin or expression becomes suppressed by other means (i.e. epigenetic silencing) if it is detrimental to cell health. Additionally, other genetic alterations may accumulate over time and allow the cell to compensate for the depletion of the specific gene. As with siRNAs, off-target effects are a serious concern, so multiple hairpins should be used in combination with other reagents to increase the confidence in attributing a specific phenotype to protein function.

Tiam2 Rescue Experiments

Even though the use of multiple individual RNAi reagents to inhibit gene expression is widely used to draw conclusions about gene function, much more confidence can be obtained by re-expression of a resistant gene that rescues the function and restores the phenotype of interest [185]. Often, another mammalian ortholog (usually mouse or rat) will have the same function as the gene of interest, but its genetic sequence will vary from that targeted by the human siRNA. It is unclear whether the mouse ortholog of Tiam2, STEF, could functionally substitute for Tiam2 in MDA-MB-231 cells after depletion by si-1 or si-3. Plasmids encoding human Tiam2 became available commercially, and these were used for further rescue experiments rather than using STEF. It was necessary to mutate the human sequence to render it resistant to the siRNA targeting sequence. The exact number and position of base pair mismatches required to ensure a gene is fully protected from silencing is still unclear. [186] In the case of Tiam2-CD, even with four mismatches there was still considerably lower Tiam2 expression than control after treatment with si-1. For Tiam2-

AB, however, just three mismatches were sufficient to protect the protein from degradation by si-3. This might relate to the position of the mutated nucleotide within the siRNA duplex, which is dictated in this case by the amino acids encoded.

Even though the protein level was unchanged for Tiam2-AB after treatment with si-3, the invasion phenotype did not return. One explanation for this is that appropriate expression levels may not be achieved by exogenous expression systems. Even if expressed at a level approaching the endogenous protein, some exogenously expressed proteins are not properly localized or modified in the same way due to the presence of epitope tags. Furthermore, especially when dealing with cancer cells, the gene of interest may harbor a mutation that changes its function.

Sequencing Endogenous Tiam2

To rule out the possibility that a mutation in Tiam2 that might, for instance, cause it to become aberrantly activated, this gene was sequenced from MDA-MB-231 cells. Only one base pair was found to be different from the reported reference sequence, resulting in an amino acid change from arginine to histidine. Although both amino acids residues are similarly polar and basic, any change might affect protein function. Database searches showed that this mutation matches a reported single nucleotide polymorphisms (SNPs) but was not associated with any disease. While other studies have linked arginine to histidine mutations to gene function in cancer [187, 188], these mutations occur within folded protein domains. This mutation falls outside of any known functional domains of Tiam2 so the likelihood that this fairly conservative mutation has an effect on protein function is low, yet has not formally been ruled out.

Other Effects of Tiam2

While preparing MDA-MB-231 cells for loading into invasion chambers, consistently, fewer cells were observed growing in samples transfected with Tiam2 si-1 and si-3 siRNA. This suggested that the invasion phenotype might be related to a defect in cell growth. To test this hypothesis, cells were subjected to cell-cycle analysis by staining the DNA content with propidium iodide and analyzed using FACS. Depletion of Tiam2 by si-1 and si-3 resulted in an increase in %G1 cells, suggesting that the effect occurred prior to DNA synthesis in S phase. Depletion of Tiam2 using si-2 effectively reduced the protein level but had a much weaker effect on cell cycle progression. The si-2 phenotype was again inconsistent with si-1 and si-3, and since the si-2 duplex was shown to confer an off-target invasion phenotype, its effect was questioned. The observed delay in the G1 phase offers insight into how Tiam2 might be functioning, but growth in 2D is very different from tumor physiology.

The ability of cells to grow in soft agar is a hallmark of malignant transformation and uncontrolled growth. To explore whether Tiam2 depletion inhibits anchorage independent growth, soft agar growth assays were utilized. The challenge experimentally is that siRNA effects typically last 7-10 days under the best circumstances. Soft agar growth assays last for 21 days, so treatment with siRNA would delay colony formation and at best we could expect to observe an approximately 50% reduction in colony number. Using shRNA to stably deplete Tiam2 levels should allow for a greater percentage difference from control cells. Four hairpins (sh-10,11,12,13) all inhibited colony growth to various degrees. However, this phenotype did not correlate with protein levels, as only expression of sh-10 and sh-13 lowered the level of Tiam2 protein.

While anchorage independent growth is considered the best in vitro assay to study tumor formation, may other factors that contribute to tumor development are absent from such

a model. Specifically, the critically important contributions from the tissue stroma and associated fibroblasts are absent in this model. [189]

In order to address the weakness of the soft agar model and directly probe the role of Tiam2 in tumor biology, I used an orthotopic xenograft model of tumor growth. The mouse xenograft model system better represents the human tumor environment. I chose orthotopic injection of MDA-MB-231 cells into the mammary fat pad to maintain physiological relevance as closely as possible even though it is more complex and time consuming. In contrast, tail vein injection is less invasive, but immediately introduces cancer cells into the circulation of animals, better facilitating the study of tumor burden and late-stage metastasis. [190] The orthotopic injection model allows the formation of a primary tumor as well as metastasis to be studied. [191] This model incorporates all stages of tumor progression, from initiation through intravasation and extravasion, and eventually metastasis formation.

While mouse tumor models are more representative than any in vitro study of cancer biology, they are not without drawbacks. One important consideration is that the mouse stromal contribution may not completely mimic that found in humans. Similarly, introduction of human cells into a mouse requires the use of immunodeficient animals. Ignoring the contribution of immune cells to tumor biology is a necessary consequence in this system, but it should be kept in mind that the immune system can play both positive and negative roles in human tumor progression. [192] Despite these caveats, this model system has been used extensively to study the role of many proteins in tumor formation, proliferation, and metastatic invasion.

The experiments performed using hairpins sh-10 and sh-13 in suggested that decreased expression of Tiam2 resulted in larger tumors that were able to metastasize into other lobes of the breast. During dissection, no obvious metastatic lesions were visible on the lungs.

Interestingly, 75% of the tumors expressing sh-10 regained expression of Tiam2. This was unexpected because all earlier evidence suggested depletion of Tiam2 slowed the growth of MDA-MB-231 cells, in which case loss of sh-10 expression would have been expected to result in larger tumors. Since sh-10 tumors express high levels of Tiam2 and yield small tumors, compared to very large tumors with low Tiam2 expression (from sh-13), it is possible that Tiam2 plays a role as a tumor suppressor in vivo. Alternatively, hairpin sh-10 may be unstable without constant puromycin selection pressure, which was discontinued after injection into mice.

To test the hypothesis that Tiam2 overexpression inhibits tumor growth, the orthotopic xenograft experiments were repeated using the MDA-MB-231 cell lines that exogenously express Tiam2. However, Tiam2-CD expressing tumors, which had very high levels of Tiam2 protein, were indistinguishable in size from control tumors.

It is not always possible to predict how protein expression will affect tumor biology in vivo based on in vitro studies. These experiments might have been more revealing had it been possible to measure tumor size throughout the growth process rather than only at the endpoint. To do this, it would have been necessary to use cell lines with a reporter such as luciferase or GFP (green fluorescent protein). This would have facilitated imaging of metastasis to other sites such as the lungs, bones, or brain. Additionally, an inducible expression system would have allowed Tiam2 levels to be modulated after tumor initiation. While the studies reported here could have been improved, the data collected strongly suggest that there is no clear role for Tiam2 either in tumor proliferation or invasion, and that the initial observations using siRNA reagents were likely due to off-target effects.

Chapter 5: Tiam2 Expression and relationship to Ras

The data presented in Chapter 4 suggest that Tiam2 does not have a specific function in invasion or proliferation. However, this does not exclude the possibility that Tiam2 plays a role in breast cancer. In order to further explore this possibility, Tiam1 and Tiam2 expression was studied in breast, and other cancer cell lines, and the mechanisms regulating its expression were investigated.

Expression of Tiam1/2 proteins in Breast Cell lines

Little is known about Tiam2 protein expression levels in breast cancer. Originally, Tiam2 was reported to be expressed only in brain and testis, [182] so it was surprising to find expression in breast cancer. The related protein, Tiam1, is a Rac GEF both in vivo and in vitro. [193] To determine whether Tiam2 expression is common among breast cancer cells, a panel of normal and breast cancer cell lines with different mutational status was assembled. MCF-10a and HMEC cell lines represented normal breast cells, since they do not express oncogenes, but they do express estrogen receptor (ER), progesterone receptor (PR) and human epidermal growth factor receptor 2 (HER2). The MDA-MB-231 cell line used throughout this work has functional p53 tumor suppressor, but is classified as "triple negative", i.e. lacking expression of ER, PR, and HER2. [194, 195] This cell line also harbors an active Ras mutation, which is not typical in breast cancer. The BT-474 cell line has normal Ras and hormone receptor expression, but lacks the tumor suppressor p53 and expresses mutant phosphatidylinositol 3-kinase (PI3K). SkBr3 cells do not express ER or PR, but have normal HER2 levels. SKBr7 and Hs578t cells do not express functional p53, they are triple negative, and both harbor an activating Ras mutation. The mutational status of these cell lines is summarized in Figure 26, panel A. Remarkably, western blot

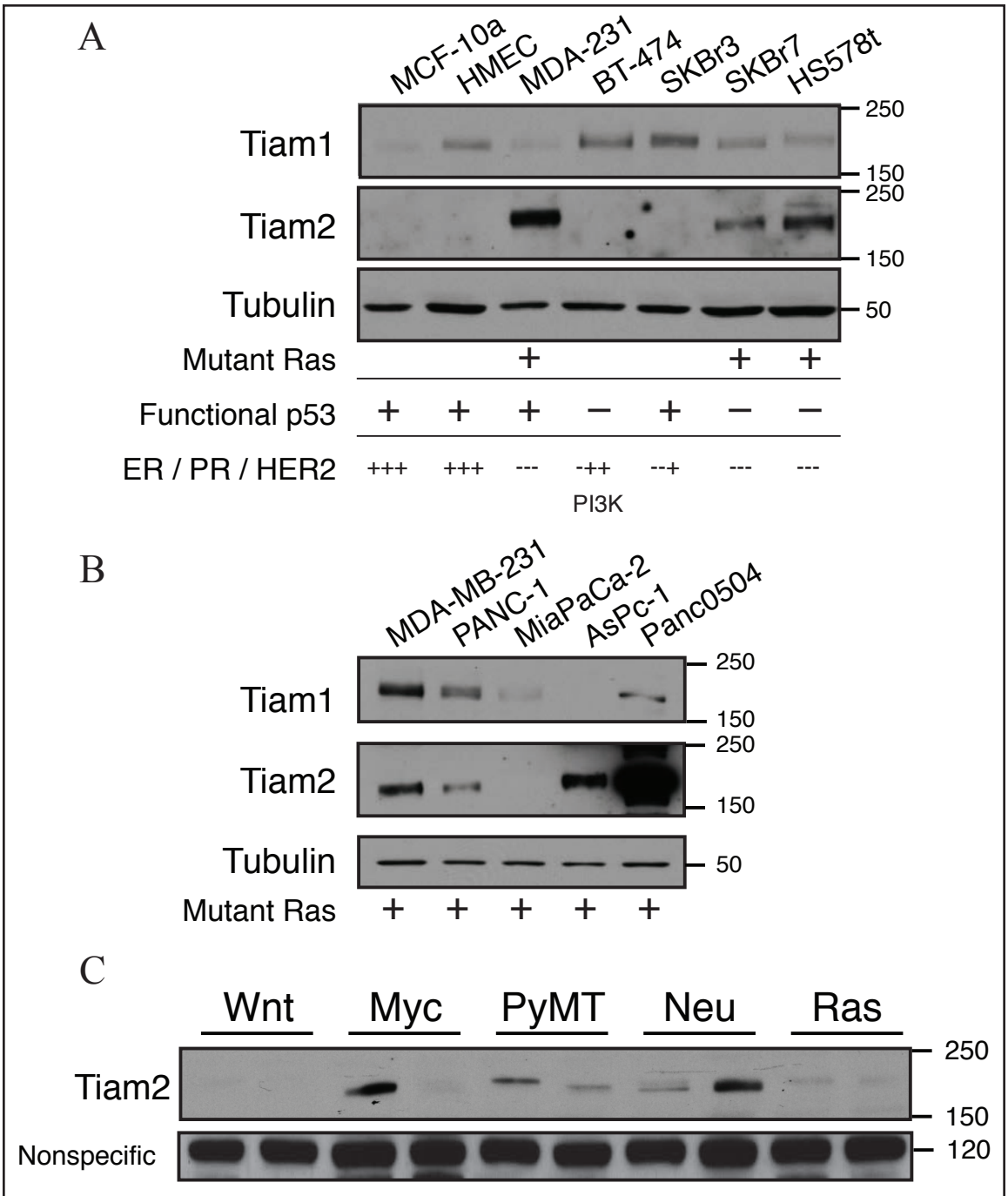

Figure 26: Tiam2 is expressed in Ras mutant cell lines

(A) A panel of indicated breast cell lines were lysed and analyzed by western blot analysis using antibodies against Tiam1, Tiam2, and Tubulin as a loading control. The mutational status of each of the cell lines is listed below. (B) A panel of indicated pancreatic cell lines were lysed and analyzed by western blot using the same antibodies as above. (C) Mammary gland tumors from mice expressing the indicated oncogenes from the MMTV promoter were lysed and analyzed by western blot using an anti-Tiam2 antibody.

analysis revealed no expression of Tiam2 in the "normal" breast or any cancer lines except MDA-MB-231, Hs578t, and SkBr7. Intriguingly, all three of these cell lines harbor Ras mutations. Tiam1 expression is higher in cell lines with normal Ras, and lower in the Ras-mutant cell lines SkBr7, Hs578t, and MDA-MB-231 (Figure 26, panel A). These data raise the possibility that mutant Ras is linked to the expression of Tiam2.

Expression of Tiam1/2 proteins in other cancer models

While mutant Ras is uncommon in breast cancer, it is prevalent in pancreatic cancers. [196] To determine if Ras-dependent Tiam2 expression is important generally or if it is specific to breast cancer, a panel of pancreatic cells was assembled. The M. Resh lab generously provided the PANC-1, MiaPaCa-2, AsPc-1, and Panc0504 cell lines, all of which harbor Ras mutations. [197] Western blot analysis revealed that Tiam2 is most strongly expressed in Panc0504 cells (Figure 26, panel B). AsPc-1 cells expressed Tiam2 at levels similar to MDA-MB-231 breast cancer cells, while PANC-1 cells showed weaker expression. Tiam1 expression in PANC-1 and Panc0504 cell lines was lower than that in MDA-MB-231 cells. MiaPaCa-2 cells show very low expression of Tiam1, while AsPc-1 cells had undetectable protein levels. This data suggests that Tiam2 expression is high in a subset of mutant Ras expressing pancreatic cell lines. Thus Tiam2 levels may be associated with Ras mutational status in multiple cancer types, but the correlation is not perfect.

Both of the previous methods used to test the link between Tiam2 and Ras were performed in cell lines. To determine if a similar link is present in vivo, we attempted to use a mouse model of breast tumor formation. The Mouse mammary tumor virus (MMTV) is used to drive expression of a variety of oncogenes as a useful mouse model for breast cancer. [198] The J. Bromberg lab generously provided two independent frozen mouse tumor samples from Wnt, Myc, PyMT, Neu, and Ras genes driven by the MMTV promoter. Western blot analysis of these samples showed sporadic expression of Tiam2 protein (Figure 26, panel

C). The MMTV-Ras and MMTV-Wnt tumors showed very low expression of Tiam2, while one of each of the MMTV-Myc and MMTV-neu tumors showed strong expression but did not appear to be consistent. Both MMTV-PyMt tumors showed modest expression of Tiam2. The data do not support a link between Ras and Tiam2 expression since the MMTV-Ras model did not show strong expression of Tiam2. This could be explained by variations in the recognition of mouse STEF protein by the Tiam2 antibody, but that is unlikely since two of the samples showed strong expression. It is highly likely, however, that there are many ways to drive tumor growth in the complex physiological tumor environment, and Tiam2 signaling may be only one of many possible avenues available.

Mutant Ras is not sufficient to induce Tiam2 expression

To test if mutant Ras expression can upregulate Tiam2 levels in breast cells directly, mutant Ras was overexpressed in normal human breast cell lines. Previously, a colleague had generated stable HMEC and MCF-10a cell lines expressing the active K-Ras V12 mutant or a matched control empty vector. Western blot analysis revealed that K-Ras V12 expression was not sufficient to increase the level of Tiam2 protein in either cell line (Figure 27, panel A). This suggests that Ras alone does not drive expression of Tiam2 in breast cancer cells. However, it does not rule out the possibility that in a different context, Ras signaling might support Tiam2 expression.

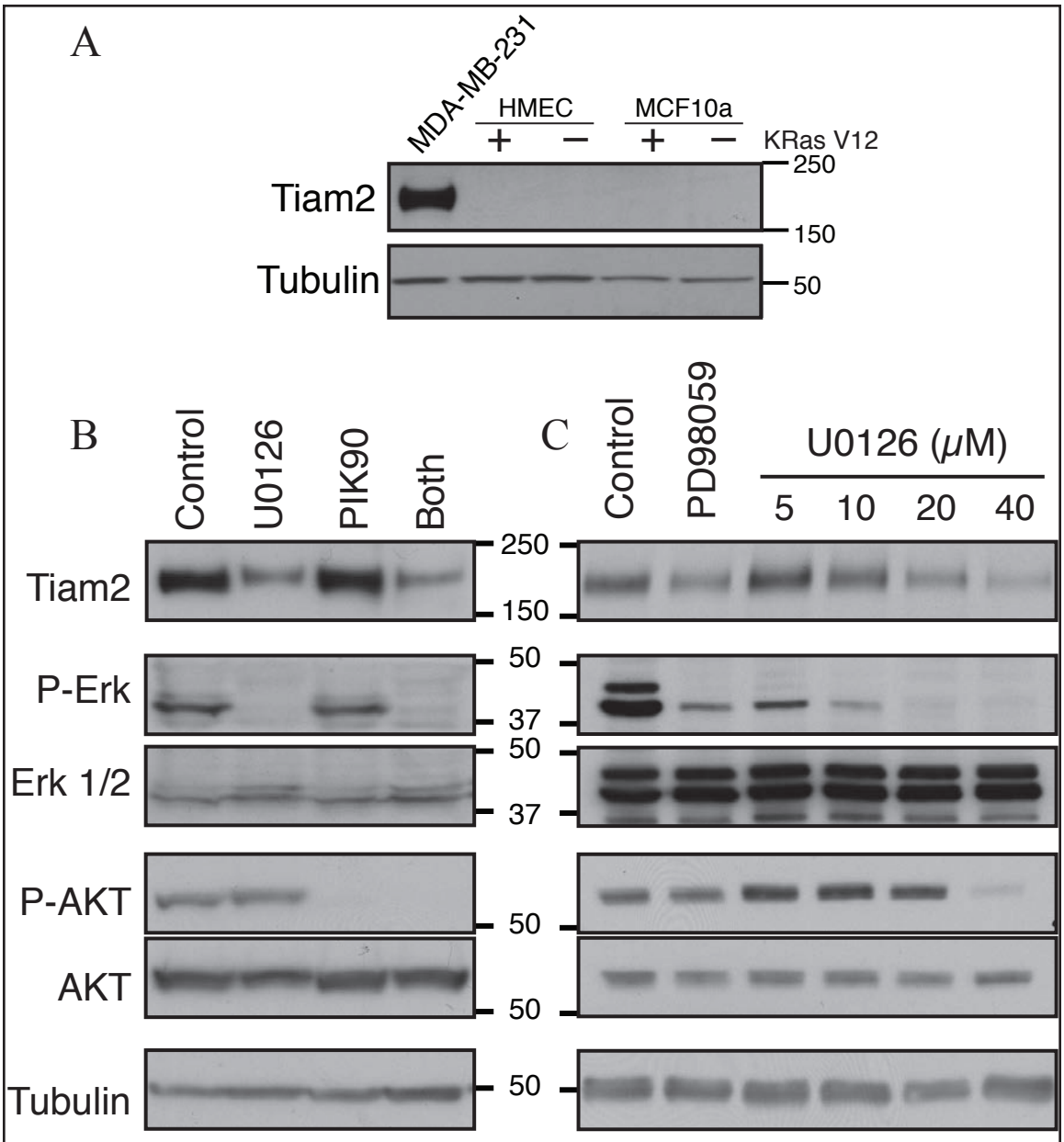

Figure 27: Ras signaling is correlated witih Tiam2 expression

(A) HMEC and MCF10a cell lines stably expressing KRas V12 (+) or empty vector (–) were lysed and analyzed by western blot alongside MDA-MB-231 cells and probed with the indicated antibodies. (B) MDA-MB-231 cells were treated with the MEK inhibitor U0126 (at 20 μM) or the PI3K inhibitor PIK90 (at 1 μM) in addition to DMSO treated control. The drugs were added to the media for 24 hours after which cells were lysed and analyzed by western blot using the indicated antibodies. (C) Cells were treated with the MEK inhibitor PD98059 (at 100 μM) or various concentrations of the MEK inhibitor U0126 for 24 hours. Cells were lysed and analyzed by western blot using the indicated antibodies.

Inhibition of MEK, but not PI3K, decreases Tiam2 expression.

To determine if Tiam2 expression is Ras-dependent in MDA-MB-231 cells, signaling was blocked from two well-characterized targets downstream of Ras: mitogen-activated protein kinase kinase (MKK, or MEK), and PI3K. The inhibitor U0126 blocks MEK signaling, and PIK90 inhibitor blocks PI3K signaling. Subconfluent MDA-MB-231 cells were treated with each inhibitor for 24 hours. Tiam2 protein levels remained unchanged after treatment with PIK90, but significantly decreased in cells treated with U0126 or a combination of both inhibitors (Figure 27, panel B). The level of MEK inhibition was determined by western blot detection of phospho-ERK, a downstream target of MEK. Similarly, phospho-AKT was used to evaluate the effectiveness of PIK90 at inhibiting PI3K signaling. This suggests that signals transduced through MEK, but not PI3K, are important for Tiam2 expression. It is possible, however, that the inhibitor is directly decreasing Tiam2 levels through some unknown mechanism. To control for this possibility, MDA-MB-231 cells were treated with a structurally unrelated MEK inhibitor, PD98059. Treatment with either MEK inhibitor resulted in decreased Tiam2 protein expression compared to DMSO control treated cells (Figure 27, panel C). The dose dependence of this effect was studied using various concentrations of U0126 inhibitor. At high concentrations, U0126 is also able to inhibit AKT phosphorylation, indicating that it loses specificity at higher doses. Tiam2 protein levels are inversely proportional to the concentration of U0126, and thus MEK activity (Figure 27, panel C). Taken together, this data suggests that signaling through the MEK/ERK pathway, but not PI3K/AKT, is important for Tiam2 protein expression in MDA-MB-231 cells.

Discussion

Breast Cancer Expression Patterns

Breast cancers can be broadly categorized based on a common histopathology into three main groups: invasive ductal carcinoma (IDC), ductal carcinoma in situ (DCIS), and invasive lobular carcinoma (ILC). [199] In order to better treat breast cancer, it is also useful to classify tumors into molecular subtypes (Triple-Negative/Basal-like, Luminal A/B, HER2-enriched, Claudin-low, Luminal ER-/AR+) based on expression of different receptors, tumor grade, and mutational status. [200-202] This work reveals that three triple-negative basal-like breast cancer cell lines that also harbor Ras mutations express significant levels of Tiam2 as compared to non-Ras-mutant cell lines. While this is not a comprehensive study, it suggests that Tiam2 may play a role in Ras signaling in this subset of cells. The expression level in MDA-MB-231 cells in particular is very high, yet has not been reported to be upregulated in any published work using DNA microarrays, including microarrays of MDA-MB-231 cells, to study gene expression. This suggests either that Tiam2 levels are not often altered in these expression studies, or more likely that current probes used are insensitive to Tiam2. While Ras mutations in breast cancer are uncommon, they still represent a large number of cases that are generally associated with poor prognosis.

Pancreatic Cancer Expression

One cancer type in which Ras mutations are much more commonly found is pancreatic cancer (>80%). [197] In order to determine if the expression of Tiam2 in Ras mutant lines was specific to breast cancer, a panel of pancreatic cancer cell lines containing Ras mutations was assembled and examined for Tiam1 and Tiam2 expression. Almost all expressed Tiam2, suggesting that Ras signaling may regulate the level of Tiam2 protein more broadly. All of the evidence for this link has been observed in cultured cells, which may behave differently than tumors in vivo.

Mouse Models of Breast Cancer

To determine if Tiam2 expression was important generally in mammary tumor formation, we examined a panel of spontaneous tumor mouse models. All of the models utilized a MMTV promoter system to drive oncogene expression specifically in mouse mammary tissue where tumors formed. There did not appear to be any pattern of Tiam2 expression driven by a particular oncogene. Surprisingly, neither of the MMTV-Ras tumors showed significant expression of Tiam2. This could be a consequence of the MMTV driver system, or suggest that upregulation of Tiam2 is specific to cultured cell lines. Tumors from the MMTV-Myc and -Neu mice, however, did show strong Tiam2 expression. This suggests that Tiam2 expression is not required in all contexts, if at all.

Ras Signaling Pathways and Tiam2 expression

Tiam1 has been shown to interact with activated Ras through its RBD (Ras binding domain), which is linked to Rac activation. [107] Since both Tiam1 and Tiam2 share a common domain organization, it suggests Tiam2 is likely to also be involved in signal transduction through Ras. It does not appear that active Ras signaling is sufficient to upregulate Tiam2 expression in normal breast cancer cells based on the experiments performed. However, the possibility still exists that Tiam2 expression and Ras activation are unrelated, and the initial observation is merely coincidental.

To further elucidate if Ras signaling pathways are involved in the regulation of Tiam2 expression, I used inhibitors of two well-characterized pathways, MEK and PI3K. These pathways are known to regulate the expression of a wide variety of genes and cellular functions, and are commonly misregulated by cancer cells. [203, 204] Inhibition of the Ras-Raf-MEK-ERK signaling pathway caused a dose-dependent reduction in Tiam2 expression while PI3K inhibition had no effect. This signaling pathway is important for a variety

of cellular behaviors, but it is still unclear where Tiam2 plays an important role. Without a defined phenotypic role for Tiam2 in MDA-MB-231 cells, further examination of Tiam2 regulation by Ras signaling pathways was not pursued further.

Chapter 6: Discussion

Rho Family GTPases control a wide variety of cellular processes including polarization, migration, and gene expression. Their activation is tightly controlled by GEFs, which stabilize nucleotide-free GTPases. This study set out to determine which regulators of Rho GTPases are important for controlling the process of cell invasion using MDA-MB-231 breast cancer cells as a model system. Unfortunately, the only GEF identified using a siRNA-based screen, Tiam2, was eventually shown to have no direct effect on invasion. Throughout the course of this work, however, it was shown that Tiam2 expression is generally high in cell lines with Ras mutations.

This approach to screening regulators of GTPases was confounded by several instances of off-target effects not only with Tiam2, but also Fam13a and PKN (data not shown). While it is a powerful technique that has yielded informative results using other cell types and cellular functions, there is a significant risk of false positives. This challenge is amplified when the proteins identified from the screen lack well-characterized reagents to distinguish between real and false effects. Recent improvements in the algorithms used to design siRNAs and the use of chemical modifications to decrease the prevalence of off-target effects may improve the results of future screens.

Nevertheless, I identified Cdc42 as an important GTPase controlling MDA-MB-231 cell invasion. One way to focus specifically on differential regulation of GTPases is to examine protein interaction through co-immunoprecipitation. For example, GTPases mutants with different known binding affinities (i.e. dominant negative, nucleotide-free, or specific effector binding) could be overexpressed with a TAP-tag and affinity purified. [205] Western blotting could be used to identify interacting proteins using a set of candidate antibodies or an unbiased identification using mass spectrometry could be employed. This biochemical

approach may be better at identifying Rho effector proteins but this depends highly on the specific mutants chosen and their behavior upon overexpression.

The mechanisms and contexts in which GEFs and GAPs regulate GTPase activity is still an open area of study. The loss-of-function screen described in this work is only one approach that could identify important regulators of invasion. While this process is critically important in embryonic development and cancer biology, it is complex, requiring complex coordination between several processes acting in concert. This implies that loss-of-function studies are likely to reveal a wide variety of candidate molecules because they could disrupt any of the component sub-processes. However, the multitude of molecular mechanisms cancer cells can use to invade, in addition to imperfect assays used to study this process, have yielded fewer candidates than expected.

One potential way to increase the likelihood of identifying a biological regulator of invasion might be to sensitize the cell line by partial reduction of Cdc42 levels. This would necessitate the creation of a stable cell line with an inducible shRNA targeting Cdc42, or co-transfection with a low concentration of siRNA. The level of knockdown could be titrated such that the invasive capacity of cells is very weakly inhibited, and then transfect a library of siRNAs to deplete GEFs and GAPs similar to the one in this study. An advantage to this method is that it may also allow identification of positive regulators of GTPases involved in invasion as well as negative regulators. Caveats remain, however, due to the variability of results using the modified Boyden chamber assay in addition to the previously discussed issues involved whenever RNAi is used. In order to avoid using siRNA, overexpression of dominant negative forms of GEFs and GAPs could be used to try and inhibit invasion.

Another alternative method of screening for regulators of invasion would be to instead use a gain-of-function study. This would require the use of a cell line that is weakly invasive.

In this case, depletion of Rho family GEFs and GAPs might be expected to increase the capacity of cells to invade. One significant challenge if using siRNA to manipulate protein expression would be identification of suitable controls that would enhance invasion. It may be necessary to use overexpression as a control, which has a different set of caveats entirely.

Proteomic and/or microarray approaches could also be used to identify regulators of specific cellular processes more globally. For instance, clonal populations from the same parental cell line with different invasive capacities could be selected after serial functional isolation and labeled for SILAC [206] or microarray [190] analysis to determine differential gene expression. This would not, however, specifically identify regulators of Rho family GTPases.

This study has revealed the unexpected result that expression of Tiam2 in breast cell lines correlates generally with mutant Ras expression. The presence of a Ras binding domain within Tiam1/2 suggests that these proteins may mediate the downstream effects of mutant Ras signaling. This signaling may be permissive for Tiam2 function, but does not directly increase Tiam2 levels. Signaling through this pathway is especially interesting in the context of cancer, where the role of Ras has been studied extensively. [195, 207-210] Whether or not Tiam2 is important in breast cancer generally, and the nature of Ras signaling specificity is still an open question.

Bibliography

1. Siegel, R., D. Naishadham, and A. Jemal, *Cancer statistics, 2012.* CA Cancer J Clin, 2012. **62**(1): p. 10-29.
2. Fidler, I.J., *Critical factors in the biology of human cancer metastasis: twenty-eighth G.H.A. Clowes memorial award lecture.* Cancer Res, 1990. **50**(19): p. 6130-8.
3. Hanahan, D. and R.A. Weinberg, *Hallmarks of cancer: the next generation.* Cell, 2011. **144**(5): p. 646-74.
4. Friedl, P., S. Borgmann, and E.B. Brocker, *Amoeboid leukocyte crawling through extracellular matrix: lessons from the Dictyostelium paradigm of cell movement.* J Leukoc Biol, 2001. **70**(4): p. 491-509.
5. Condeelis, J., *Understanding the cortex of crawling cells: insights from Dictyostelium.* Trends Cell Biol, 1993. **3**(11): p. 371-6.
6. Abercrombie, M., G.A. Dunn, and J.P. Heath, *The shape and movement of fibroblasts in culture.* Soc Gen Physiol Ser, 1977. **32**: p. 57-70.
7. Lauffenburger, D.A. and A.F. Horwitz, *Cell migration: a physically integrated molecular process.* Cell, 1996. **84**(3): p. 359-69.
8. Ridley, A.J., et al., *Cell migration: integrating signals from front to back.* Science, 2003. **302**(5651): p. 1704-9.
9. Parri, M. and P. Chiarugi, *Rac and Rho GTPases in cancer cell motility control.* Cell Commun Signal, 2010. **8**: p. 23.
10. Huttenlocher, A. and A.R. Horwitz, *Integrins in cell migration.* Cold Spring Harb Perspect Biol, 2011. **3**(9): p. a005074.
11. Itoh, R.E., et al., *Activation of rac and cdc42 video imaged by fluorescent resonance energy transfer-based single-molecule probes in the membrane of living cells.* Mol Cell Biol, 2002. **22**(18): p. 6582-91.
12. Etienne-Manneville, S., *Cdc42--the centre of polarity.* J Cell Sci, 2004. **117**(Pt 8): p. 1291-300.
13. Etienne-Manneville, S. and A. Hall, *Rho GTPases in cell biology.* Nature, 2002. **420**(6916): p. 629-35.
14. Rodriguez, O.C., et al., *Conserved microtubule-actin interactions in cell movement and morphogenesis.* Nat Cell Biol, 2003. **5**(7): p. 599-609.
15. Welchman, D.P., L.D. Mathies, and J. Ahringer, *Similar requirements for CDC-42 and the PAR-3/PAR-6/PKC-3 complex in diverse cell types.* Dev Biol, 2007. **305**(1): p. 347-57.
16. Nishimura, T., et al., *PAR-6-PAR-3 mediates Cdc42-induced Rac activation through the Rac GEFs STEF/Tiam1.* Nat Cell Biol, 2005. **7**(3): p. 270-7.
17. Yang, H.W., et al., *Cooperative activation of PI3K by Ras and Rho family small GTPases.* Mol Cell, 2012. **47**(2): p. 281-90.
18. Merlot, S. and R.A. Firtel, *Leading the way: Directional sensing through phosphatidylinositol 3-kinase and other signaling pathways.* J Cell Sci, 2003. **116**(Pt 17): p. 3471-8.
19. Iijima, M. and P. Devreotes, *Tumor suppressor PTEN mediates sensing of chemoattractant gradients.* Cell, 2002. **109**(5): p. 599-610.
20. Li, Z., et al., *Regulation of PTEN by Rho small GTPases.* Nat Cell Biol, 2005. **7**(4): p. 399-404.

21. Srinivasan, S., et al., *Rac and Cdc42 play distinct roles in regulating PI(3,4,5)P3 and polarity during neutrophil chemotaxis.* J Cell Biol, 2003. **160**(3): p. 375-85.
22. Welch, H.C., et al., *Phosphoinositide 3-kinase-dependent activation of Rac.* FEBS Lett, 2003. **546**(1): p. 93-7.
23. Condeelis, J., *Life at the leading edge: the formation of cell protrusions.* Annu Rev Cell Biol, 1993. **9**: p. 411-44.
24. Mullins, R.D., J.A. Heuser, and T.D. Pollard, *The interaction of Arp2/3 complex with actin: nucleation, high affinity pointed end capping, and formation of branching networks of filaments.* Proc Natl Acad Sci U S A, 1998. **95**(11): p. 6181-6.
25. Yarar, D., et al., *The Wiskott–Aldrich syndrome protein directs actin-based motility by stimulating actin nucleation with the Arp2/3 complex.* Current Biology, 1999. **9**(10): p. 555-S1.
26. Pollard, T.D. and C.C. Beltzner, *Structure and function of the Arp2/3 complex.* Curr Opin Struct Biol, 2002. **12**(6): p. 768-774.
27. Carlsson, L., et al., *Actin polymerizability is influenced by profilin, a low molecular weight protein in non-muscle cells.* J Mol Biol, 1977. **115**(3): p. 465-83.
28. Nakano, K. and I. Mabuchi, *Actin-capping protein is involved in controlling organization of actin cytoskeleton together with ADF/cofilin, profilin and F-actin crosslinking proteins in fission yeast.* Genes Cells, 2006. **11**(8): p. 893-905.
29. Ammer, A.G. and S.A. Weed, *Cortactin branches out: roles in regulating protrusive actin dynamics.* Cell Motil Cytoskeleton, 2008. **65**(9): p. 687-707.
30. Sun, H.Q., et al., *Gelsolin, a multifunctional actin regulatory protein.* J Biol Chem, 1999. **274**(47): p. 33179-82.
31. Friederich, E., et al., *Villin function in the organization of the actin cytoskeleton. Correlation of in vivo effects to its biochemical activities in vitro.* J Biol Chem, 1999. **274**(38): p. 26751-60.
32. Mattila, P.K. and P. Lappalainen, *Filopodia: molecular architecture and cellular functions.* Nat Rev Mol Cell Biol, 2008. **9**(6): p. 446-54.
33. Lebrand, C., et al., *Critical role of Ena/VASP proteins for filopodia formation in neurons and in function downstream of netrin-1.* Neuron, 2004. **42**(1): p. 37-49.
34. Edwards, R.A. and J. Bryan, *Fascins, a family of actin bundling proteins.* Cell Motil Cytoskeleton, 1995. **32**(1): p. 1-9.
35. Lidke, D.S., et al., *Reaching out for signals: filopodia sense EGF and respond by directed retrograde transport of activated receptors.* J Cell Biol, 2005. **170**(4): p. 619-26.
36. Linder, S., *The matrix corroded: podosomes and invadopodia in extracellular matrix degradation.* Trends Cell Biol, 2007. **17**(3): p. 107-17.
37. Yamaguchi, H., et al., *Molecular mechanisms of invadopodium formation: the role of the N-WASP-Arp2/3 complex pathway and cofilin.* J Cell Biol, 2005. **168**(3): p. 441-52.
38. Yamaguchi, H., et al., *Lipid rafts and caveolin-1 are required for invadopodia formation and extracellular matrix degradation by human breast cancer cells.* Cancer Res, 2009. **69**(22): p. 8594-602.
39. Yamaguchi, H., J. Wyckoff, and J. Condeelis, *Cell migration in tumors.* Curr Opin Cell Biol, 2005. **17**(5): p. 559-64.
40. Humphries, M.J., *Integrin structure.* Biochem Soc Trans, 2000. **28**(4): p. 311-39.
41. Hynes, R.O., *Integrins: bidirectional, allosteric signaling machines.* Cell, 2002. **110**(6): p. 673-87.

42. Zaidel-Bar, R. and B. Geiger, *The switchable integrin adhesome.* J Cell Sci, 2010. **123**(Pt 9): p. 1385-8.
43. Geiger, B., et al., *Transmembrane crosstalk between the extracellular matrix--cytoskeleton crosstalk.* Nat Rev Mol Cell Biol, 2001. **2**(11): p. 793-805.
44. Zaidel-Bar, R., et al., *Hierarchical assembly of cell-matrix adhesion complexes.* Biochem Soc Trans, 2004. **32**(Pt3): p. 416-20.
45. Zaidel-Bar, R., et al., *Functional atlas of the integrin adhesome.* Nat Cell Biol, 2007. **9**(8): p. 858-67.
46. Abercrombie, M., J.E. Heaysman, and S.M. Pegrum, *The locomotion of fibroblasts in culture. IV. Electron microscopy of the leading lamella.* Exp Cell Res, 1971. **67**(2): p. 359-67.
47. Heath, J.P. and G.A. Dunn, *Cell to substratum contacts of chick fibroblasts and their relation to the microfilament system. A correlated interference-reflexion and high-voltage electron-microscope study.* J Cell Sci, 1978. **29**: p. 197-212.
48. Turner, C.E., *Paxillin and focal adhesion signalling.* Nat Cell Biol, 2000. **2**(12): p. E231-6.
49. Zamir, E. and B. Geiger, *Components of cell-matrix adhesions.* J Cell Sci, 2001. **114**(Pt 20): p. 3577-9.
50. Zhang, X., et al., *Talin depletion reveals independence of initial cell spreading from integrin activation and traction.* Nat Cell Biol, 2008. **10**(9): p. 1062-8.
51. Xu, W., H. Baribault, and E.D. Adamson, *Vinculin knockout results in heart and brain defects during embryonic development.* Development, 1998. **125**(2): p. 327-37.
52. Enterline, H.T. and D.R. Coman, *The ameboid motility of human and animal neoplastic cells.* Cancer, 1950. **3**(6): p. 1033-8.
53. Yumura, S., H. Mori, and Y. Fukui, *Localization of actin and myosin for the study of ameboid movement in Dictyostelium using improved immunofluorescence.* J Cell Biol, 1984. **99**(3): p. 894-9.
54. Mandeville, J.T., M.A. Lawson, and F.R. Maxfield, *Dynamic imaging of neutrophil migration in three dimensions: mechanical interactions between cells and matrix.* J Leukoc Biol, 1997. **61**(2): p. 188-200.
55. Lewis, W.H., *On the locomotion of the polymorphonuclear neutrophiles of the rat in autoplasma cultures.* Bull. Johns Hopkins Hosp., 1934. **4**(55): p. 273-279.
56. Friedl, P. and K. Wolf, *Tumour-cell invasion and migration: diversity and escape mechanisms.* Nat Rev Cancer, 2003. **3**(5): p. 362-74.
57. Sahai, E. and C.J. Marshall, *Differing modes of tumour cell invasion have distinct requirements for Rho/ROCK signalling and extracellular proteolysis.* Nat Cell Biol, 2003. **5**(8): p. 711-9.
58. Wolf, K., et al., *Amoeboid shape change and contact guidance: T-lymphocyte crawling through fibrillar collagen is independent of matrix remodeling by MMPs and other proteases.* Blood, 2003. **102**(9): p. 3262-9.
59. Davidson, L.A. and R.E. Keller, *Neural tube closure in Xenopus laevis involves medial migration, directed protrusive activity, cell intercalation and convergent extension.* Development, 1999. **126**(20): p. 4547-56.
60. Klinowska, T.C., et al., *Laminin and beta1 integrins are crucial for normal mammary gland development in the mouse.* Dev Biol, 1999. **215**(1): p. 13-32.
61. Simian, M., et al., *The interplay of matrix metalloproteinases, morphogens and growth factors is necessary for branching of mammary epithelial cells.* Development, 2001. **128**(16): p. 3117-31.

62. Hegerfeldt, Y., et al., *Collective cell movement in primary melanoma explants: plasticity of cell-cell interaction, beta1-integrin function, and migration strategies.* Cancer Res, 2002. **62**(7): p. 2125-30.
63. Friedl, P., et al., *Migration of coordinated cell clusters in mesenchymal and epithelial cancer explants in vitro.* Cancer Res, 1995. **55**(20): p. 4557-60.
64. Thiery, J.P., *Epithelial-mesenchymal transitions in tumour progression.* Nat Rev Cancer, 2002. **2**(6): p. 442-54.
65. Alexander, S. and P. Friedl, *Cancer invasion and resistance: interconnected processes of disease progression and therapy failure.* Trends Mol Med, 2012. **18**(1): p. 13-26.
66. Friedl, P., et al., *Classifying collective cancer cell invasion.* Nat Cell Biol, 2012. **14**(8): p. 777-83.
67. Wolf, K., et al., *Multi-step pericellular proteolysis controls the transition from individual to collective cancer cell invasion.* Nat Cell Biol, 2007. **9**(8): p. 893-904.
68. Kalluri, R. and R.A. Weinberg, *The basics of epithelial-mesenchymal transition.* J Clin Invest, 2009. **119**(6): p. 1420-8.
69. Mani, S.A., et al., *The epithelial-mesenchymal transition generates cells with properties of stem cells.* Cell, 2008. **133**(4): p. 704-15.
70. Pietras, K. and A. Ostman, *Hallmarks of cancer: interactions with the tumor stroma.* Exp Cell Res, 2010. **316**(8): p. 1324-31.
71. Mizejewski, G.J., *Role of integrins in cancer: survey of expression patterns.* Proc Soc Exp Biol Med, 1999. **222**(2): p. 124-38.
72. McHugh, B.J., et al., *Loss of the integrin-activating transmembrane protein Fam38A (Piezo1) promotes a switch to a reduced integrin-dependent mode of cell migration.* PLoS ONE, 2012. **7**(7): p. e40346.
73. Morozevich, G., et al., *Integrin alpha5beta1 controls invasion of human breast carcinoma cells by direct and indirect modulation of MMP-2 collagenase activity.* Cell Cycle, 2009. **8**(14): p. 2219-25.
74. Friedl, P. and K. Wolf, *Plasticity of cell migration: a multiscale tuning model.* J Cell Biol, 2010. **188**(1): p. 11-9.
75. Jechlinger, M., S. Grunert, and H. Beug, *Mechanisms in epithelial plasticity and metastasis: insights from 3D cultures and expression profiling.* J Mammary Gland Biol Neoplasia, 2002. **7**(4): p. 415-32.
76. Wolf, K., et al., *Compensation mechanism in tumor cell migration: mesenchymal-amoeboid transition after blocking of pericellular proteolysis.* J Cell Biol, 2003. **160**(2): p. 267-77.
77. Coussens, L.M., B. Fingleton, and L.M. Matrisian, *Matrix metalloproteinase inhibitors and cancer: trials and tribulations.* Science, 2002. **295**(5564): p. 2387-92.
78. Overall, C.M. and C. Lopez-Otin, *Strategies for MMP inhibition in cancer: innovations for the post-trial era.* Nat Rev Cancer, 2002. **2**(9): p. 657-72.
79. McSherry, E.A., et al., *Molecular basis of invasion in breast cancer.* Cell Mol Life Sci, 2007. **64**(24): p. 3201-18.
80. Wolf, K. and P. Friedl, *Molecular mechanisms of cancer cell invasion and plasticity.* Br J Dermatol, 2006. **154 Suppl 1**: p. 11-5.
81. Fritz, G., I. Just, and B. Kaina, *Rho GTPases are over-expressed in human tumors.* Int J Cancer, 1999. **81**(5): p. 682-7.
82. Gomez del Pulgar, T., et al., *Rho GTPase expression in tumourigenesis: evidence for a significant link.* Bioessays, 2005. **27**(6): p. 602-13.

83. Tang, Y., et al., *Role of Rho GTPases in breast cancer.* Front Biosci, 2008. **13**: p. 759-76.
84. Farina, K.L., et al., *Cell motility of tumor cells visualized in living intact primary tumors using green fluorescent protein.* Cancer Res, 1998. **58**(12): p. 2528-32.
85. Sahai, E. and C.J. Marshall, *RHO-GTPases and cancer.* Nat Rev Cancer, 2002. **2**(2): p. 133-42.
86. Bar-Sagi, D. and A. Hall, *Ras and Rho GTPases: a family reunion.* Cell, 2000. **103**(2): p. 227-38.
87. Madaule, P. and R. Axel, *A novel ras-related gene family.* Cell, 1985. **41**(1): p. 31-40.
88. Anderson, P.S. and J.C. Lacal, *Expression of the Aplysia californica rho gene in Escherichia coli: purification and characterization of its encoded p21 product.* Mol Cell Biol, 1987. **7**(10): p. 3620-8.
89. Boureux, A., et al., *Evolution of the Rho family of ras-like GTPases in eukaryotes.* Mol Biol Evol, 2007. **24**(1): p. 203-16.
90. Ellenbroek, S.I. and J.G. Collard, *Rho GTPases: functions and association with cancer.* Clin Exp Metastasis, 2007. **24**(8): p. 657-72.
91. Ridley, A.J., *Historical overview of Rho GTPases.* Methods Mol Biol, 2012. **827**: p. 3-12.
92. Bourne, H.R., D.A. Sanders, and F. McCormick, *The GTPase superfamily: a conserved switch for diverse cell functions.* Nature, 1990. **348**(6297): p. 125-32.
93. Karnoub, A.E., C.J. Der, and S.L. Campbell, *The insert region of Rac1 is essential for membrane ruffling but not cellular transformation.* Mol Cell Biol, 2001. **21**(8): p. 2847-57.
94. Mitin, N., et al., *Posttranslational lipid modification of Rho family small GTPases.* Methods Mol Biol, 2012. **827**: p. 87-95.
95. Jaffe, A.B. and A. Hall, *Rho GTPases: biochemistry and biology.* Annu Rev Cell Dev Biol, 2005. **21**: p. 247-69.
96. Ridley, A.J. and A. Hall, *The small GTP-binding protein rho regulates the assembly of focal adhesions and actin stress fibers in response to growth factors.* Cell, 1992. **70**(3): p. 389-99.
97. Ridley, A.J., et al., *The small GTP-binding protein rac regulates growth factor-induced membrane ruffling.* Cell, 1992. **70**(3): p. 401-10.
98. Jaffe, A.B., et al., *Cdc42 controls spindle orientation to position the apical surface during epithelial morphogenesis.* J Cell Biol, 2008. **183**(4): p. 625-33.
99. Melendez, J., M. Grogg, and Y. Zheng, *Signaling role of Cdc42 in regulating mammalian physiology.* J Biol Chem, 2011. **286**(4): p. 2375-81.
100. Schmidt, A. and A. Hall, *Guanine nucleotide exchange factors for Rho GTPases: turning on the switch.* Genes Dev, 2002. **16**(13): p. 1587-609.
101. DerMardirossian, C. and G.M. Bokoch, *GDIs: central regulatory molecules in Rho GTPase activation.* Trends Cell Biol, 2005. **15**(7): p. 356-63.
102. Robbe, K., et al., *Dissociation of GDP dissociation inhibitor and membrane translocation are required for efficient activation of Rac by the Dbl homology-pleckstrin homology region of Tiam.* J Biol Chem, 2003. **278**(7): p. 4756-62.
103. Olofsson, B., *Rho guanine dissociation inhibitors: pivotal molecules in cellular signalling.* Cell Signal, 1999. **11**(8): p. 545-54.
104. Boulter, E., et al., *Regulation of Rho GTPase crosstalk, degradation and activity by RhoGDI1.* Nat Cell Biol, 2010. **12**(5): p. 477-83.
105. Keep, N.H., et al., *A modulator of rho family G proteins, rhoGDI, binds these*

G proteins via an immunoglobulin-like domain and a flexible N-terminal arm. Structure, 1997. **5**(5): p. 623-33.
106. Iden, S. and J.G. Collard, *Crosstalk between small GTPases and polarity proteins in cell polarization.* Nat Rev Mol Cell Biol, 2008. **9**(11): p. 846-59.
107. Lambert, J.M., et al., *Tiam1 mediates Ras activation of Rac by a PI(3) K-independent mechanism.* Nat Cell Biol, 2002. **4**(8): p. 621-5.
108. Sander, E.E., et al., *Rac downregulates Rho activity: reciprocal balance between both GTPases determines cellular morphology and migratory behavior.* J Cell Biol, 1999. **147**(5): p. 1009-22.
109. Nimnual, A.S., L.J. Taylor, and D. Bar-Sagi, *Redox-dependent downregulation of Rho by Rac.* Nat Cell Biol, 2003. **5**(3): p. 236-41.
110. Sakumura, Y., et al., *A molecular model for axon guidance based on cross talk between rho GTPases.* Biophys J, 2005. **89**(2): p. 812-22.
111. Fujisawa, K., et al., *Identification of the Rho-binding domain of p160ROCK, a Rho-associated coiled-coil containing protein kinase.* J Biol Chem, 1996. **271**(38): p. 23022-8.
112. Riento, K. and A.J. Ridley, *Rocks: multifunctional kinases in cell behaviour.* Nat Rev Mol Cell Biol, 2003. **4**(6): p. 446-56.
113. Totsukawa, G., et al., *Distinct roles of ROCK (Rho-kinase) and MLCK in spatial regulation of MLC phosphorylation for assembly of stress fibers and focal adhesions in 3T3 fibroblasts.* J Cell Biol, 2000. **150**(4): p. 797-806.
114. Bagrodia, S., et al., *Cdc42 and PAK-mediated signaling leads to Jun kinase and p38 mitogen-activated protein kinase activation.* J Biol Chem, 1995. **270**(47): p. 27995-8.
115. Alberts, A.S., et al., *Analysis of RhoA-binding proteins reveals an interaction domain conserved in heterotrimeric G protein beta subunits and the yeast response regulator protein Skn7.* J Biol Chem, 1998. **273**(15): p. 8616-22.
116. Flynn, P., et al., *Multiple interactions of PRK1 with RhoA. Functional assignment of the Hr1 repeat motif.* J Biol Chem, 1998. **273**(5): p. 2698-705.
117. Marinissen, M.J. and J.S. Gutkind, *Scaffold proteins dictate Rho GTPase-signaling specificity.* Trends Biochem Sci, 2005. **30**(8): p. 423-6.
118. Baranwal, S. and S.K. Alahari, *Rho GTPase effector functions in tumor cell invasion and metastasis.* Curr Drug Targets, 2011. **12**(8): p. 1194-201.
119. Phillips-Mason, P.J., et al., *The receptor protein-tyrosine phosphatase PTPmu interacts with IQGAP1.* J Biol Chem, 2006. **281**(8): p. 4903-10.
120. Bustelo, X.R., V. Sauzeau, and I.M. Berenjeno, *GTP-binding proteins of the Rho/Rac family: regulation, effectors and functions in vivo.* Bioessays, 2007. **29**(4): p. 356-70.
121. Aflaki, E., et al., *Impaired Rho GTPase activation abrogates cell polarization and migration in macrophages with defective lipolysis.* Cell Mol Life Sci, 2011. **68**(23): p. 3933-47.
122. Hall, A., *Rho GTPases and the actin cytoskeleton.* Science, 1998. **279**(5350): p. 509-14.
123. Maekawa, M., et al., *Signaling from Rho to the actin cytoskeleton through protein kinases ROCK and LIM-kinase.* Science, 1999. **285**(5429): p. 895-8.
124. Lin, M. and K.L. van Golen, *Rho-regulatory proteins in breast cancer cell motility and invasion.* Breast Cancer Res Treat, 2004. **84**(1): p. 49-60.
125. Wittmann, T. and C.M. Waterman-Storer, *Cell motility: can Rho GTPases and microtubules point the way?* J Cell Sci, 2001. **114**(Pt 21): p. 3795-803.

126. Adams, A.E., et al., *CDC42 and CDC43, two additional genes involved in budding and the establishment of cell polarity in the yeast Saccharomyces cerevisiae.* J Cell Biol, 1990. **111**(1): p. 131-42.
127. Walsh, S.V., et al., *Rho kinase regulates tight junction function and is necessary for tight junction assembly in polarized intestinal epithelia.* Gastroenterology, 2001. **121**(3): p. 566-79.
128. Minden, A., et al., *Selective activation of the JNK signaling cascade and c-Jun transcriptional activity by the small GTPases Rac and Cdc42Hs.* Cell, 1995. **81**(7): p. 1147-57.
129. Salh, B., et al., *Dysregulation of phosphatidylinositol 3-kinase and downstream effectors in human breast cancer.* Int J Cancer, 2002. **98**(1): p. 148-54.
130. Vadlamudi, R.K., et al., *Regulatable expression of p21-activated kinase-1 promotes anchorage-independent growth and abnormal organization of mitotic spindles in human epithelial breast cancer cells.* J Biol Chem, 2000. **275**(46): p. 36238-44.
131. Kamai, T., et al., *Overexpression of RhoA, Rac1, and Cdc42 GTPases is associated with progression in testicular cancer.* Clin Cancer Res, 2004. **10**(14): p. 4799-805.
132. Feig, L.A., *Guanine-nucleotide exchange factors: a family of positive regulators of Ras and related GTPases.* Curr Opin Cell Biol, 1994. **6**(2): p. 204-11.
133. Rossman, K.L., C.J. Der, and J. Sondek, *GEF means go: turning on RHO GTPases with guanine nucleotide-exchange factors.* Nat Rev Mol Cell Biol, 2005. **6**(2): p. 167-80.
134. Eva, A. and S.A. Aaronson, *Isolation of a new human oncogene from a diffuse B-cell lymphoma.* Nature, 1985. **316**(6025): p. 273-5.
135. Drubin, D.G., *Development of cell polarity in budding yeast.* Cell, 1991. **65**(7): p. 1093-6.
136. Whitehead, I.P., et al., *Dbl family proteins.* Biochim Biophys Acta, 1997. **1332**(1): p. F1-23.
137. Zheng, Y., *Dbl family guanine nucleotide exchange factors.* Trends Biochem Sci, 2001. **26**(12): p. 724-32.
138. Soisson, S.M., et al., *Crystal structure of the Dbl and pleckstrin homology domains from the human Son of sevenless protein.* Cell, 1998. **95**(2): p. 259-68.
139. Haslam, R.J., H.B. Koide, and B.A. Hemmings, *Pleckstrin domain homology.* Nature, 1993. **363**(6427): p. 309-10.
140. Karnoub, A.E., et al., *Molecular basis for Rac1 recognition by guanine nucleotide exchange factors.* Nat Struct Biol, 2001. **8**(12): p. 1037-41.
141. Bellanger, J.M., et al., *The Rac1- and RhoG-specific GEF domain of Trio targets filamin to remodel cytoskeletal actin.* Nat Cell Biol, 2000. **2**(12): p. 888-92.
142. Cote, J.F. and K. Vuori, *Identification of an evolutionarily conserved superfamily of DOCK180-related proteins with guanine nucleotide exchange activity.* J Cell Sci, 2002. **115**(Pt 24): p. 4901-13.
143. Meller, N., S. Merlot, and C. Guda, *CZH proteins: a new family of Rho-GEFs.* J Cell Sci, 2005. **118**(Pt 21): p. 4937-46.
144. Hasegawa, H., et al., *DOCK180, a major CRK-binding protein, alters cell morphology upon translocation to the cell membrane.* Mol Cell Biol, 1996. **16**(4): p. 1770-6.
145. Cote, J.F. and K. Vuori, *GEF what? Dock180 and related proteins help Rac to polarize cells in new ways.* Trends Cell Biol, 2007. **17**(8): p. 383-93.

146. Yang, J., et al., *Activation of Rho GTPases by DOCK exchange factors is mediated by a nucleotide sensor.* Science, 2009. **325**(5946): p. 1398-402.
147. Cote, J.F., et al., *A novel and evolutionarily conserved PtdIns(3,4,5)P3-binding domain is necessary for DOCK180 signalling.* Nat Cell Biol, 2005. **7**(8): p. 797-807.
148. Premkumar, L., et al., *Structural basis of membrane targeting by the Dock180 family of Rho family guanine exchange factors (Rho-GEFs).* J Biol Chem, 2010. **285**(17): p. 13211-22.
149. Moon, S.Y. and Y. Zheng, *Rho GTPase-activating proteins in cell regulation.* Trends Cell Biol, 2003. **13**(1): p. 13-22.
150. Garrett, M.D., et al., *Identification of distinct cytoplasmic targets for ras/R-ras and rho regulatory proteins.* J Biol Chem, 1989. **264**(1): p. 10-3.
151. Barrett, T., et al., *The structure of the GTPase-activating domain from p50rhoGAP.* Nature, 1997. **385**(6615): p. 458-61.
152. Gamblin, S.J. and S.J. Smerdon, *GTPase-activating proteins and their complexes.* Curr Opin Struct Biol, 1998. **8**(2): p. 195-201.
153. Li, R., B. Zhang, and Y. Zheng, *Structural determinants required for the interaction between Rho GTPase and the GTPase-activating domain of p190.* J Biol Chem, 1997. **272**(52): p. 32830-5.
154. Levay, M., J. Settleman, and E. Ligeti, *Regulation of the substrate preference of p190RhoGAP by protein kinase C-mediated phosphorylation of a phospholipid binding site.* Biochemistry, 2009. **48**(36): p. 8615-23.
155. Ligeti, E., et al., *Phospholipids can switch the GTPase substrate preference of a GTPase-activating protein.* J Biol Chem, 2004. **279**(7): p. 5055-8.
156. Hodis, E., et al., *A landscape of driver mutations in melanoma.* Cell, 2012. **150**(2): p. 251-63.
157. Fritz, G., et al., *Rho GTPases in human breast tumours: expression and mutation analyses and correlation with clinical parameters.* Br J Cancer, 2002. **87**(6): p. 635-44.
158. Schnelzer, A., et al., *Rac1 in human breast cancer: overexpression, mutation analysis, and characterization of a new isoform, Rac1b.* Oncogene, 2000. **19**(26): p. 3013-20.
159. Engers, R., et al., *Tiam1 mutations in human renal-cell carcinomas.* Int J Cancer, 2000. **88**(3): p. 369-76.
160. Fields, A.P. and V. Justilien, *The guanine nucleotide exchange factor (GEF) Ect2 is an oncogene in human cancer.* Adv Enzyme Regul, 2010. **50**(1): p. 190-200.
161. Kamynina, E., et al., *Regulation of proto-oncogenic dbl by chaperone-controlled, ubiquitin-mediated degradation.* Mol Cell Biol, 2007. **27**(5): p. 1809-22.
162. Sosa, M.S., et al., *Identification of the Rac-GEF P-Rex1 as an essential mediator of ErbB signaling in breast cancer.* Mol Cell, 2010. **40**(6): p. 877-92.
163. Citterio, C., et al., *The rho exchange factors vav2 and vav3 control a lung metastasis-specific transcriptional program in breast cancer cells.* Sci Signal, 2012. **5**(244): p. ra71.
164. Wertheimer, E., et al., *Rac signaling in breast cancer: a tale of GEFs and GAPs.* Cell Signal, 2012. **24**(2): p. 353-62.
165. Holeiter, G., et al., *The RhoGAP protein Deleted in Liver Cancer 3 (DLC3) is essential for adherens junctions integrity.* Oncogenesis, 2012. **1**: p. e13.
166. Johnstone, C.N., et al., *ARHGAP8 is a novel member of the RHOGAP family related to ARHGAP1/CDC42GAP/p50RHOGAP: mutation and expression*

analyses in colorectal and breast cancers. Gene, 2004. **336**(1): p. 59-71.
167. Ren, X.D. and M.A. Schwartz, *Determination of GTP loading on Rho.* Methods Enzymol, 2000. **325**: p. 264-72.
168. Cailleau, R., et al., *Breast tumor cell lines from pleural effusions.* J Natl Cancer Inst, 1974. **53**(3): p. 661-74.
169. Farina, A.R., et al., *Transforming growth factor-beta1 enhances the invasiveness of human MDA-MB-231 breast cancer cells by up-regulating urokinase activity.* Int J Cancer, 1998. **75**(5): p. 721-30.
170. Repesh, L.A., *A new in vitro assay for quantitating tumor cell invasion.* Invasion Metastasis, 1989. **9**(3): p. 192-208.
171. Garcia-Mata, R., E. Boulter, and K. Burridge, *The 'invisible hand': regulation of RHO GTPases by RHOGDIs.* Nat Rev Mol Cell Biol, 2011. **12**(8): p. 493-504.
172. Bishop, A.L. and A. Hall, *Rho GTPases and their effector proteins.* Biochem J, 2000. **348 Pt 2**: p. 241-55.
173. Liu, B.P. and K. Burridge, *Vav2 activates Rac1, Cdc42, and RhoA downstream from growth factor receptors but not beta1 integrins.* Mol Cell Biol, 2000. **20**(19): p. 7160-9.
174. Lin, D., et al., *A mammalian PAR-3-PAR-6 complex implicated in Cdc42/Rac1 and aPKC signalling and cell polarity.* Nat Cell Biol, 2000. **2**(8): p. 540-7.
175. Noda, Y., et al., *Human homologues of the Caenorhabditis elegans cell polarity protein PAR6 as an adaptor that links the small GTPases Rac and Cdc42 to atypical protein kinase C.* Genes Cells, 2001. **6**(2): p. 107-19.
176. Suzuki, A. and S. Ohno, *The PAR-aPKC system: lessons in polarity.* J Cell Sci, 2006. **119**(Pt 6): p. 979-87.
177. Jackson, A.L. and P.S. Linsley, *Recognizing and avoiding siRNA off-target effects for target identification and therapeutic application.* Nat Rev Drug Discov, 2010. **9**(1): p. 57-67.
178. Semizarov, D., et al., *Specificity of short interfering RNA determined through gene expression signatures.* Proc Natl Acad Sci U S A, 2003. **100**(11): p. 6347-52.
179. Jackson, A.L., et al., *Position-specific chemical modification of siRNAs reduces "off-target" transcript silencing.* RNA, 2006. **12**(7): p. 1197-205.
180. Khan, A.A., et al., *Transfection of small RNAs globally perturbs gene regulation by endogenous microRNAs.* Nat Biotechnol, 2009. **27**(6): p. 549-55.
181. Habets, G.G., et al., *Identification of an invasion-inducing gene, Tiam-1, that encodes a protein with homology to GDP-GTP exchangers for Rho-like proteins.* Cell, 1994. **77**(4): p. 537-49.
182. Chiu, C.Y., et al., *Cloning and characterization of T-cell lymphoma invasion and metastasis 2 (TIAM2), a novel guanine nucleotide exchange factor related to TIAM1.* Genomics, 1999. **61**(1): p. 66-73.
183. Terawaki, S., et al., *The PHCCEx domain of Tiam1/2 is a novel protein- and membrane-binding module.* Embo J, 2010. **29**(1): p. 236-50.
184. Bantounas, I., L.A. Phylactou, and J.B. Uney, *RNA interference and the use of small interfering RNA to study gene function in mammalian systems.* J Mol Endocrinol, 2004. **33**(3): p. 545-57.
185. Cullen, B.R., *Enhancing and confirming the specificity of RNAi experiments.* Nat Methods, 2006. **3**(9): p. 677-81.
186. Schultz, N., et al., *Off-target effects dominate a large-scale RNAi screen for modulators of the TGF-beta pathway and reveal microRNA regulation of*

TGFBR2. Silence, 2011. **2**: p. 3.
187. Beitel, L.K., et al., *Substitution of arginine-839 by cysteine or histidine in the androgen receptor causes different receptor phenotypes in cultured cells and coordinate degrees of clinical androgen resistance.* J Clin Invest, 1994. **94**(2): p. 546-54.
188. Hachiya, M., et al., *Mutant p53 proteins behave in a dominant, negative fashion in vivo.* Anticancer Res, 1994. **14**(5A): p. 1853-9.
189. Shekhar, M.P., et al., *Breast stroma plays a dominant regulatory role in breast epithelial growth and differentiation: implications for tumor development and progression.* Cancer Res, 2001. **61**(4): p. 1320-6.
190. Minn, A.J., et al., *Genes that mediate breast cancer metastasis to lung.* Nature, 2005. **436**(7050): p. 518-24.
191. Niu, Z., et al., *Small interfering RNA targeted to secretory clusterin blocks tumor growth, motility, and invasion in breast cancer.* Acta Biochim Biophys Sin (Shanghai), 2012.
192. Zamarron, B.F. and W. Chen, *Dual roles of immune cells and their factors in cancer development and progression.* Int J Biol Sci, 2011. **7**(5): p. 651-8.
193. Michiels, F., et al., *A role for Rac in Tiam1-induced membrane ruffling and invasion.* Nature, 1995. **375**(6529): p. 338-40.
194. Riaz, M., et al., *Low-risk susceptibility alleles in 40 human breast cancer cell lines.* BMC Cancer, 2009. **9**: p. 236.
195. Hollestelle, A., et al., *Phosphatidylinositol-3-OH kinase or RAS pathway mutations in human breast cancer cell lines.* Mol Cancer Res, 2007. **5**(2): p. 195-201.
196. Pellegata, N.S., et al., *K-ras and p53 gene mutations in pancreatic cancer: ductal and nonductal tumors progress through different genetic lesions.* Cancer Res, 1994. **54**(6): p. 1556-60.
197. Laghi, L., et al., *Common occurrence of multiple K-RAS mutations in pancreatic cancers with associated precursor lesions and in biliary cancers.* Oncogene, 2002. **21**(27): p. 4301-6.
198. Taneja, P., et al., *MMTV mouse models and the diagnostic values of MMTV-like sequences in human breast cancer.* Expert Rev Mol Diagn, 2009. **9**(5): p. 423-40.
199. Eheman, C.R., et al., *The changing incidence of in situ and invasive ductal and lobular breast carcinomas: United States, 1999-2004.* Cancer Epidemiol Biomarkers Prev, 2009. **18**(6): p. 1763-9.
200. Prat, A. and C.M. Perou, *Deconstructing the molecular portraits of breast cancer.* Mol Oncol, 2011. **5**(1): p. 5-23.
201. Lehmann, B.D., et al., *Identification of human triple-negative breast cancer subtypes and preclinical models for selection of targeted therapies.* J Clin Invest, 2011. **121**(7): p. 2750-67.
202. *Comprehensive molecular portraits of human breast tumours.* Nature, 2012. **490**(7418): p. 61-70.
203. Castellano, E. and J. Downward, *RAS Interaction with PI3K: More Than Just Another Effector Pathway.* Genes Cancer, 2011. **2**(3): p. 261-74.
204. Kolch, W., *Meaningful relationships: the regulation of the Ras/Raf/MEK/ERK pathway by protein interactions.* Biochem J, 2000. **351 Pt 2**: p. 289-305.
205. Goldfinger, L.E., et al., *An experimentally derived database of candidate Ras-interacting proteins.* J Proteome Res, 2007. **6**(5): p. 1806-11.
206. Mann, M., *Functional and quantitative proteomics using SILAC.* Nat Rev Mol Cell

Biol, 2006. **7**(12): p. 952-8.
207. Prior, I.A., P.D. Lewis, and C. Mattos, *A comprehensive survey of Ras mutations in cancer.* Cancer Res, 2012. **72**(10): p. 2457-67.
208. Fernandez-Medarde, A. and E. Santos, *Ras in cancer and developmental diseases.* Genes Cancer, 2011. **2**(3): p. 344-58.
209. Janku, F., et al., *PIK3CA mutations frequently coexist with RAS and BRAF mutations in patients with advanced cancers.* PLoS ONE, 2011. **6**(7): p. e22769.
210. von Lintig, F.C., et al., *Ras activation in human breast cancer.* Breast Cancer Res Treat, 2000. **62**(1): p. 51-62.